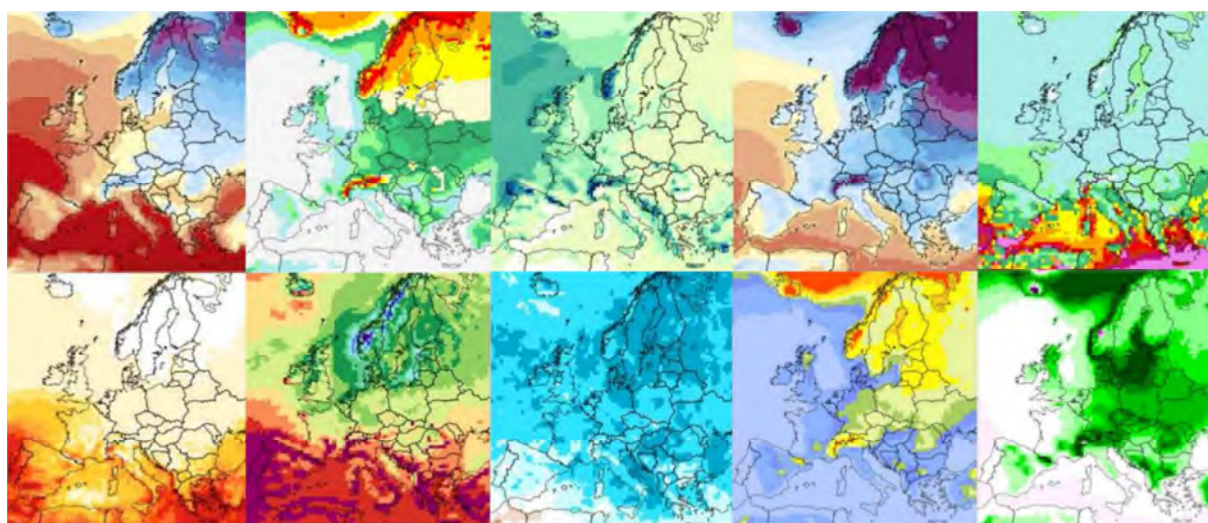# CORDEX scenarios for Europe from the Rossby Centre regional climate model RCA4

Gustav Strandberg, Lars Bärring, Ulf Hansson, Christer Jansson, Colin Jones, Erik Kjellström, Michael Kolax, Marco Kupiainen, Grigory Nikulin, Patrick Samuelsson, Anders Ullerstig and Shiyu Wang

CORDEX scenarios for Europe from the Rossby Centre regional climate model RCA4

Gustav Strandberg, Lars Bärring, Ulf Hansson, Christer Jansson, Colin Jones, Erik Kjellström, Michael Kolax, Marco Kupiainen, Grigory Nikulin, Patrick Samuelsson, Anders Ullerstig and Shiyu Wang

Swedish Meteorological and Hydrological Institute, SE 601 76 Norrköping, Sweden

Corresponding author
Gustav Strandberg, Swedish Meteorological and Hydrological Institute
SE-601 76 Norrköping, Sweden
Telephone: +46(0)11 495 8268 E-mail: gustav.strandberg@smhi.se

Studies published in the SMHI Report series RMK are quality reviewed.
This report has been quality reviewed by Joakim Langner, SMHI. Results and conclusions
were presented at a seminar (June 2, 2015) prior to publication.

....
Signature & date, quality reviewer

Summary

This report documents Coordinated Regional Downscaling Experiment (CORDEX) climate model simulations at 50 km horizontal resolution over Europe with the Rossby Centre regional atmospheric model (RCA4) for i) a ERA-Interim-driven (ERAINT) simulation used to evaluate model performance in the recent past climate, ii) historical simulations of the recent decades with forcing from nine different global climate models (GCMs) and iii) future scenarios RCP 4.5 and RCP 8.5 forced by the same nine different GCMs. Those simulations represent a subset of all CORDEX simulations produced at the Rossby Centre and a general conclusion drawn at the Rossby Centre is that such large ensembles could not have been produced without the establishment of an efficient production chain as outlined here.

The first part of this report documents RCA4 and its performance in a perfect boundary simulation where ERAINT was downscaled. RCA4 is to a large extent replicating the large-scale circulation in ERAINT, but some local biases in mean sea level pressure appear. In general the seasonal cycles of temperature and precipitation are simulated in relatively close agreement to observations. Some biases occur, such as too much precipitation in northern Europe and too little in the south. In winter, there is also too much precipitation in eastern Europe. Temperatures are generally biased low in northern Europe and in the Mediterranean region in winter while overestimated temperatures are seen in southeastern Europe in winter and in the Mediterranean area in summer.

RCA4 performs generally well when simulating the recent past climate taking boundary conditions from the GCMs. A large part of the RCA4 simulated climate is attributed to the driving GCMs, but RCA4 creates its own climate inside the model domain and adds details due to higher resolution. All nine downscaled GCMs share problems in their representation of the large-scale circulation in winter. This feature is inherited in RCA4. The biases in large-scale circulation induce some biases in temperature and precipitation in RCA4.

The climate change signal in the RCP 4.5 and RCP 8.5 ensembles simulated by RCA4 is very similar to what has been presented previously. Both scenarios RCP 4.5 and RCP 8.5 project Europe to be warmer in the future. In winter the warming is largest in northern Europe and in summer in southern Europe. The summer maximum daily temperature increases in a way similar to summer temperature, but somewhat more in southern Europe. The winter minimum daily temperature in northern Europe is the temperature that changes the most. Precipitation is projected to increase in all seasons in northern Europe and decrease in southern Europe. The largest amount of rainfall per day (and per seven day period) is projected to increase in almost all of Europe and in all seasons. At the same time the longest period without precipitation is projected to be longer in southern Europe. Small changes in mean wind speed are generally projected. There are, however, regions with significant changes in wind.

The ensemble approach is a way to describe the uncertainties in the scenarios, but there are other possible ensembles using other models which would give other results. Still, the ensemble used here is found to be similar enough to these other possible ensembles to be representative of the whole set of GCMs. Dynamical downscaling using RCA4 changes the climate change signal, and the ensemble spread is sometimes reduced, but the ensemble of nine RCA4 simulations, using different GCMs, is considered to be representative of the full ensemble. All scenarios agree on a climate change pattern; the amplitude of the change is determined by the choice of scenario. The relative importance of the chosen scenario increases with time.

Sammanfattning

Denna rapport dokumenterar klimatmodellsimuleringar på 50 km horisontell upplösning över Europa med Rossby Centres regionala atmosfärsmodell (RCA4) gjorda inom projektet Coordinated Regional Downscaling Experiment (CORDEX) för i) ERA-Interim-drivna (ERAINT) simuleringar för att utvärdera förmågan hos RCA4 att simulera den senaste tidens klimat, ii) historiska simuleringar av de senaste årtiondena med drivning från nio olika globala klimatmodeller (GCM:er) och iii) framtidsscenarierna RCP 4,5 och RCP 8,5 drivna med samma GCM:er. Dessa simuleringar representerar en delmängd av alla CORDEX-simuleringar producerade vid Rossby Centre och en allmän slutsats dragen vid Rossby Centre är att en sådan ensemble inte varit möjlig utan att först etablera den effektiva produktionskedja som beskrivs här.

Första delen av rapporten dokumenterar RCA4 och dess förmåga i en simulering där ERAINT skalades ner. RCA4 återskapar till stor del den storskaliga cirkulationen från ERAINT, men några lokala avvikelser förekommer. I allmänhet simuleras säsongscykler för temperatur och nederbörd i överensstämmelse med observationer. Några avvikelser finns, som för mycket nederbörd i norra Europa och för lite i södra. På vintern är det även för mycket nederbörd i östra Europa. Temperaturen är i allmänhet underskattad i norra Europa och i medelhavsområdet på vintern, medan för höga temperaturer ges i sydöstra Europa på vintern och i medelhavsområdet på sommaren.

RCA4 presterar i allmänhet bra i simuleringar av den senaste tidens klimat med randvillkor från GCM:er. En stor del av det simulerade klimatet i RCA4 kan tillskrivas den drivande GCM:en, men RCA4 skapar sitt eget klimat inuti modelldomänen och lägger till detaljer på grund av högre upplösning. Alla nio nedskalade GCM:er har gemensamma problem i representationen av den storskaliga cirkulationen på vintern. Denna egenskap förs vidare till RCA4. Avvikelserna i storskalig cirkulation medför avvikelser i temperatur och nederbörd i RCA4.

Klimatförändringssignalen som den simuleras av RCA4-ensembler enligt RCP 4,5 och RCP 8,5 är mycket lika tidigare resultat. I både scenario RCP 4,5 och RCP 8,5 beräknas Europa bli varmare i framtiden. På vintern är uppvärmningen störst i norra Europa, och på sommaren i södra Europa. Den högsta dygnsmedeltemperaturen på sommaren ökar på ungefär samma sätt som sommartemperaturen, men något mer i södra Europa. Den lägsta dygnsmedeltemperaturen på vintern i norra Europa är den temperatur som förändras mest. Nederbörden beräknas öka under alla årstider i norra Europa och minska i södra Europa. Den största dygnsnederbörden (och per sjudagarsperiod) beräknas öka i nästan hela Europa och i alla årstider. Samtidigt beräknas den längsta perioden utan nederbörd att bli längre i södra Europa. I allmänhet förutses små förändringar i medelvindhastighet. Det finns emellertid områden med signifikanta förändringar i vind.

Att använda ensembler är ett sätt att beskriva osäkerheterna i scenarierna, men det finns andra möjliga ensembler som använder andra modeller och som skulle ge andra resultat. Ändå anses den ensemble som används här vara tillräckligt lik dessa andra ensembler för att vara representativ för den hela mängden GCM:er. Dynamisk nedskalning med RCA4 förändrar klimatförändringssignalen, och spridningen i ensemblen minskar ibland, men ensemblen med nio RCA4 simuleringar med olika GCM:er anses vara representativ för den hela ensemblen. Alla scenarier är överens om mönstret på klimatförändringen, men storleken på förändringen bestäms av valet av scenario. Den relativa betydelsen av valet av scenario ökar med tiden.

Table of contents

Empty page

Introduction

The Rossby Centre, which is a part of SMHI, pursues advanced climate modelling. The efforts include the development, verification, validation, evaluation and application of global and regional climate models in climate and climate change research. Over the last few years there has been an extensive work to produce a very large number of regional climate modelling experiments with the latest version of the Rossby Centre regional atmospheric model, RCA4, for several regions of the world including Europe, the Arctic, Africa, the Middle East and North Africa, South Asia and North, Central and South America. This report documents part of this work by presenting results from the European domain.

A large number of global climate change scenarios have been produced in the fifth coupled model intercomparison project (CMIP5 (Taylor et al., 2012)). These scenarios are extensively used in the fifth assessment report (AR5) from the Intergovernmental Panel on Climate Change (IPCC, 2013). CMIP5 models are more complex, have a better representation of external forcing and run at higher resolution than those used in the preceding intercomparison project (CMIP3). Scenarios for the future in CMIP3 and CMIP5 are remarkably similar (Knutti and Sedláček, 2013), confirming that even though more and more complex models are used we can have some confidence with the results.

Even these most recent modern global climate change scenarios have the problem that the CMIP5 global climate models (GCMs) generally operate on a relatively coarse horizontal resolution of 100-300 km. This implies that regional details of the land-sea distribution and altitude of mountains are not well resolved. Further, the coarse resolution implies that some processes are handled in a crude way, including weather phenomena like mid-latitude low pressure systems. As it is computationally expensive to run GCMs at high resolution, downscaling techniques are applied to increase the resolution and thereby improve the degree of local and regional detail compared to the GCM. Both statistical and dynamical downscaling techniques can be used in this context. Statistical downscaling utilizes empirical relationships between large-scale features and local conditions assuming that these relations stay the same in a changing climate. Dynamical downscaling makes use of regional climate models (RCM) that are set up on a smaller domain at higher resolution compared to the GCM (e.g. Rummukainen, 2010). RCMs typically operate on a horizontal scale of 10-50 km. Previously, earlier CMIP results have been downscaled creating ensembles of RCM data for Europe (e.g. Christensen and Christensen, 2007; Haugen and Iversen, 2008; Kjellström et al., 2011 and 2013). Recently, a substantial number of CMIP5 GCMs have been downscaled in the Coordinated Regional Downscaling Experiment (CORDEX, Giorgi et al., 2009). For Europe, CORDEX is producing a large number of RCM scenarios at 12.5 km horizontal resolution which is higher than in most previous studies (e.g. Jacob et al., 2013; Vautard et al., 2013). In addition to these simulations, an even larger number of simulations are being performed at 50 km to better sample the uncertainties related to future climate change. We note here that dynamical downscaling cannot, albeit the higher resolution of the RCMs, resolve all problems inherited from the GCMs (Mauran et al., 2010). For instance, there are still problems in the CMIP5 simulations like the overestimated meridional pressure gradient in winter and spring over the North Atlantic, which gives to moist and mild conditions in continental Europe (Brands et al., 2013; Cattiaux et al., 2013).

There are three main sources of uncertainties in climate scenarios for the future: 1) natural variability, 2) model uncertainty and 3) emissions scenario uncertainty. The relative importance of these uncertainties varies with prediction length and resolution (Hawkins and Sutton, 2009). Natural variability is the internal variations in climate occurring on time scales ranging from days through months and seasons up to years, decades, centuries or longer. These variations are inherent features of the climate system and if the variability is large climate change signals can be difficult to detect. This

uncertainty is largest in the first few decades of a climate simulation when the forced climate change signal is still relatively small. Natural variability in the climate system can also change with time when the climate is changing. For instance, climate models indicate increasing frequency of extreme El Niño events in a future warmer climate (Cai et al., 2014), a change that would have an impact on the interannual variability of global mean temperature and on regional precipitation patterns. The uncertainty from natural variability can be reduced by better initialization of climate model runs (Hawkins and Sutton, 2009).

The model uncertainty is an effect of differences between climate models. This can be further subdivided into limitations in the description of physical phenomena in the model, discretization error due to discrete approximations, round-off error due to finite precision computers, erroneous treatment of mathematical processes (e.g. setting of boundary conditions or the use of non-mass-conserving numerical schemes) and actual computer program errors (bugs). Different models have a different set of these ingredients and hence describe the climate system differently, and will therefore produce different results. As an example two models with the same climate sensitivity may give different regional response to the global forcing. The relative importance of the model uncertainty is largest after 50-60 years. This uncertainty can be reduced by improving climate models.

The scenario uncertainty is different from the two previous uncertainties. The scenarios build on assumptions of the future and will be uncertain per se. There are several forcing components influencing future climate. The most important components are greenhouse gases, aerosols and changes in the land surface. Different forcing components work on different spatial scales and can be both warming and cooling. The relative importance of scenario uncertainty grows over time.

As part of the Euro-CORDEX effort the Rossby Centre has downscaled nine different GCMs in 46 runs at 12.5 km or 50 km resolution. Results from the 50 km scenarios are presented in this report. For a more comprehensive assessment of potential changes in the European climate additional Euro-CORDEX simulations with other RCMs should be included. We note, however, that the number of GCMs that have been downscaled with RCA4 is larger than what has been downscaled with any other RCM to date, making the Rossby Centre ensemble unique in its sampling of the uncertainty related to choice of GCM. In addition to presenting results from the RCA4 simulations of future climate change we also describe differences in RCA4 compared to the previous model version RCA3 and perform a validation of the model. The RCA4 simulations cover the period 1961-2100 which makes it possible both to validate the performance in the historical climate and to explore potential future climate change in Europe on short, medium and long-term time perspectives under different scenarios. Differences in the climate response in the regional climate model compared to the underlying GCMs are discussed.

1   Method

1.1   The Rossby Centre regional climate model, RCA4

RCA is originally based on the numerical weather prediction model HIRLAM (Undén et al., 2002). Earlier versions of the RCA model are described by Rummukainen et al. (1998, 2001); Räisänen et al. (2003, 2004), Jones et al. (2004), Kjellström et al. (2005) and Samuelsson et al. (2011). Since RCA3 (Samuelsson et al., 2011), RCA has undergone substantial both physical and technical changes. In the development of RCA4 the aims have been that RCA should be a transferable model, i.e. that it can be applied for any domain worldwide without retuning, and that RCA4 should be efficient and user

friendly to apply. The main two shortcomings with RCA3 were that it was in principle a Europe-tuned RCM and that it was technically very complicated to setup.

Reaching the first aim of technically developing RCA includes the use of globally valid physiography data bases as ECOCLIMAP (Masson et al., 2003) for vegetation, Gtopo30 (USGS, 1996) for topography, lake depth (Kourzeneva, 2010) and soil carbon density (Global Soil Data Task, 2000). The code is easy to port to different architectures via standard gmake, which also obsoletes the complicated scripting system of RCA3. No pre-processing is needed to run RCA4 since all data used for a simulation are read from global databases and also the number of MPI-ranks is determined runtime by using built-in MPI-calls and the domain decomposition is also done runtime (the number of MPI-ranks was a hard-coded preprocessing step in RCA3). Most other settings are controlled via namelist files, which are read in at the start of the simulation. The restart procedure in RCA4 is exact, which was not the case for RCA3. All together, these technical developments of RCA made it possible for Rossby Centre to go for a highly ambitious scenario production for CORDEX.

The second aim was to improve the physical parameterisation of RCA. The mean climate over Europe was simulated fairly well by RCA3 (Samuelsson et al., 2011). However, when the development version of RCA4, including global physiography, was applied over other domains it was obvious that RCA3 included Europe-climate adapted parameterisations and compensating errors which did not perform well over e.g. Africa and the Arctic. Consequently a number of physical parameterisation packages have been improved to reach a more transferable model; in the surface model a new lake model (FLake) has been implemented (Samuelsson et al., 2010), soil processes are improved with respect to heat transfer and soil moisture to account for e.g. high-latitude high-carbon soils and low-latitude deep-rooted forests, snow albedo is improved to account for e.g. Arctic cold climate conditions. For more details on developments of surface processes in RCA4 please refer to Samuelsson et al. (2014). Modifications in the atmospheric part of the model include introduction of a numerically more stable turbulent kinetic energy (TKE) scheme (Lenderink and Holtslag, 2004) into the original CBR (Cuxart et al., 2000) scheme. At the same time the variables diffused in the TKE scheme are switched from dry (temp, humidity, liquid water) to moist conservation (liquid water potential temp and total water) following Grenier and Bretherton. (2001). Treatment of convection has been adjusted by switching the deep and shallow convection schemes from the standard Kain-Fritsch scheme (Kain and Fritsch, 1990) to the Bechtold-KF scheme (Bechtold et al., 2001). A few additional modifications including a diluted CAPE (Convective Available Potential Energy) profile for calculating the CAPE closure have also been implemented (Jiao and Jones, 2008). Finally, the threshold relative humidity for cloud formation was adjusted and the representation of cloud short wave reflectivity and long wave emissivity was modified to account for in-cloud cloud-water heterogeneity, loosely following Tiedtke (1996).

All together, these modifications have contributed to a more transferable RCA where parameterisations are more physical than in RCA3 and where compensating errors are reduced. All parameterisations are empirical and some of the parameterisations used in RCA4 are more tuned to a specific location, e.g. the radiation scheme, which makes a fully transferable code difficult to achieve. Nevertheless, exactly the same version of RCA4 is now used for CORDEX domains over Europe, Africa and the Arctic. However, the drawback is that for Europe specifically the new version has degraded some aspects of the RCA3 good mean climate, i.e. for precipitation. This degrade is considered to be acceptable taking into account less compensating errors and the benefit of higher transferability.

A few additional developments are also available for RCA4, although not used for the CORDEX simulations presented here but for specific other studies. For instance, spectral nudging is implemented and so far applied mostly for the Arctic domain (Berg et al.,

Table 1. List of CMIP5 GCMs that have been used to provide boundary conditions for the RCA4 runs presented here. Transient climate response (TCR) is defined as the immediate temperature change after a doubling of CO_2 (Cubash et al., 2001). The two rightmost columns indicate which RCP scenarios that have been run.

| No	Modelling Centre	Model name	Reference	TCR (°C)	0.44°	0.11°
1	Canadian Centre for Climate Modelling and Analysis	CanESM2	Chylek et al., 2011	2.4	4.5, 8.5	-
2	Centre National de Recherches Météorologiques / Centre Européen de Recherche et Formation Avancée en Calcul Scientifique	CNRM-CM5	Voldoire et al., 2012	2.1	4.5, 8.5	4.5, 8.5
3	EC-EARTH consortium	EC-EARTH	Hazeleger et al., 2010	2.0	2.6, 4.5, 8.5	2.6, 4.5, 8.5
4	NOAA Geophysical Fluid Dynamics Laboratory	GFDL-ESM2M	Dunne et al., 2012	1.3	4.5, 8.5	-
5	Met Office Hadley Centre	HadGEM2-ES	Collins et al., 2011	2.5	2.6, 4.5, 8.5	4.5, 8.5
6	Institut Pierre-Simon Laplace	IPSL-CM5A-MR	Dufresne et al., 2013	2.0	4.5, 8.5	4.5, 8.5
7	Atmosphere and Ocean Research Institute (The University of Tokyo), National Institute for Environmental Studies, and Japan Agency for Marine-Earth Science and Technology	MIROC5	Watanabe et al., 2011	1.5	4.5, 8.5	-
8	Max Planck Institute for Meteorology	MPI-ESM-LR	Popke et al., 2013	2.0	2.6, 4.5, 8.5	4.5, 8.5
9	Norwegian Climate Centre	NorESM1-M	Bentsen et al., 2013	1.4	4.5, 8.5	-
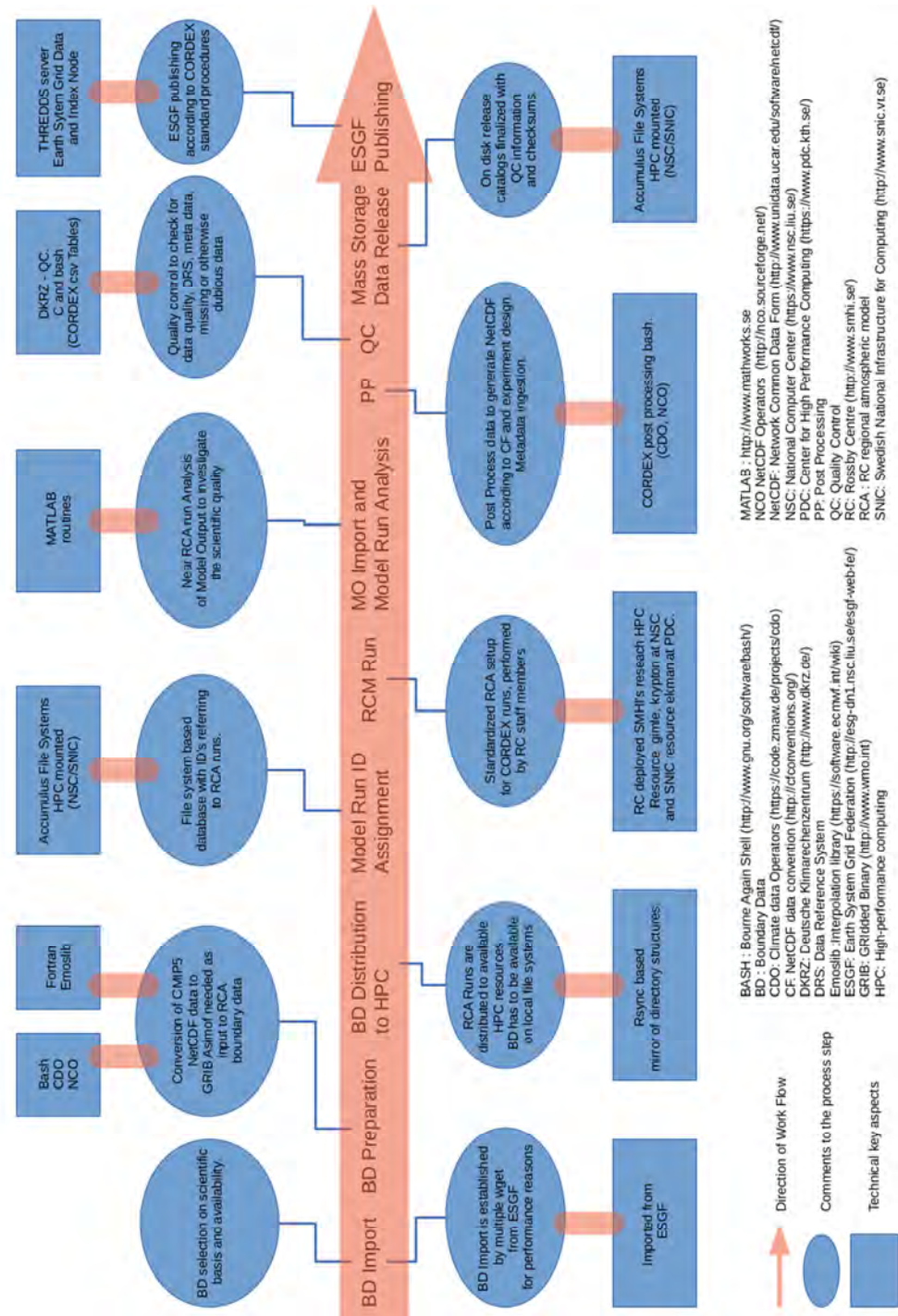
Figure 1. CORDEX workflow at the Rossby Centre. Boundary data (BD) is imported from ESGF and prepared to be read by RCA. An RCA run is started, model output (MO) is analysed, post processed (PP) to fulfil demands on file formats and quality controlled (QC). Final output files are stored at NSC and published via ESGF. Accumulus is the name given to the main storage facility.

2013). RCA4 can be coupled to the regional ocean model NEMO 3.3.1 (Madec, 2011), sea ice model LIM3 (Vancoppenolle et al., 2009) and river routing model CaMa_Flood 3.0 (Yamazaki, 2011) via the coupler OASIS3 (Valcke, 2013). This coupling has been applied over a European domain by Wang et al. (2015) where the Baltic Sea and North Sea are simulated by NEMO. RCA4 can be coupled to the dynamic vegetation model LPJ-GUESS (Smith et al., 2001). RCA4-GUESS has been applied over the Arctic (Zhang et al. 2014) and over Africa (Wu et al., 2014).

1.2   CORDEX simulations for Europe with RCA4

RCA4 has been set up and run for the European CORDEX domain at two different horizontal resolutions, 0.44° and 0.11° corresponding to c. 50 and c. 12.5 km grid spacing. A first set of runs consists of downscaling of the ERA-Interim reanalysis data (ERAINT, Dee et al., 2011). These simulations are used for evaluating model performance in the recent past climate. In a second round RCA4 has been used to downscale results from a total of nine different GCMs as listed in Table 1. The simulations have been performed for i) the historical period 1961-2005 for which historical forcing was applied and ii) for different future scenarios in which the so called RCP scenarios (Representative Concentration Pathways (Moss et al., 2010)) have been applied to prescribe future radiative forcing. Greenhouse gas concentrations are expressed as equivalent CO_2 concentrations following the RCP scenarios, and interpolated from one year to the next. Here we use three different RCP scenarios:

- RCP 2.6: Strategies for reducing greenhouse gas emissions cause radiative forcing to stabilise at 2.6 W/m² before the year 2100 (used by IPCC, AR5).
- RCP 4.5: Strategies for reducing greenhouse gas emissions cause radiative forcing to stabilise at 4.5 W/m² before the year 2100 (used by IPCC, AR5).
- RCP 8.5: Increased greenhouse gas emissions mean that radiative forcing will reach 8.5 W/m² by the year 2100 (used by IPCC, AR5).

Table 1 gives an overview of forcing GCMs and scenarios at the two horizontal resolutions. The RCP 4.5 and 8.5 scenarios have been downscaled for all nine GCMs at 50 km while the RCP 2.6 scenario has been downscaled for three GCMs. At 12.5 km a subset of the 50 km simulations have been repeated.

1.2.1   CORDEX - Data Processing and Technical Experiment Layout

The Rossby Centre has produced and made available a very large number of CORDEX simulations. The data set is unique not only as it is large but also as RCA4 takes lateral boundary conditions from a very large number of different GCMs. To achieve this the Rossby Centre required access to different components of large scale technical infrastructure and built up a work flow to handle all aspects from data import, high-performance computer (HPC) based RCM integrations, post processing, quality control and publishing to the end user. The technical resources required by experiment modules needed to be estimated and weighted against the available facilities. Priorities were made and experiment modules were distributed on the available HPC and mass storage systems. A tight collaboration with NSC (the National Supercomputer Centre at Linköping University) was established to implement a data publishing work flow suitable for the scale of the project. Output data is published via the Earth System Grid Foundation (ESGF). ESGF is an international collaboration with the aim of providing a gateway to scientific data collections from institutes across the world mainly within CMIP. RCA output can be retrieved via the Swedish ESGF node (http://esg-dn1.nsc.liu.se).

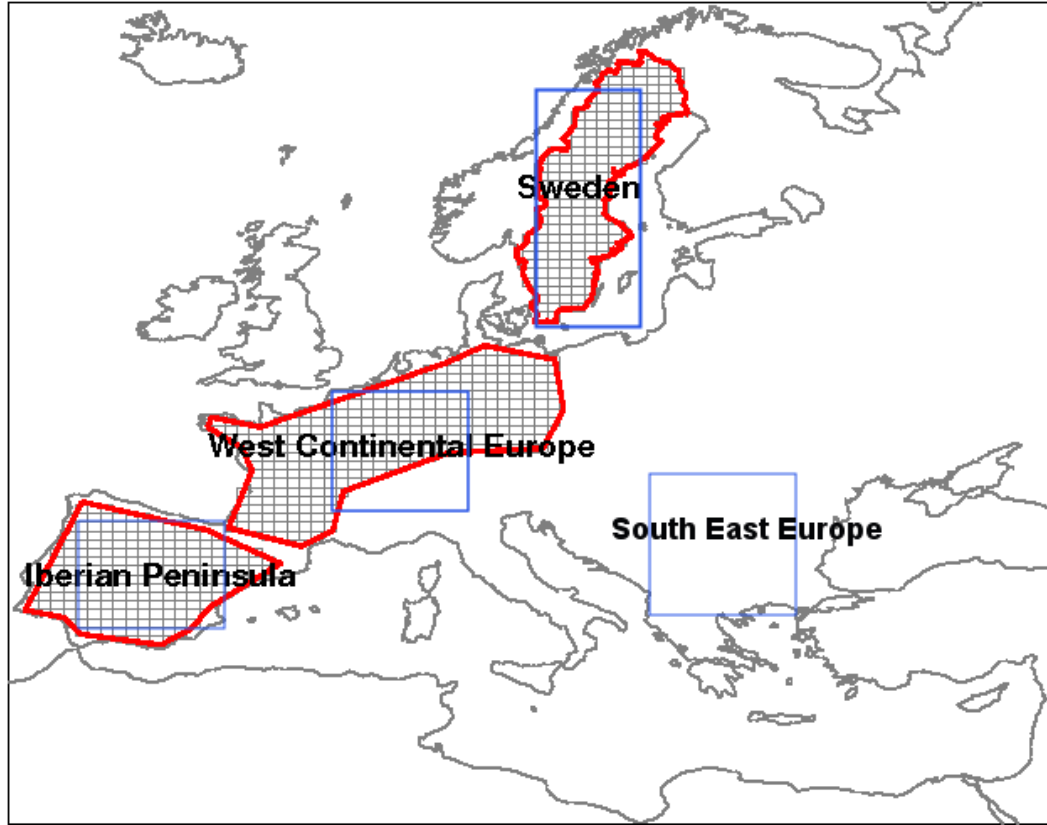Figure 1 presents the established work flow.

Figure 2. Areas in which RCA4 is evaluated against observations (red) and areas used to compare the climate change signal in GCMs and RCA4 in section 4 (blue).

Table 1. Observational data sets

Name	Reference	Time period	Resolution	Coverage
CRU	Harris et al., 2014	1901-2009	0.5°	Land only
E-OBS	Haylock et al., 2008	1950-2006	25 km	Land only
GLOBSNOW	Takala et al., 2011	1980-2010	25 km	Land only
GPCP	Adler et al., 2003	1979-2014	2.5°	Ocean and land
ISCCP	Rossow and Schiffer, 1999	1983-2009	250 km	Ocean and land
WILLMOTT	Willmott and Matsuura, 1995	1900-2010	0.5°	Land only

2   Results – Recent past climate

2.1   Recent past climate in the RCA4 ERA Interim run

Here we compare results from RCA4 at 50 km horizontal resolution forced with ERA-Interim (ERAINT, Dee et al., 2011) with ERAINT itself. In such a "perfect boundary" experiment, when the model results are compared with the forcing data, it is possible to see how RCA4 changes the climate produced by ERAINT. This tells us about potential systematic errors in RCA4 but also about potential benefits as RCA4 is run at higher horizontal resolution than ERAINT. As RCA4 is free to develop its own state in the interior model domain some deviations between ERAINT and RCA4 are to be expected on both small and large temporal and spatial scales. As there is no data assimilation in RCA4 it cannot be expected to follow the actual evolution of the atmosphere on a day-to-day basis. However, in a climatological sense it should represent observed long-term means and higher-order variability. Deviations from this are attributed to simplifications in the model formulation. Identification of such, systematic, model errors can be used to distinguish between errors introduced by the GCMs and those introduced by RCA4. To further extend the validation RCA4 results are compared with other observational datasets as well: CRU, E-OBS, GLOBSNOW, GPCP, ISCCP and WILLMOTT (Table 1). Note that the observational data sets are different. Hence, there is no clear definition of "real" or "observed" climate in the validation of a model. To be able to use these observations (with sometimes short timeseries) some comparisons are limited to the years 1990-1999. Annual cycles are presented for three regions: Sweden, West Continental Europe and Iberian Peninsula (Figure 2).

2.1.1   Sea level pressure

Simulated sea level pressure is generally in close resemblance with ERAINT. For winter (here December-February) some notable differences include higher pressure by 1-2 hPa over the southernmost parts of the domain and also around Iceland in the northwest (Figure 3). At the same time underestimates of up to 4 hPa are seen in parts of eastern Europe. For summer, differences in sea level pressure are small between RCA4 and ERAINT; ±0-1 hPa in most of Europe except Iceland, Scandinavia and parts of the Mediterranean where the pressure in RCA4 is 1-2 hPa higher than in ERAINT. The generally good agreement between RCA4 and ERAINT implies that the representation of the large scale circulation is realistic in RCA4. Particularly, the small bias over the North Atlantic implies that the prevailing westerlies are simulated in a good way.
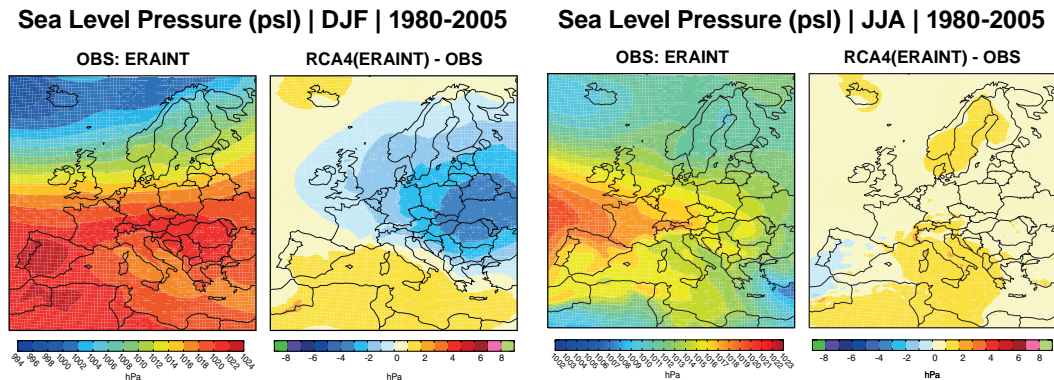

Figure 3. Observed (ERAINT) sea level pressure (hPa) in the present climate 1980-2005 (columns 1 and 3) and the difference between a RCA4 simulation forced with ERAINT and observations (columns 2 and 4). Left: winter (December – February), right: summer (June – August).

2.1.2 Temperature

In Figure 4 and Figure 5 the difference between RCA4 temperature and observations is shown. In Sweden RCA4 is too cold in spring and summer; the largest difference is in summer where RCA4 is around 2 °C too cold on a monthly mean basis. In central and southern Europe the differences are smaller and less systematic. In these areas, the annual temperature range in RCA4 is larger than in the observations. RCA4 is too cold in winter and too warm in summer; the differences lies around -1 - +2 °C. The two observational data sets and ERAINT are relatively close to each other generally agreeing within 0.5°C apart for winter in Sweden where ERAINT is colder by up to 1°C. The good correspondence between the datasets lends stronger confidence in quantifying RCA4 biases.
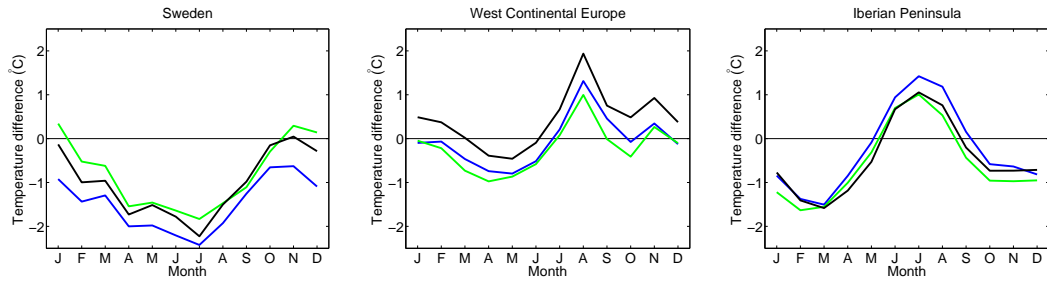

Figure 4. Annual cycles of temperature differences (°C) between RCA4 and observations (RCA4-OBS) for CRU (green) and WILLMOTT (black). For comparison we also show the difference to ERAI reference data (blue). Panels show Sweden (left), West Continental Europe (middle) and the Iberian Peninsula (right).
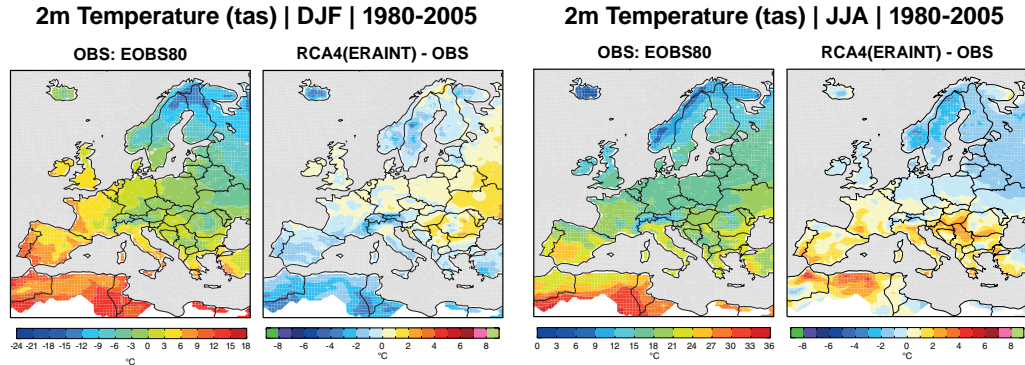

Figure 5. Observed (E-OBS 8.0) temperature (°C) in the recent past climate 1980-2005 (columns 1 and 3) and the difference between a RCA4 simulation forced with ERAINT and observations (columns 2 and 4). Left: winter (December – February), right: summer (June – August).

2.1.3 Precipitation

Figure 6 shows precipitation in RCA4 and four different observational datasets. In general the seasonal cycles are replicated in a good way with maxima and minima in the right months. However, the amount of precipitation is not always in accordance with the observations. In Sweden RCA4 overestimates precipitation with 10-50% in all four seasons. In West Central Europe and the Iberian Peninsula the differences are smaller, but RCA4 has a tendency to underestimate precipitation; in summer in West Continental Europe and generally over the Iberian Peninsula. Compared to E-OBS winter precipitation is higher in RCA4 in most of the domain (Figure 7). The differences are biggest in mountainous areas and parts of eastern Europe. In the mountainous areas this

could be a result of differences in resolution and hence topography. Precipitation is know to be better reproduced in higher resolution RCMs (e.g. Rauscher et al. 2010; Kendon et al., 2012; Ban et al., 2014). However, it is not just a displacement of the precipitation; the total amount of precipitation that falls in the domain is about 16% higher in RCA4 than in E-OBS (ranging from 5-15% in summer and autumn to 30-40% higher in spring). Part of the differences may also be attributed to undercatch of precipitation that can be relatively large, especially in winter and/or at high altitudes (Rubel and Hantel, 2001). We also note that the deviations between model and E-OBS are emphasized in some areas that to a relatively large degree coincides with country borders (e.g. Poland, Romania). This indicates that there may be differences between different countries in sampling and/or treatment of precipitation data and as discussed by Christensen et al. (2010) this is an area where RCMs can be used to identify such problems.

In summer precipitation in RCA4 is higher than in E-OBS in the mountain ranges, but lower in the surrounding areas (Figure 7). Apart from this systematic feature of RCA4 precipitation is generally overestimated with respect to E-OBS in northern Europe and underestimated in the south.
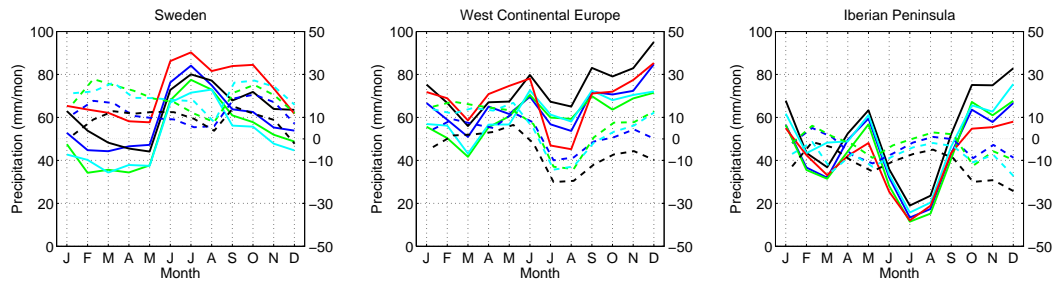

Figure 6. Annual cycles of precipitation (mm/month) in RCA4 (red), ERAINT (blue), CRU (green), GPCP (black) and WILLMOTT (cyan); Sweden (left), West Continental Europe (middle) and the Iberian Peninsula (right). Differences RCA4 – observation/reanalysis are represented by dashed lines on the right hand y-axis.
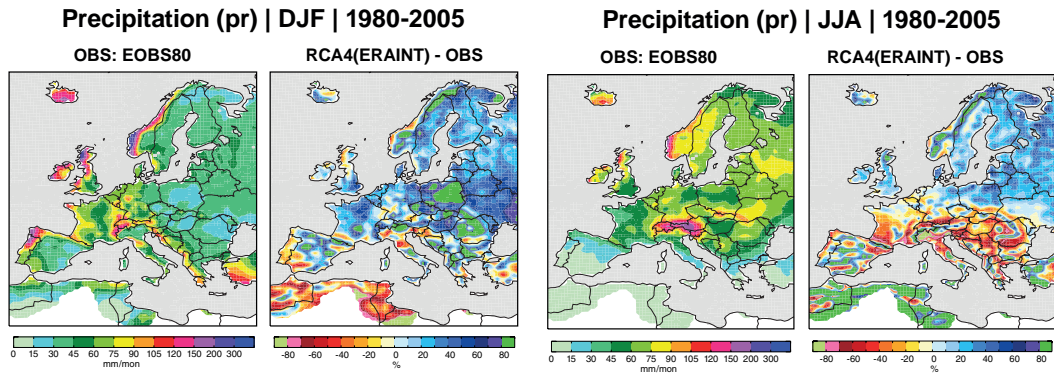

Figure 7. Observed (E-OBS 8.0) precipitation (mm/mon) in the recent past climate 1980-2005 (columns 1 and 3) and the difference (%) between a RCA4 simulation forced with ERAINT and observations (columns 2 and 4). Left: winter (December – February), right: summer (June – August).

2.1.4   Cloud cover

In general simulated total cloud cover in RCA4 is close to the ERAINT cloud cover, albeit with some notable differences. Compared to ERAINT RCA4 overestimates the cloud cover in spring and summer in Sweden, and to some extent in West Continental Europe. This is the case also for late summer and autumn in the Iberian Peninsula (Figure 8). These over estimations are about 5-10% on a monthly mean basis. We note also that there are some relatively large differences between the observational estimates and that RCA4 mostly lies between ERAINT and the ISCCP estimate. For Sweden the agreement with ISCCP is very good in the summer half of the year while RCA4 underestimates cloud cover with respect to ISCCP in the other two areas in most months.
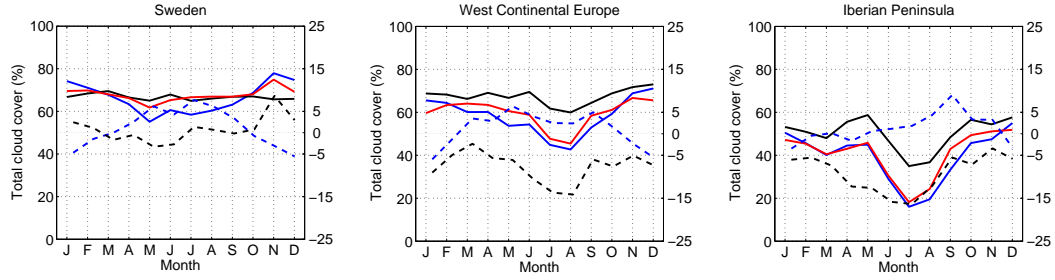

Figure 8. Annual cycles of total cloud cover (%) in RCA (red), ERAINT (blue) and ISCCP (black); Sweden (left), West Continental Europe (middle) and the Iberian Peninsula (right). Differences RCA4 – observation/reanalysis are represented by dashed lines on the right hand y-axis.

Figure 9. Annual cycles of incoming short wave radiation (top row, W/m^2) and incoming long wave radiation (bottom row, W/m^2) in RCA (red) and ERAINT (blue); Sweden (left), West Continental Europe (middle) and the Iberian Peninsula (right). Differences RCA4 – observation/reanalysis are represented by dashed lines on the right hand y-axis.
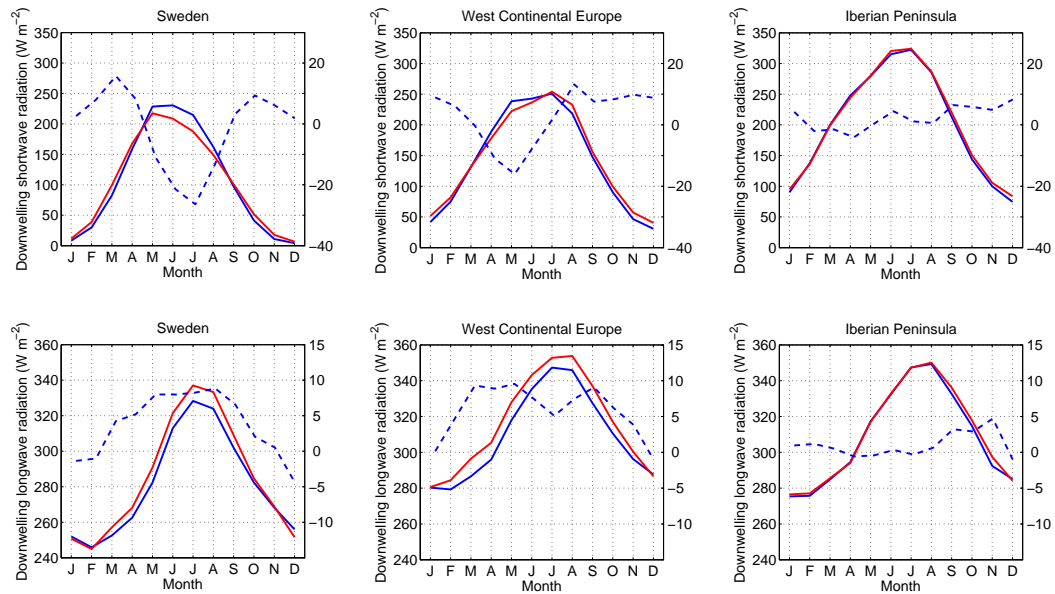
2.1.5   Radiation

Figure 9 shows incoming short wave and long wave radiation at the surface. The short wave radiation in RCA4 is similar to ERAINT over the Iberian Peninsula and West

11

Central Europe, but in Sweden there is a clear underestimation in RCA4 of the short wave radiation during the summer months. This correlates well to differences in cloud cover.

RCA4 gives more incoming long wave radiation than ERAINT for most of the year in Sweden and West Central Europe, while it is similar to ERAINT over the Iberian Peninsula. This extra radiation almost compensates for the shortage of short wave radiation in summer over Sweden; the sum of incoming radiation is 35 W/m^2 ($\approx$ 2% of the total summer insolation) lower in RCA4 than in ERAINT. This net shortage of incoming radiation could not explain the cold bias in summer temperatures over Sweden in RCA4.

2.1.6   Snow cover

The snow season in Sweden is similar in RCA4 and ERAINT. RCA4 gives a later onset of the snow season and less snow in winter. In spring complete removal of the snow cover occurs one month later than in the reanalysis (Figure 10). Even if RCA4 give less snow than ERAINT it is still well above the GLOBSNOW estimate. Observations of the length of the snow season in Sweden give similar results as GLOBSNOW in Figure 10 (Wern, 2015). The overestimation of snow in RCA4 could explain the cold bias in winter.
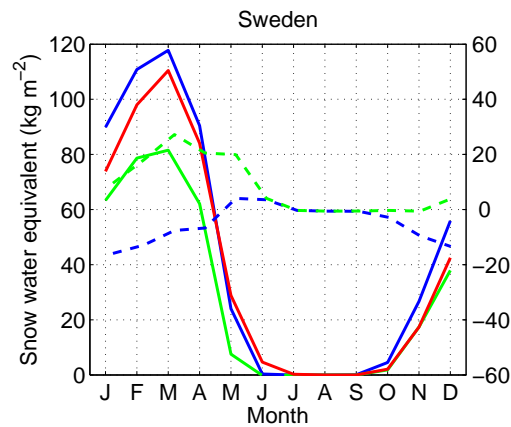

Figure 10. Seasonal cycle of snow water equivalent (kg/m^2) in RCA (red), ERAINT (blue) and GLOBSNOW (green) for Sweden. Differences RCA4 – observation/reanalysis are represented by dashed lines on the right hand y-axis.

2.2   Recent past climate in the RCA4 GCM-driven runs

The simulated climate is compared with E-OBS observational data and ERAINT. We choose to focus on annual mean, winter (December – February, DJF) and summer (June – August, JJA) changes in temperature, precipitation and wind speed. Results are shown as ensemble-averages with a measure of the spread between individual models. Results for individual runs are given in the appendix.

2.2.1   Sea level pressure

In winter the sea level pressure field is dominated by low pressure west of Iceland and high pressure in Portugal and Spain (Figure 11). The models are capturing the overall pressure pattern rather well. The depth of the Icelandic Low is overestimated in some models, underestimated in others and more or less correctly captured in a few, resulting in an ensemble mean in relatively close agreement to ERAINT. However, most models place it too far south (Appendix Figure A1). At the same time most simulations gives too high sea level pressure in the southwest leading to a too strong meridional pressure gradient over the North Atlantic. The resulting bias pattern shows a strong low pressure
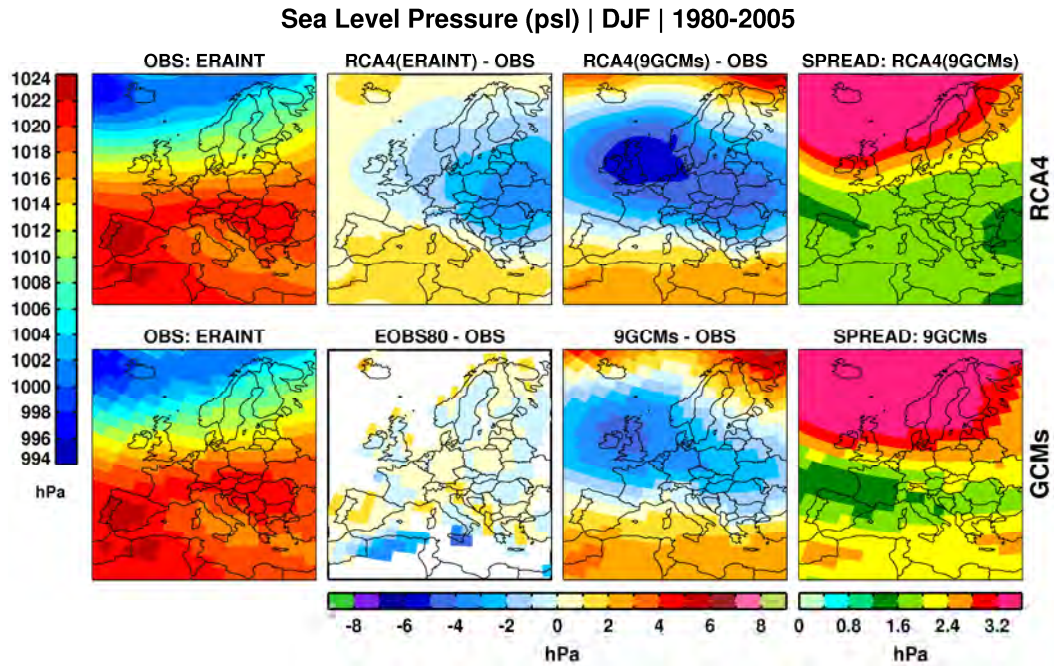
12

Sea Level Pressure (psl) | DJF | 1980-2005

Figure 11. Reanalysed (ERAINT) winter (December – February) sea level pressure (hPa) in the recent past climate 1980-2005 (left). The three other columns show difference between a model simulation forced with ERAINT and observations (second from left), difference between the mean of the 9 ensemble members and observations (third from left) and the spread between the individual model simulations in the ensemble (rightmost). The upper row shows conditions in RCA4 and the lower the corresponding fields taken directly from the underlying GCMs.

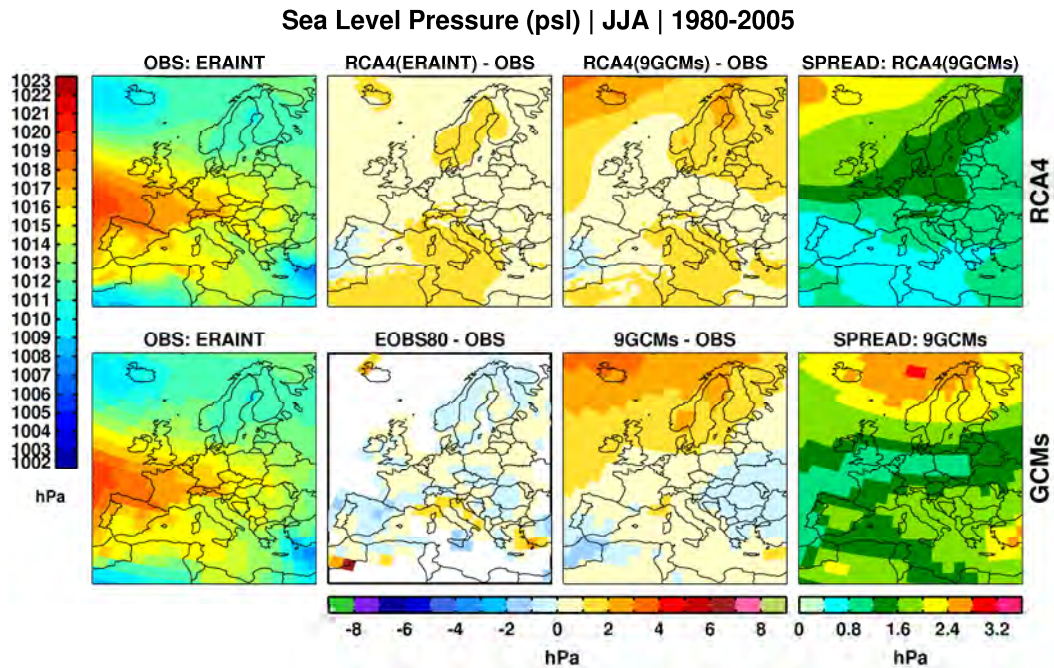**Sea Level Pressure (psl) | JJA | 1980-2005**

Figure 12. Same as Figure 11, but for summer (June – August).

anomaly centred in the area surrounding the British Isles (Figure 11). As a consequence the transport of mild and moist air from the Atlantic becomes too strong south of the British Isles and too weak north of them. The pressure pattern in RCA4 is inherited from the GCMs; we can see that apart from the resolution there are only small differences in mean sea level pressure between the ensemble of 9 RCA4 simulations and the ensemble of 9 GCMs, although the spread between models is reduced in the RCA4 ensemble in southern Europe. That the pressure pattern is inherited from the GCMs is a well know fact (e.g. Jacob et al., 2007; Rummukainen, 2010; Kjellström et al., 2011).

In summer, the meridional pressure gradient is weaker and the Azores high is moved northwards (Figure 12 and Figure A2). The models capture the overall pressure pattern, but the exact locations and strengths of the high and low pressures vary among the models. On average the sea level pressure is too high in the extreme north indicative of a somewhat too weak cyclone activity in this area. Again, the pressure pattern in RCA4 is to a large degree inherited from the GCMs. In the Mediterranean area a positive anomaly shows up in RCA4 that is not present in the GCMs but also in the RCA4 ERAINT-driven run. This indicates a systematic bias in RCA4; possibly as an effect of the formulation of lateral boundaries.

2.2.2 Temperature

The winter temperature is underestimated in the RCA4 simulations in northern and south-western Europe, and overestimated in south-eastern Europe (Figure 13). This bias pattern is similar to the one in RCA4-ERAINT (cf. section 2.1.2) and may therefore reflect the bias of RCA4. However, the amplitudes are larger with a stronger warm bias in the southeast and a stronger cold bias in the north. A part of this is related to the biases in large-scale circulation in the forcing GCMs as discussed above (cf. section 2.2.1) and is also clearly indicated by the bias pattern in the GCM ensemble mean (Figure 13). In northern Europe the individual RCA4 simulations span between being warmer than observations and being much colder while in the south-east most simulations are too warm (see Appendix Figure A3). It is interesting to note that the spread between the simulations in RCA4 is large in northern Europe and small in southern Europe, while the spread between the GCM simulations is on a similar level across the whole domain, with a minimum over parts of western Europe. The large spread in northern Europe in RCA4 could be an amplification caused by differences in snow cover. Similarly, the large spread between GCMs in the north may be a result of differences in snow cover. At the same time, however, there is also a large spread in southeastern Europe for which we do not know the reason.

Summer temperature is underestimated in the RCA4 simulations in practically all of Europe (Figure 14 and Figure A4). This could to some extent be a result of the large precipitation amounts in the simulations, which would have a cooling effect, but when looking at the individual simulations there is no clear correlation between low (high) summer temperature and high (low) spring or summer precipitation anywhere in Europe (not shown). The simulated temperatures in the GCMs and RCA4 are very different. While the RCA4 simulations are colder than observations, the GCM simulations are warmer than observations in large parts of central and eastern Europe and only slightly colder in the rest of Europe. It is clear that the low summer temperature is a feature produced by RCA4. Another striking feature seen in Figure 14 is the strong reduction in spread in summer temperature in RCA4 compared to the spread in the GCMs. As for the summer precipitation, the summer temperature is less influenced by large scale circulation; hence RCA4 is allowed to become more independent of the GCM forcing.
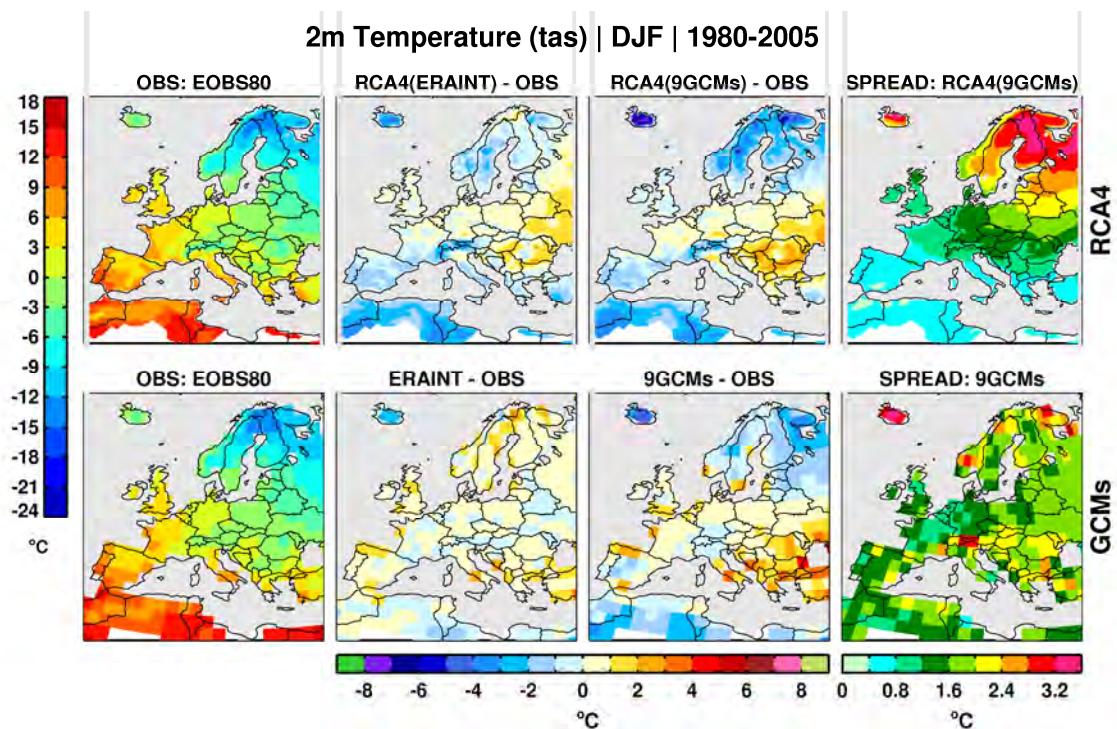
2m Temperature (tas) | DJF | 1980-2005

Figure 13. Observed (E-OBS 8.0) winter (December – February) temperature (°C) in the recent past climate 1980-2005 (left). The three other columns show difference between a model simulation forced with ERAINT and observations (second from left), difference between the mean of the 9 ensemble members and observations (third from left) and the spread between the individual model simulations in the ensemble (rightmost). The upper row shows conditions in RCA4 and the lower the corresponding fields taken directly from the underlying GCMs.

2m Temperature (tas) | JJA | 1980-2005

Figure 14. Same as Figure 13, but for summer (June – August).

15

Figure 15. Observed (E-OBS 8.0) winter (December – February) precipitation (mm/mon) in the recent past climate 1980-2005 (left). The three other columns show difference (%) between a model simulation forced with ERAINT and observations (second from left), difference (%) between the mean of the 9 ensemble members and observations (third from left) and the spread (mm/mon) between the individual model simulations in the ensemble (rightmost). The upper row shows conditions in RCA4 and the lower the corresponding fields taken directly from the underlying GCMs.
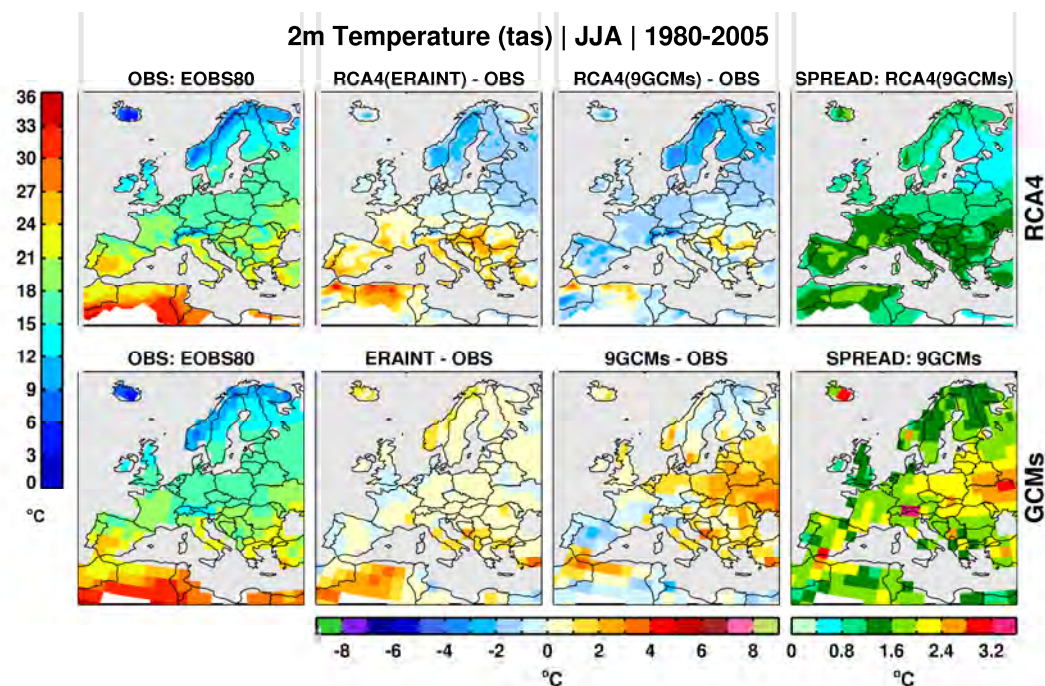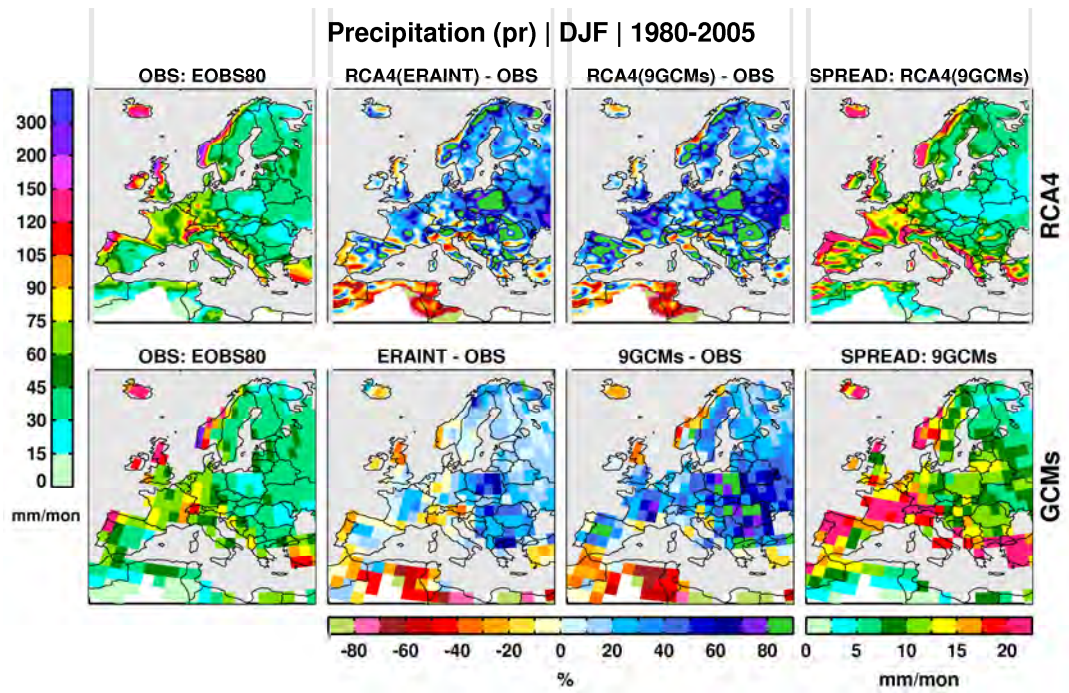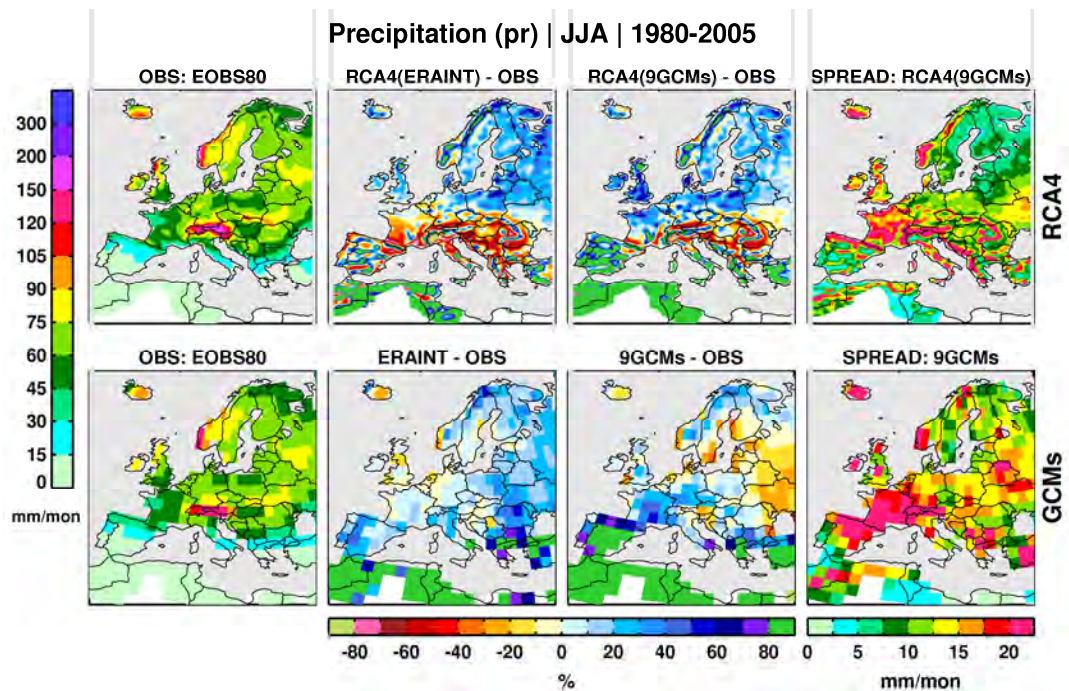

Figure 16. Same as Figure 15, but for summer (June – August).

16

2.2.3   Precipitation

In winter, RCA4 overestimates the precipitation amounts in all simulations, in some regions with as much as 100% (Figure 15 and Figure A5). This is more than in the ERAINT-driven RCA4 simulations, and is, in central and southern Europe, a consequence of the too zonal pressure pattern in the GCMs (cf. Figure 11). At the same time precipitation is underestimated in northern Britain and along the Norwegian west coast. This is possibly an effect of the resolution of the topography in RCA4. The coastline in RCA4 is not as steep as in reality, and the precipitation falls farther in over land (where RCA4 instead overestimates precipitation). The overall precipitation distribution is similar in the GCM and RCA4 simulations. This supports the fact that the precipitation anomalies are large scale features caused by biases in the GCMs including differences in pressure, but the RCA4 simulations offer a more detailed distribution of precipitation than the GCMs, especially in regions with complex topography such as mountainous regions and along coastlines. The spread between simulations are generally smaller in the RCA4 ensemble than in the GCM ensemble. There are however areas where the opposite is true and the spread between RCA4 simulations are larger than in the GCMs. This includes some high-altitude areas like the Pyrenees where differences are reinforced by the fine-scale more steep orography in RCA4.

Summer precipitation is less dominated by large scale circulation and more dependent on topography and local/regional scale convection. Therefore RCA4 is able to produce its own precipitation climate more independent of the GCM simulations and consequently the bias pattern resembles that in the ERAINT-driven simulation. However, the GCM-driven simulations tend to show higher precipitation in large parts of southern and central Europe than in the ERAINT-driven simulation (Figure 16 and Figure A6). This is consistent with the differences between the GCMs themselves and ERAINT. In Eastern Europe and parts of Russia summertime precipitation is lower in the GCMs than in ERAINT. This is also reflected in the RCA4 GCM-driven simulations that show somewhat reduced wet bias compared to the ERAINT-driven simulation. As for winter precipitation the RCA4 simulations generally give less spread compared to the underlying GCMs.

2.3   Summary of simulated recent past climate

Perfect boundary experiments with RCMs (see chapter **Fel! Hittar inte referenskälla.**) enables validation with reduced systematic bias in the large-scale forcing. Biases with respect to observations in such experiments are, in practice, RCM induced. The validation is limited by availability of suitable observations. Preferably, RCMs should be validated in terms of physical processes, such as budgets and fluxes, of which observations are limited (Rummukainen, 2010). Nevertheless, model evaluation should also be performed with focus on usability; a physically correct model that produces erroneous results may not be useful. In spite of the induced biases in the RCM simulations there is added value in the RCMs compared to the GCMs (Kjellström & Giorgi, 2010). As seen above different observations and reanalyses give different estimates of the past climate; every model validation must be done with this uncertainty in mind.

There are clear biases in RCA4 forced by ERAINT that can not be explained by uncertainties in observations; these are described above. Some biases can not be easily explained and the reduction of them is a constantly ongoing theme in model development. Biases in the GCM-driven RCA4-simulations can to some extent be attributed to the driving GCMs as shown above. Based on the RCA4 validations in this chapter we conclude that the biases in RCA4 compares with biases in other state-of-the-art RCMs for both perfect boundary and GCM-driven simulations (e.g. Jacob et al., 2007; Christensen et al., 2010; Wibig et al., 2015).

3 Results – future climate scenarios

This section concentrates on changes in climate in the end of the century (2071-2100) according to scenario RCP 8.5. Changes until then are gradual, but not linear. The choice of RCP 8.5 gives a distinct climate change signal which makes it suitable for studying interactions between changes in radiative forcing and changes in climate. Other scenarios (RCP 2.6, RCP 4.5) would give smaller changes, which are in line with what is presented here. Results for RCP 4.5 are show in Appendix.

3.1 Changes in seasonal mean conditions in the RCA4 CORDEX-ensemble
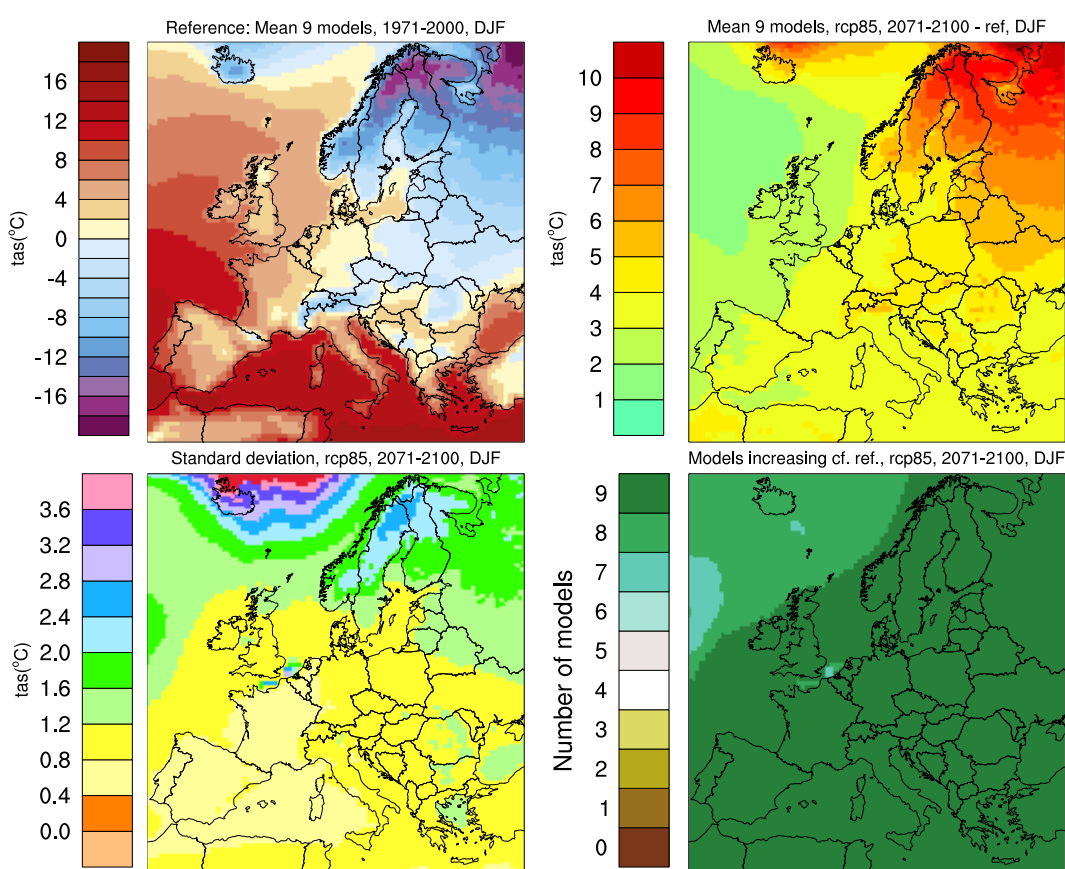
3.1.1 Temperature

Figure 17. Ensemble mean winter (December – February) temperature (°C) in the control period 1971-2000 (upper left). Change in ensemble mean (°C) for 2071-2100 compared with 1971-2000 (upper right). Standard deviation (°C) for members of the ensemble for the period 2071-2100 (lower left). Number of climate scenarios in the ensemble that show an increase for the period 2071-2100 compared to the control period 1971-2000 (lower right). All according to the RCP 8.5 scenario.

Figure 18. Ensemble mean summer (June – August) temperature (˚C) in the control period 1971-2000 (upper left). Change in ensemble mean (°C) for 2071-2100 compared with 1971-2000 (upper right). Standard deviation (°C) for members of the ensemble for the period 2071-2100 (lower left). Number of climate scenarios in the ensemble that show an increase for the period 2071-2100 compared to the control period 1971-2000 (lower right). All according to the RCP 8.5 scenario.
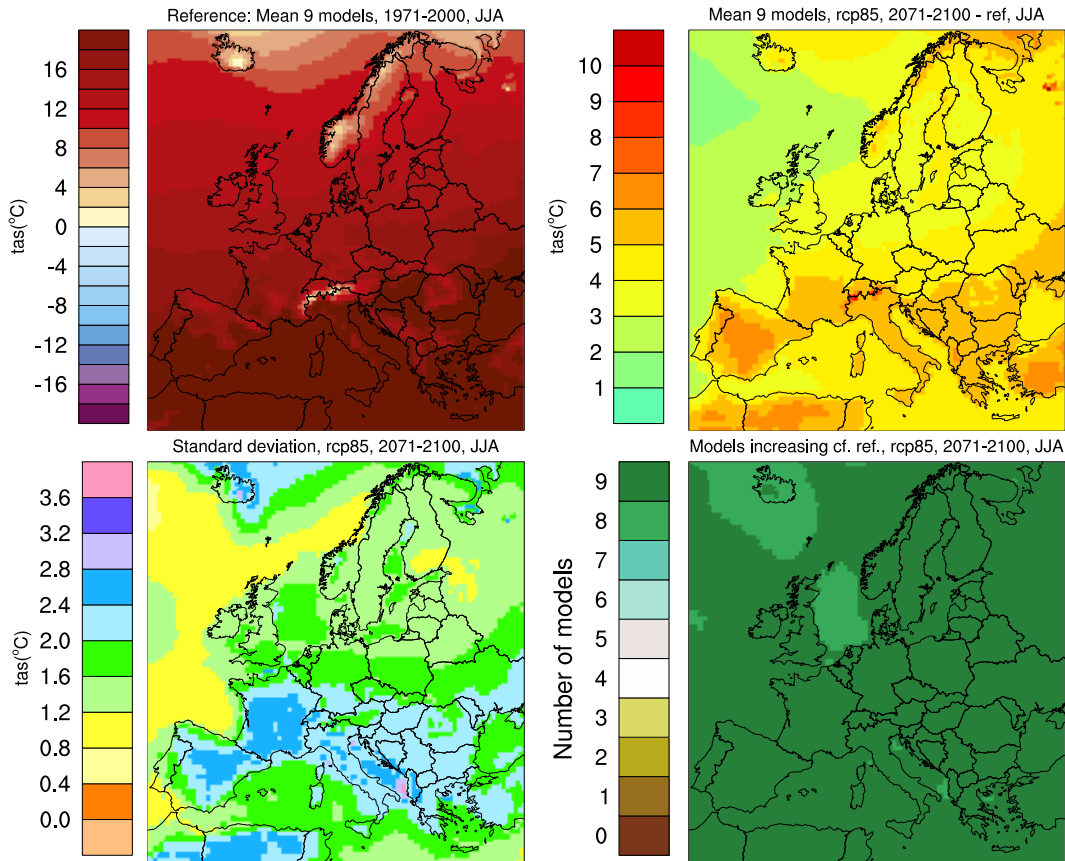
The geographic patterns of temperature changes in RCA4 shown in Figure 17 and Figure 18 are very close to those found in earlier RCM modelling experiments (e.g. Christensen et al., 2007; Kjellström et al., 2011). The largest temperature signals are seen in the northern and north-eastern parts of the continent during winter (Figure 17). Northern Europe is projected to be up to 10 °C warmer and southern Europe 2-4 °C in the end of the century in the scenario RCP 8.5 showed in Figure 17. In RCP 4.5 (Figure A8) and RCP 2.6 the changes are weaker. In summer the signal is more or less reversed with the largest warming in southern and south-eastern Europe (4-6 °C in RCP 8.5) and less warming in the northern parts (2-4 °C) as seen in Figure 18. These strong changes are connected to positive feedbacks involving retreating snow and sea-ice during winter (and in the far north also in summer) and reduced soil moisture during summer. In contrast, the weakest signal is found over the North Atlantic, south of Iceland, in all seasons. In this area the relatively slow warming of the ocean dampens the temperature increase in the lower atmosphere. Notably, the climate change signal for temperature is very robust as all model simulations show increasing temperatures in the entire model domain. It is only in a small area south of Iceland where some model(s) does not show increasing temperatures. However, the amplitude of the response in the model simulations varies widely over the ensemble, particularly in the north and northeast as reflected by the large standard deviation between the simulations. This is caused by substantial differences in how GCMs project changes in sea-ice concentration and sea-surface temperature. Also in southern Europe there are large differences in response in temperature between the GCMs. This is probably related to changes in soil moisture and its feedback on the lower

atmosphere (e.g. Rowell and Jones, 2006; Fischer and Schär, 2009). See also Figure A7 in Appendix.

The seasonal maximum of the highest daily temperature is projected to change in a similar way as the summer mean temperature. The change is largest where the temperatures are the highest, i.e. in southern Europe summer; here the highest daily temperature is projected to be 4-6 °C warmer by the end of the century (Figure A10). Correspondingly, the lowest daily temperature is projected to change most where the temperatures are the lowest, i.e. northern Europe winter. The temperature change is much larger than for the mean temperature, however; more than 10 °C in large parts of northern Europe by the end of the century (Figure A9). With the large amplitude in change there is also a large spread between the ensemble members (Figure A9). Interestingly the spread is larger in the RCP 4.5 scenario compared to the RCP 8.5 scenario. An interpretation of this could be that in the warmer RCP 8.5 scenario snow in winter is much reduced in all models leading to a more uniform temperature increase. In the more moderate RCP 4.5 scenario some models give large changes in snow and thereby in temperature while in others there is still snow.

The number of days per year with zero-crossings (maximum temperature above zero, minimum temperature below zero) is expected to decrease with around 10-30 days across Europe (Figure 19A). When the temperature rises there will be less days with temperatures below zero. The change is complex, however. In northern Scandinavia and the Alps the number of days with zero-crossings is expected to increase with around 10 days in winter (Figure 19B). In these regions the winters are cold and only few days have zero-crossings in the present climate. When the temperature is rising the winter temperature is reaching zero and more days with zero-crossings are possible. The change in days with zero-crossing is therefore highly dependent on which region and which season that is of interest.

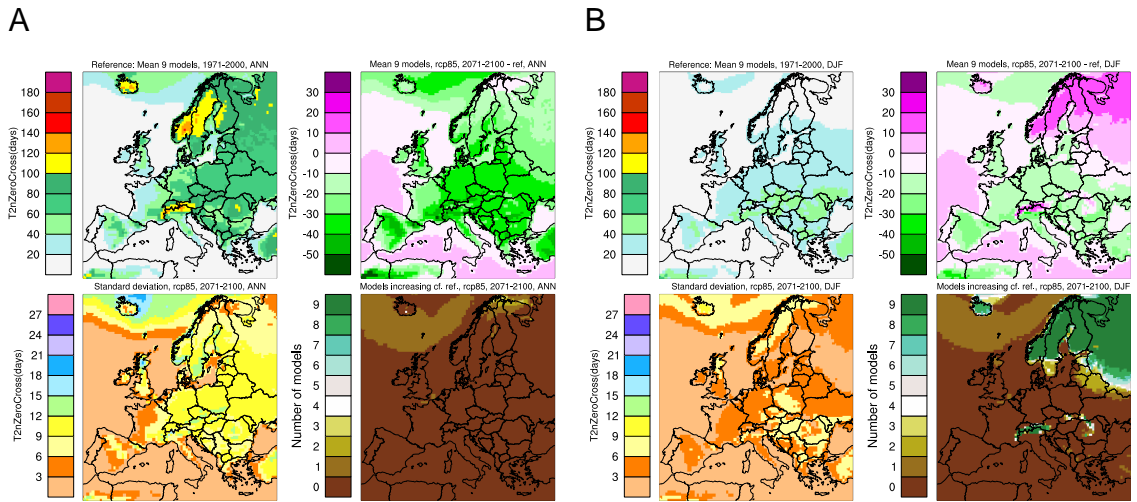A   B

Figure 19. A: Ensemble mean annual number of days with zero-crossings (days) in the control period 1971-2000 (upper left). Change in ensemble mean (days) for 2071-2100 compared with 1971-2000 (upper right). Standard deviation (days) for members of the ensemble for the period 2071-2100 (lower left). Number of climate scenarios in the ensemble that show an increase for the period 2071-2100 compared to the control period 1971-2000 (lower right). All according to the RCP 8.5 scenario. B: Same as A, but for winter (December – February) mean.

The vegetation period defined as days with mean temperature above 5 °C (after the exclusion of single warm days in the beginning and end of the year) is expected to become longer in all of Europe, except in areas where the vegetation period already covers the whole year (Figure 20). The change is largest in central and eastern Europe (1-

3 months longer depending on scenario) where the climate is warm but still have the potential for a longer vegetation period. In interior parts of Scandinavia and Finland changes are somewhat smaller indicating that even if the climate change signal is very large temperatures will still be below 5 °C for a substantial part of the year. Around the Mediterranean the change is small, since the vegetation period defined with the present temperature criteria already now covers most of the year. The changes in the length of the vegetation period include both an earlier start and a later end of the vegetation period. These changes are not symmetrical over the year, however. The beginning of the vegetation period is projected to change more than the end (Figure A11).
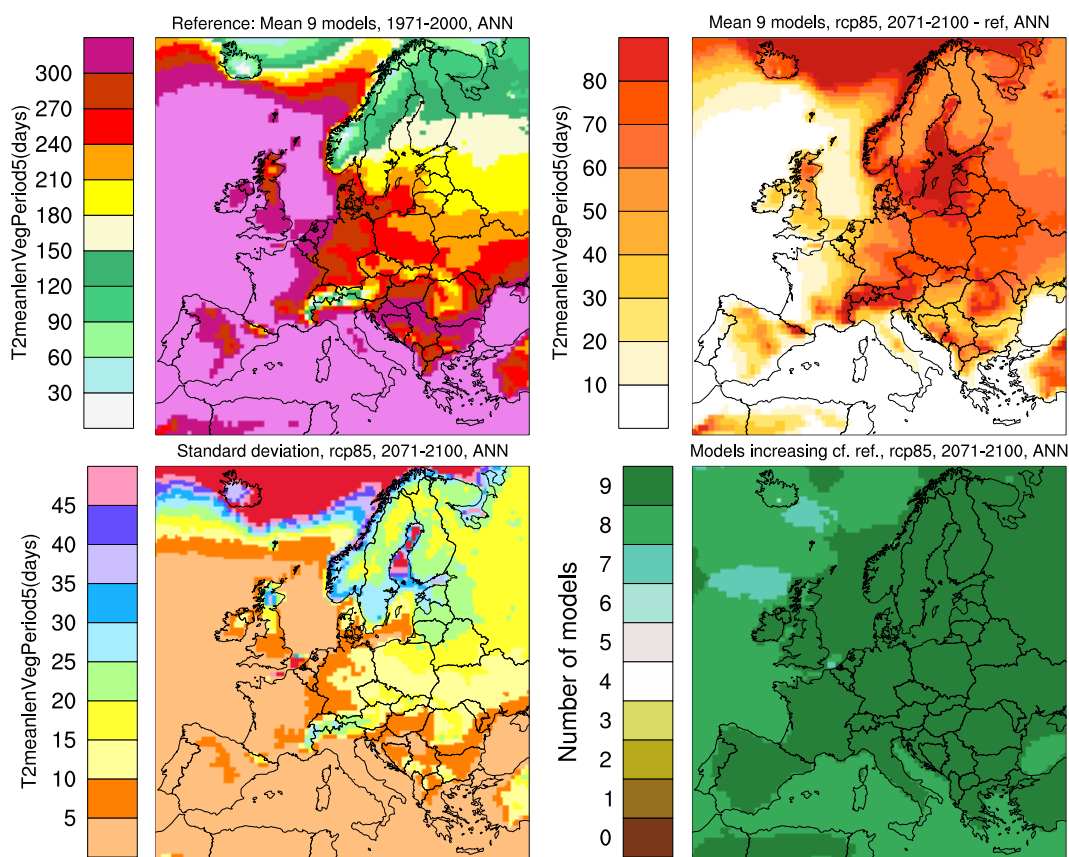

Figure 20. Ensemble mean annual length of the vegetation period (days) in the control period 1971-2000 (upper left). Change in ensemble mean (days) for 2071-2100 compared with 1971-2000 (upper right). Standard deviation (days) for members of the ensemble for the period 2071-2100 (lower left). Number of climate scenarios in the ensemble that show an increase for the period 2071-2100 compared to the control period 1971-2000 (lower right). All according to the RCP 8.5 scenario.

3.1.2 Precipitation

Precipitation changes follow what is expected from an intensification of the global hydrological cycle. This includes increasing precipitation in the north and decreasing in the south. According to scenario RCP 8.5, there is a pronounced shift from north to south between summer and winter of the borderline between areas receiving less and more precipitation in the future (Figure 21 and Figure 22). Taken as annual averages precipitation is projected to decrease with 10-20 % in the Mediterranean area and increase with 10-30 % in the Baltic Sea region, changes in between those areas are relatively small although individual simulations show increases or decreases of up to 10-20% also in these areas (Figure A12). Figure A12 shows that many models give relatively strong increases

in precipitation over the Baltic Sea. This is a feature previously noted in many RCM simulations that may be a result of the relatively crude description of the Baltic Sea in the underlying GCMs from which seas surface temperatures are taken (e.g. Kjellström and Ruosteenoja, 2007; van Haren et al., 2013) It is clear from the figures that the exact location of the borderline between increased and decreased precipitation differs between the simulations making this an area of high uncertainty (Figure 21, Figure 22 and Figure A13)
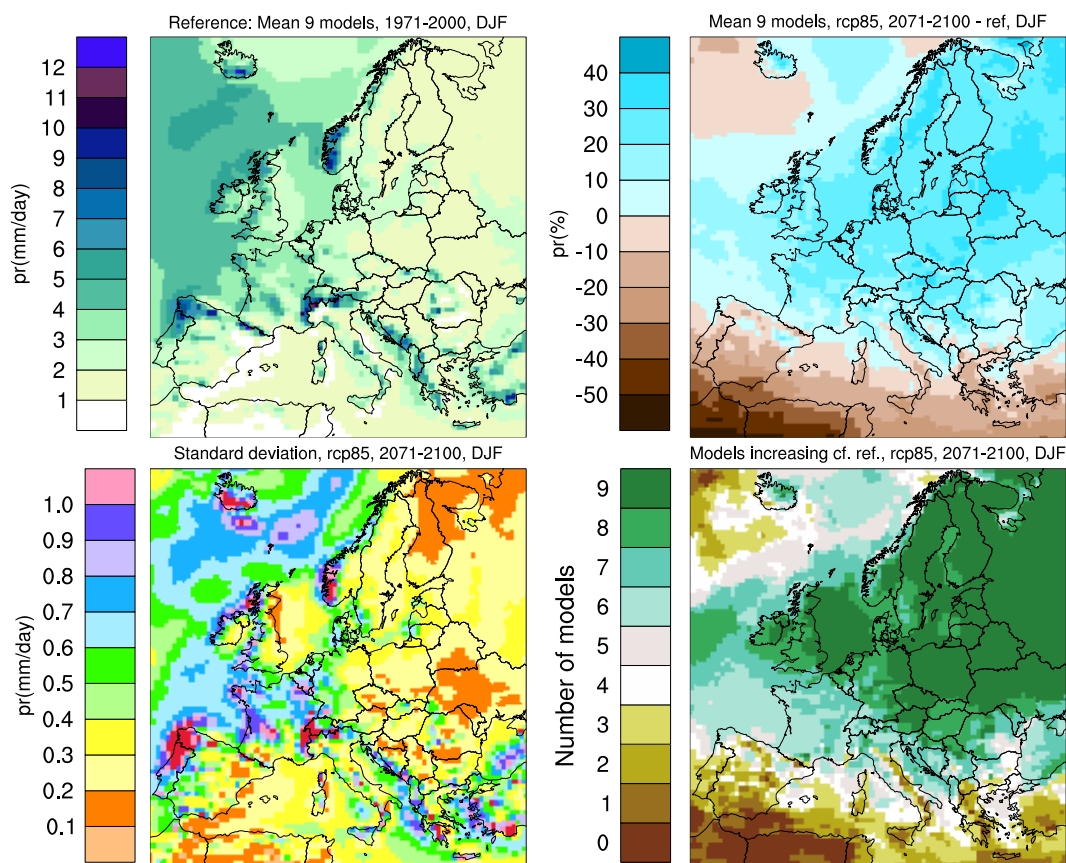

Figure 21. Ensemble mean winter (December – February) precipitation (mm/day) in the control period 1971-2000 (upper left). Change in ensemble mean (%) for 2071-2100 compared with 1971-2000 (upper right). Standard deviation (mm/day) for members of the ensemble for the period 2071-2100 (lower left). Number of climate scenarios in the ensemble that show an increase for the period 2071-2100 compared to the control period 1971-2000 (lower right). All according to the RCP 8.5 scenario.

Another sign of the intensified hydrological cycle is that the maximum daily precipitation increases in most of Europe, even in areas where the total precipitation decreases (Figure A14). The maximum daily precipitation increases everywhere but in Mediterranean summer; from 10-30 % more in Scandinavia to 0-20 % less around the Mediterranean. In a corresponding way the maximum precipitation amount in a seven day period increases also in areas with decreasing total precipitation (Figure A15). The number of days with heavy precipitation (more than 10 mm/day) increases when the total precipitation increases, and decreases when the total precipitation decreases (Figure A16). The longest dry period (consecutive days with precipitation less than 1 mm/day) will be 2-3 weeks longer around the Mediterranean and more or less unchanged in Scandinavia (Figure A17). This is a feedback from the deficit of soil moisture in southern Europe (e.g. Rowell and Jones, 2006; Fischer and Schär, 2009) (cf. Figure 7).

A very noticeable difference between the underlying GCMs and RCA4 is that RCA4 simulates more intense precipitation in mountainous regions. This is partly a result of the higher resolution and thereby higher mountains in the RCM that contributes to generate stronger vertical winds and more precipitation. This also leads to larger differences between the RCM ensemble members in some of the mountainous areas compared to those in the underlying models (e.g. part of southern Norway in Figure 15 and Figure 16).
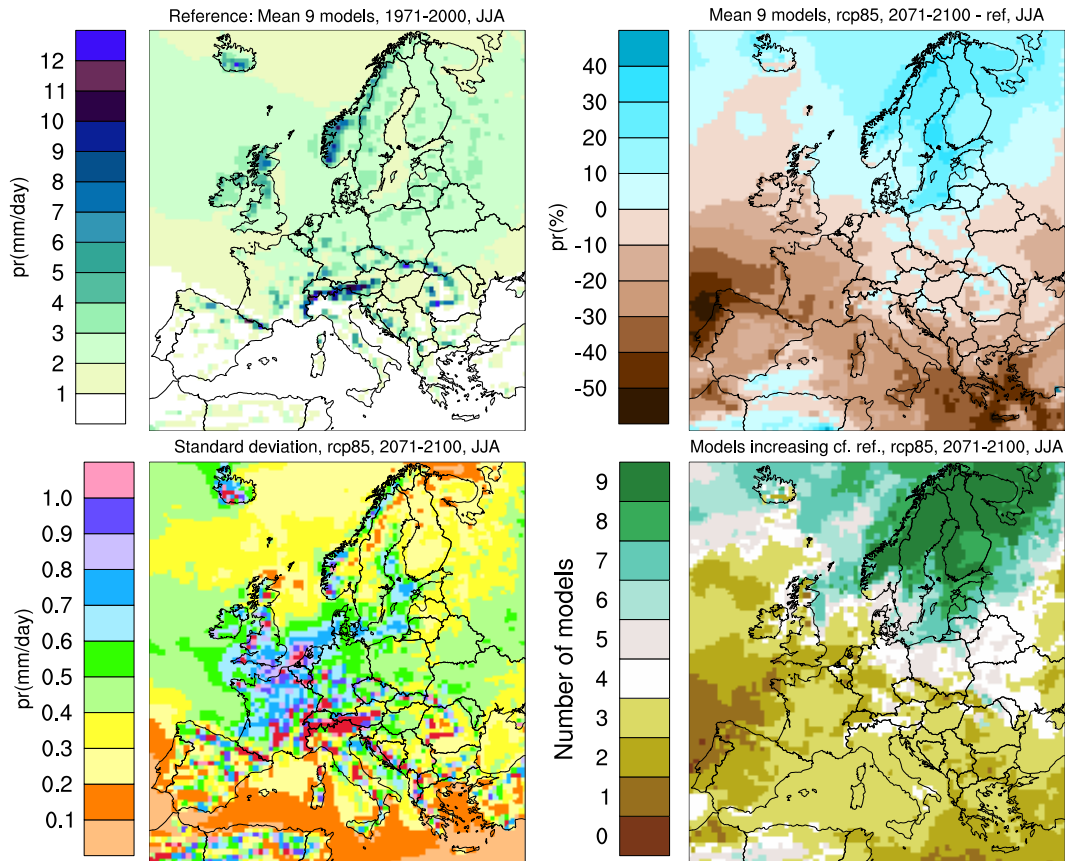

Figure 22. Ensemble mean summer (June – August) precipitation (mm/day) in the control period 1971-2000 (upper left). Change in ensemble mean (%) for 2071-2100 compared with 1971-2000 (upper right). Standard deviation (mm/day) for members of the ensemble for the period 2071-2100 (lower left). Number of climate scenarios in the ensemble that show an increase for the period 2071-2100 compared to the control period 1971-2000 (lower right). All according to the RCP 8.5 scenario.

Another feature of the RCA4 simulations is that they often tend to strengthen the response in precipitation compared to the underlying GCMs, at least in northern Europe. This is clearly seen in the scatter plot showing changes in both temperature and precipitation as averaged over the Baltic Sea (Figure 23). At this stage it is still unclear why the response is larger in RCA4 compared to the underlying GCMs but we note that there is also a wet bias in the model in the control period indicating that RCA4 is (possibly) too sensitive in this respect. A similar behaviour has been discussed by Boberg and Christensen (2012) for summertime temperatures in southern Europe where many models that tend to show warm biases in the extremes in today's climate show stronger climate change signals than other. Future studies including more RCMs can reveal if there is a similar amplification of the climate change signal here for models with large bias in the control period.

Another notable feature of Figure 23 is that the downscaling procedure can act to change the order between different climate scenarios. This can be illustrated by the Hadley Centre GCM, HadGEM-ES2 that only shows a very modest increase in precipitation over the Baltic Sea by the end of the century (red dot number 6 in Figure 23). In RCA4, however, the corresponding simulation shows a much larger response being among the "wetter" simulations. This example clearly shows that the regional model has an impact on the results, not just in terms of the absolute numbers but also in terms of the climate change signal. Figure 23 also illustrates that the spread in the climate change signal decreases somewhat in RCA4 compared to the underlying GCMs. Here, the change in precipitation is more correlated with the change in temperature in RCA4.

Even if there are notable differences between RCA4 and the underlying GCMs there are also common features. The most striking one is of course the difference in response with different forcing as illustrated by: i) the gradual change over time from near future (green) over the mid-century (blue) to the later parts of the century (red) and by ii) the difference between the different scenarios with the response being larger in the RCP 8.5 scenario compared to that in RCP 4.5. The latter is only valid from around the mid of the century and onwards, at earlier stages the difference in forcing is still relatively modest and the uncertainty in the climate change signal is not governed by the forcing as discussed previously by for instance Hawkins and Sutton (2009). Also noticeable is the increase in spread over time.
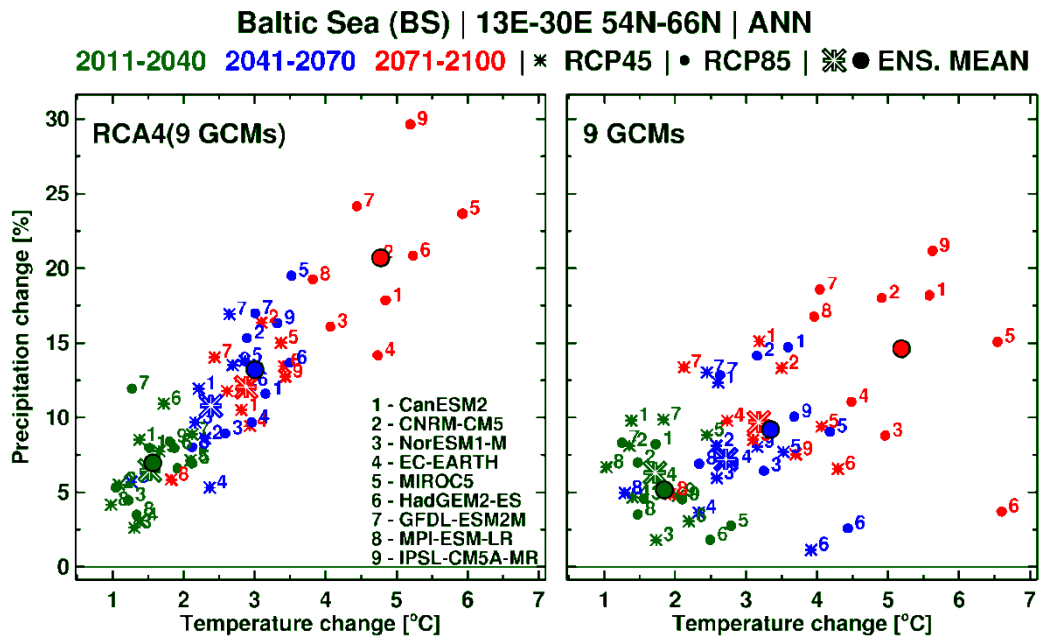

Figure 23. Simulated change in annual mean temperature and precipitation in RCA4 (left) and in the corresponding GCMs (right) in the Baltic Sea area. Results are shown for three time periods (green for 2011-2040, blue for 2041-2070, red for 2071-2100) and two emission scenarios (stars for RCP 4.5, circles for RCP 8.5) for all individual simulations as well as for the ensemble means (large symbols).

3.1.3   Wind

For mean wind there is a poor agreement among different simulations on the sign of the change in wind for large parts of the domain. There are tendencies for decreases in wind-speed in parts of the model domain both in winter and summer. Most notably, this occurs over parts of the North Atlantic and parts of the Mediterranean. Contrastingly, indications of locally higher wind speed are seen over parts of the ocean at the northernmost fringe of

the model domain in winter. Also the Baltic Sea is a region where mean wind speed tends to increase in many of the simulations both in winter and summer. This may be related to changes in stability as the sea and the lowermost atmosphere warms considerably in many of the scenarios (e.g. Figure 17 and Figure 18). The strong temperature increase over the Baltic Sea is partly due to removal of sea ice in the northern parts of the Sea in winter. In summer, the SST increase given by the GCMs is relatively high in the Baltic Sea yielding a local maximum in warming in this area. As an annual mean the wind is projected to change by less than ±1 m/s in all areas (Figure 24).
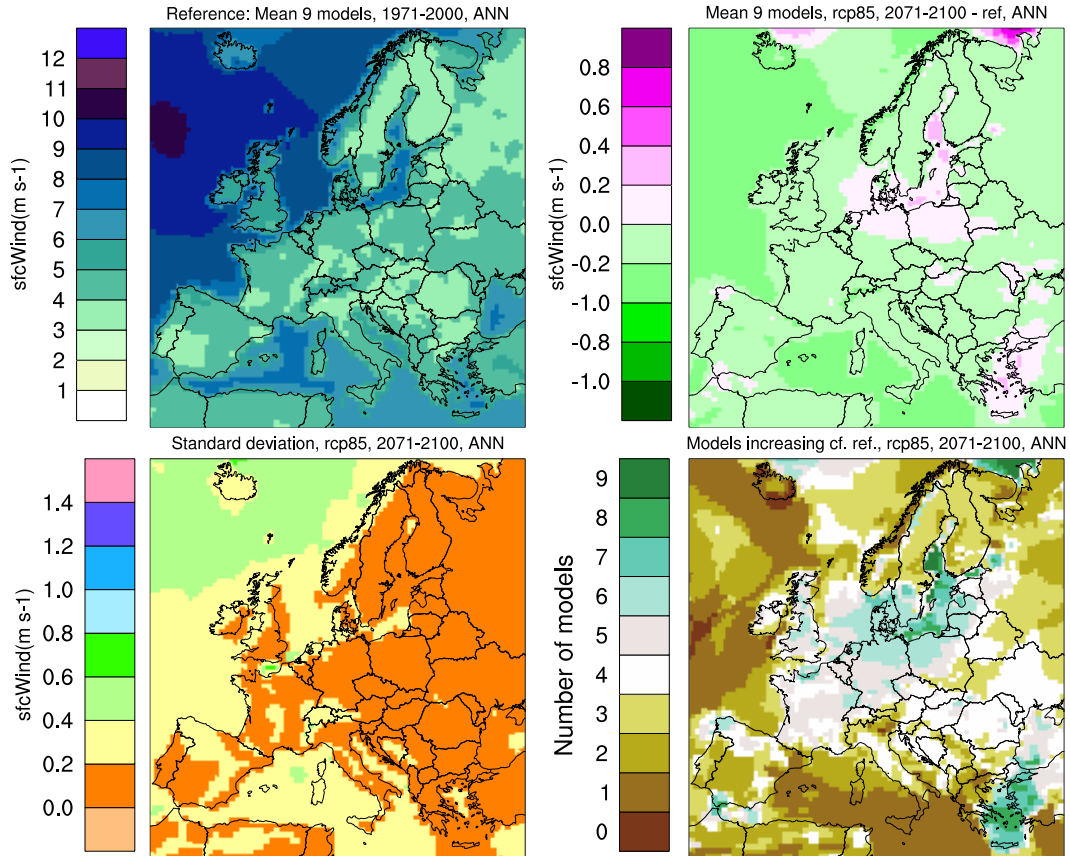

Figure 24. Ensemble mean annual surface wind (m/s) in the control period 1971-2000 (upper left). Change in ensemble mean (m/s) for 2071-2100 compared with 1971-2000 (upper right). Standard deviation (m/s) for members of the ensemble for the period 2071-2100 (lower left). Number of climate scenarios in the ensemble that show an increase for the period 2071-2100 compared to the control period 1971-2000 (lower right). All according to the RCP 8.5 scenario.

3.2   Changes in daily extremes in the RCA4 CORDEX-ensemble

In this section we show ensemble mean statistics for daily extremes in summer and winter temperature conditions and in annual daily maximum precipitation amounts and daily wind speed. The statistics have been calculated according to Nikulin et al. (2011). The statistical significance is determined by a bootstrapping technique where 500 bootstrap samples are used to estimate the inter-annual variability of seasonal and annual means. The analysis is done for 20-year return levels of the variables in question.

Figure 25 shows changes in cold extremes during winter. From the figure it is clear that the response is larger than in seasonal mean temperature (cf. Figure 17). The pattern of

change is fairly similar with the largest differences in northern and north-eastern parts of the domain but also in large parts of eastern Europe. The spread between the simulations are largest in eastern Europe and over the Baltic Sea and ocean areas in the northernmost part of the domain. The differences in the latter areas are connected to differences in SSTs and sea ice in the GCMs. Locally and regionally there can be large differences between the RCA4 ensemble and GCM ensemble (e.g. in Scandinavia).

20-yr ret. values of Daily Minimum Temperature (tasmin)
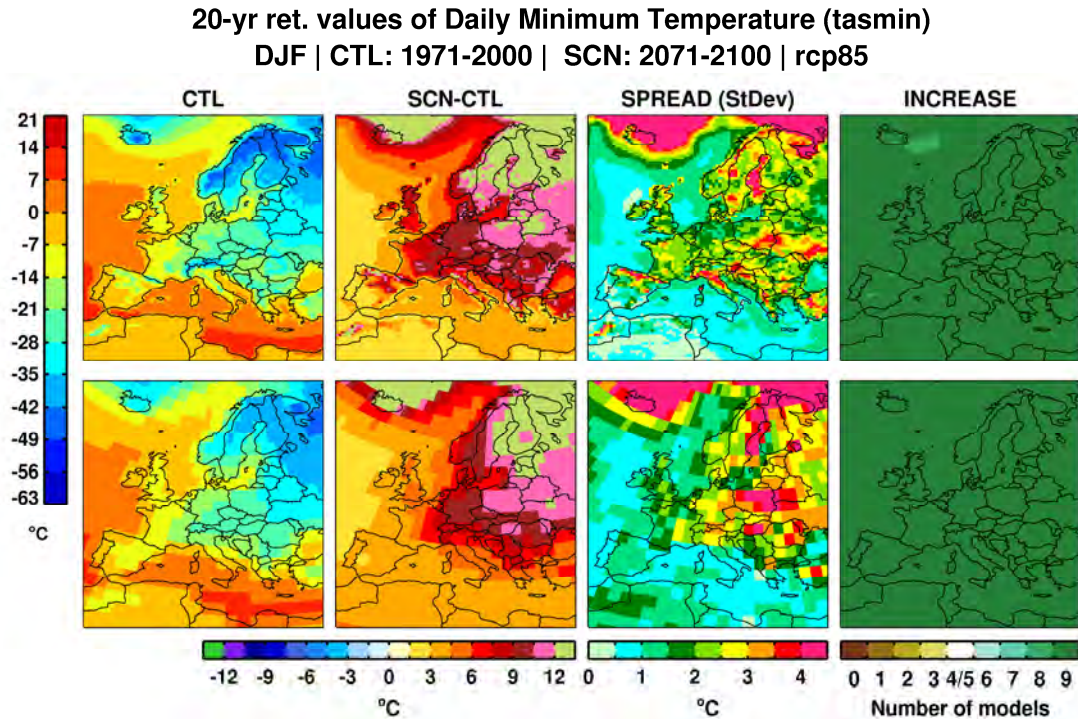**DJF | CTL: 1971-2000 | SCN: 2071-2100 | rcp85**

Figure 25. Ensemble mean winter (December – February) 20-year return values for daily minimum temperatures in the control period 1971-2000 (left). The three other columns show changes between the period 2071-2100 under the RCP 8.5 scenario as compared to the control period for the return levels (second from left), the standard deviation calculated from the nine ensemble members (third from left) and number of models that simulate an increase (rightmost). The upper row shows conditions in RCA4 and the lower the corresponding fields taken directly from the underlying GCMs.

Figure 26 shows changes in warm extremes during summer. For this time period and scenario the amplitude of these changes is 1-2 °C larger than the change in seasonal mean conditions (Figure 18). Towards the end of the century in the high end scenario (RCP 8.5) the changes in extremes are larger than the corresponding changes in seasonal mean conditions paralleling what is seen for wintertime cold extremes above. There are, however, individual models that show a weaker response and there are even models showing no change at all in parts of northern Scandinavia in the future (Figure 26). A notable difference between RCA4 and the GCMs is the weaker signal in RCA4 both in northern and southern Europe; it is only in a zone across northern central Europe that the signal is equally large. For northern Europe, we note that RCA4 is colder than the underlying GCMs in the control period while in the south it is the contrary. This cold bias is a known feature of RCA4 (cf. Figure 5).

20-yr ret. values of Daily Maximum Temperature (tasmax)
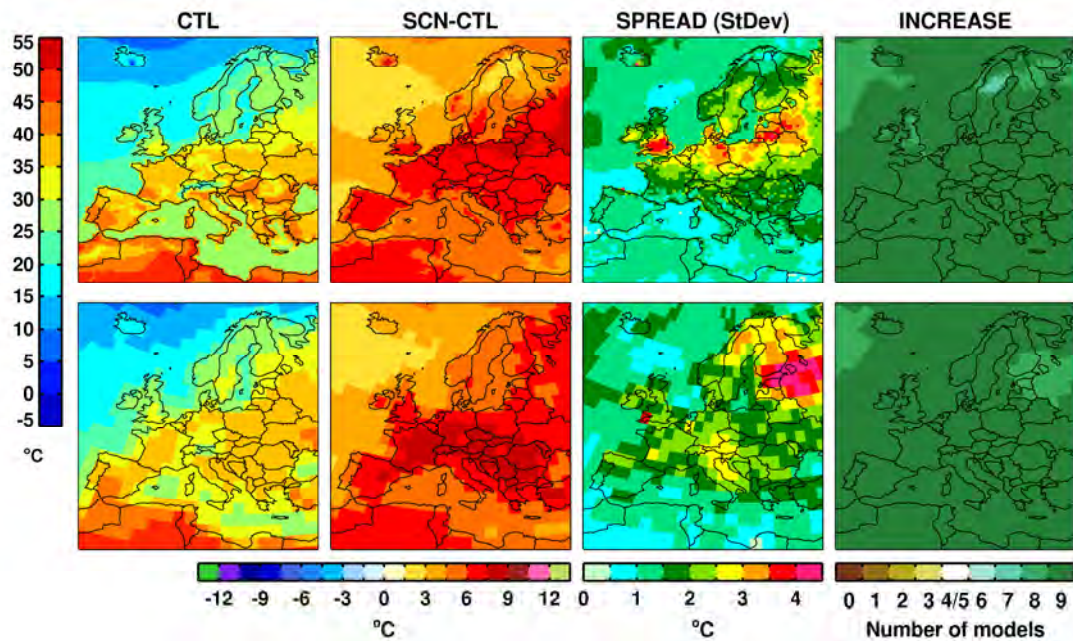**JJA | CTL: 1971-2000 | SCN: 2071-2100 | rcp85**

Figure 26. Ensemble mean summer (June – August) 20-year return values for daily maximum temperatures in the control period 1971-2000 (left). The three other columns show changes between the period 2071-2100 under the RCP 8.5 scenario as compared to the control period for the return levels (second from left), the standard deviation calculated from the nine ensemble members (third from left) and number of models that simulate an increase (rightmost). The upper row shows conditions in RCA4 and the lower the corresponding fields taken directly from the underlying GCMs.

Figure 27 shows changes in daily precipitation extremes. The climate change signal indicates heavier precipitation extremes in the future. This is true also for other time periods, scenarios and for different seasons. It is only in parts of southernmost Europe in summer when these extremes are not projected to increase in all models. These patterns of change are similar to what has been reported from many other studies over the years (e.g. Christensen and Christensen, 2003; Fischer et al., 2013; Sillmann et al., 2013). Another striking feature is the difference in precipitation amount in the control period as simulated by RCA4 and the underlying GCMs. This is one of the main benefits of running regional climate models that heavy precipitation is more intense and hence in better agreement to observations (e.g. Prein et al., 2015). We note, however, that it does not substantially change the overall pattern of change as projected by the GCMs.

Changes in wind speed extremes are relatively modest in the model. For annual daily maximum wind gust conditions there is a tendency for an increase in many models in an area in central western Europe (Figure 28) that grows with time and forcing. This feature is relatively robust as it is seen in many of the models. We did not have access to corresponding wind gusts from the GCMs so we can not deduce whether this is a RCM feature or not. Part of the area coincides with the area where there is an increase in annual mean wind speed (cf. Figure 24). Subsequent analysis comparing the RCA4 results to other RCMs is needed here.

20-yr ret. values of Daily Precipitation (pr)
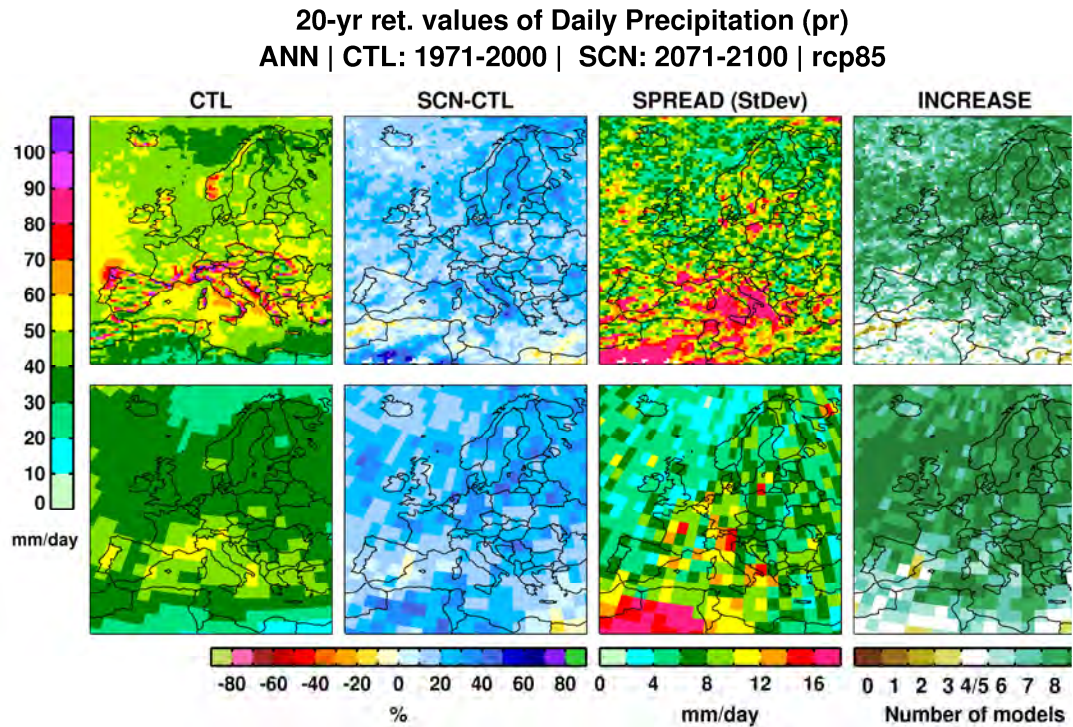**ANN | CTL: 1971-2000 | SCN: 2071-2100 | rcp85**

Figure 27. Ensemble mean 20-year return values for daily precipitation in the control period 1961-1990 (left). The three other columns show changes between the period 2071-2100 under the RCP 8.5 scenario as compared to the control period for the return levels (second from left), the standard deviation calculated from the nine ensemble members (third from left) and number of models that simulate an increase (rightmost). The upper row shows conditions in RCA4 and the lower the corresponding fields taken directly from the underlying GCMs.

20-yr ret. values of Daily Maximum Gust Wind (wsgsmax)
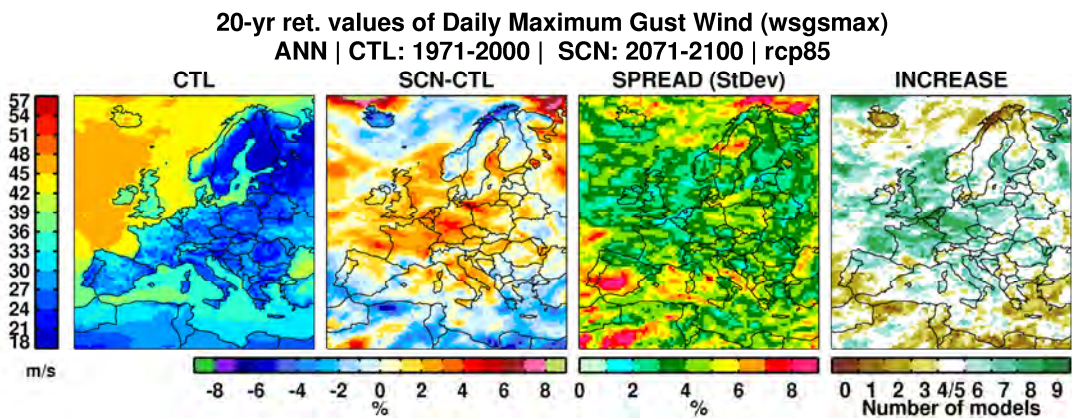**ANN | CTL: 1971-2000 | SCN: 2071-2100 | rcp85**

Figure 28. Ensemble mean 20-year return values for daily maximum wind gusts as simulated by RCA4 in the control period 1971-21000 (left). The three other columns show changes between the control period and a future period under the RCP 8.5 scenario as compared to the control period for the return levels (second from left), the standard deviation calculated from the nine ensemble members (third from left) and number of models that simulate an increase (rightmost).

4   Validation of the ensemble method

4.1   Climate sensitivity and ensemble representativity

Even if the ensemble of simulations with RCA4 driven by nine different GCMs under two different forcing scenarios clearly samples a substantial fraction of all available GCM scenarios in CMIP5 there is still a number of GCM simulations that are not downscaled by RCA4. A central question therefore relates to how different would the results be if a larger or different ensemble of GCMs where sampled? Another broader question is how representative are the CMIP5 GCMs of the total uncertainty in future climate change? In this respect we note that the climate sensitivity defined as the transient climate response (TCR) in the GCMs used here (Table 1) range from 1.3 to 2.5°C at the time of CO_2 doubling. This range compares well to the estimate put forward in the IPCC assessment of 1.0-2.5 °C (Collins et al., 2013). An initial conclusion is therefore that the GCMs used here are representative of the response in climate change as a result of increasing CO_2-concentrations in the atmosphere.

4.2   Sampling of GCMs

Next, we try to see to what degree results would differ given another subset of GCMs. To investigate this, the GCMs used in the ensemble presented in this report are compared with 25 other CMIP5 models. This is done for four regions. Since the resolution in the GCMs is coarse the detailed descriptions of the regions used to validate RCA4 (red regions in Figure 2) can not be used, instead for this section a more simplified description of the regions are used (blue boxes in Figure 2). Figure 29 and Figure 30 show temperature and precipitation changes as simulated by 34 CMIP5 GCMs (coloured crosses if used by RCA4, otherwise black), nine RCA4 simulations (squares of the same colours as the driving GCMs) and six other RCMs (triangles). Generally, the spread between models are smaller in winter than in summer, and smaller in northern and western Europe than in southern and eastern Europe. The GCMs used in this report (multi coloured crosses in Figure 29 and Figure 30) show some spread between them without being outliers, but captures most of the spread even in areas and seasons with a large spread (e.g. summer in South East Europe). To further quantify this, the mean value and standard deviation of temperature and precipitation and the correlation between temperature and precipitation is calculated for the four regions above. This is done for the full ensemble (all GCMs), the GCM ensemble used by RCA4, four randomly selected nine-GCM ensembles and the downscaled RCA4 ensemble (Table A1). If the RCA4-GCM ensemble (GCMs used by RCA4) can capture the statistical properties of the full ensemble it is considered to be representative of the full ensemble; and if the randomly selected ensembles also capture the statistical properties of the full ensemble and are similar to the RCA4-GCM ensemble, we know that the RCA4-GCM ensemble is not biased in any way. The statistical properties of the seven different ensembles are relatively similar. However, differences in mean temperature change can be almost ±1°C and in mean precipitation ±5%. Based on mean and standard deviation we conclude that the nine GCMs used in this study is considered to be representative of the full ensemble. Another ensemble, using nine or more GCMs, would give a different, yet similar result. The sampling of a few (here 9 out of 34) models shows that the correlation between the variables is not necessarily representative for the larger set. We also note that the correlation can differ considerably between different ensembles, implying that interpretation of the results may be erroneous. We note that other combinations of variables with stronger interdependence may be less sensitive to the size of the ensemble. The statistical properties are collected in Table A1 in appendix.
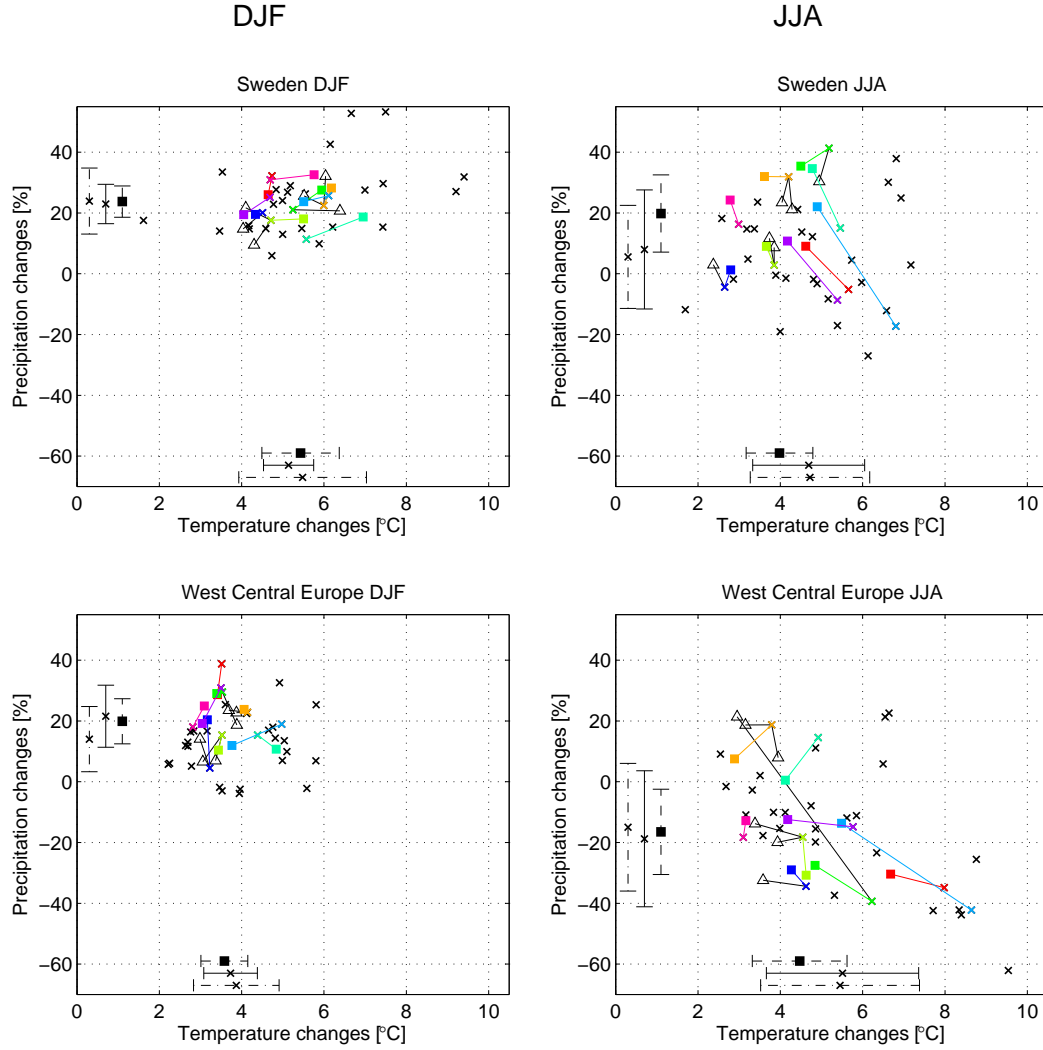
Figure 29. Temperature (°C) and precipitation (%) changes 2071-2100 compared with 1971-2000 for winter (DJF, left column) and summer (JJA, right column); Sweden (top row) and West Central Europe (bottom row). Filled squares represent RCA4 simulations, connected by a line to the corresponding GCM (cross of the same colour as the square). Black crosses represent other CMIP5 GCMs. Triangles indicate simulations with other RCMs than RCA4. Mean values and ±1 standard deviations are shown along the x-axis for temperature and the y-axis for precipitation for: the full GCM ensemble (represented by crosses for mean values and dash dotted line for ±1 standard deviation), the ensemble of GCMs used by RCA4 (crosses and full lines) and the RCA4 ensemble (filled squares and dashed lines).

4.3 Influence of dynamical downscaling

The next step is to investigate the influence of RCA4. Temperature and precipitation changes as simulated by RCA4 are represented by squares in Figure 29 and Figure 30 with lines connecting the individual RCA4 simulations with their respective driving GCMs. For winter conditions in Sweden the difference between GCMs and RCA4 is relatively small (Figure 29). RCA4 gives either higher temperatures and more precipitation or lower temperature and less precipitation. In summer RCA4 gives larger increases in precipitation than the GCMs in all but one simulation, and smaller increases in temperature in all but one simulation. The conditions in West Central Europe are similar to those in Sweden but with a somewhat larger spread between models and larger differences between RCA4 and GCMs, especially for summer. In West Central European summer RCA4 gives smaller temperature increases than the GCMs. When the spread

30

between models are large the difference between GCMs and RCMs are large, in some cases the precipitation difference is of different sign in the RCM and the driving GCM, which suggests that the difference in climate is generally more uncertain in those regions and seasons. Despite some systematic differences in precipitation the RCA4 simulations are representative for the ensemble as a whole.

The spread between the simulations is in most areas smaller in RCA4 forced by a number of GCMs than between the GCMs themselves. We hypothesize that this reduction in spread is something that is a consequence of the fact that the RCM only holds one description of the climate system while each GCM has its own, adding up to in total nine different ones. For instance, RCA4 has one formulation of snow on the ground while each GCM has a different formulation of the corresponding processes. Future comparisons with other RCMs will reveal if this is a correct interpretation.
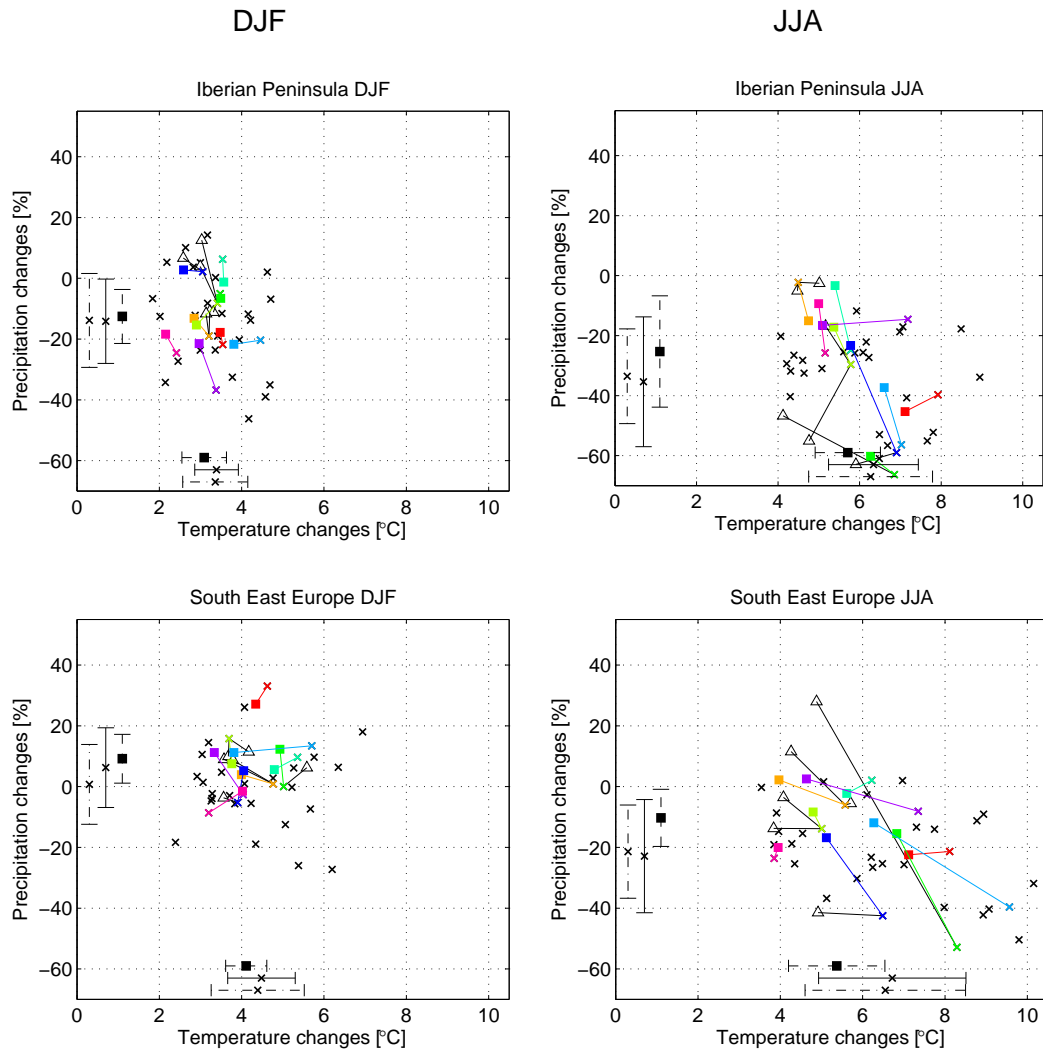

Figure 30. Same as Figure 29, but for Iberian Peninsula (top row) and South East Europe (bottom row).

Figure 30 shows temperature and precipitation differences over the Iberian Peninsula and in South East Europe. In winter over the Iberian Peninsula the spread between GCMs are larger than in the northern regions (cf. Figure 29), especially the spread in precipitation differences, but the differences between GCMs and RCA4 are relatively small. In summer the spread is even larger and the differences between GCMs and RCA4 are

larger than in winter. In most cases RCA4 gives smaller temperature and precipitation differences than the corresponding GCMs. For the other RCMs the differences between GCMs and RCMs are less systematic. The conditions in South East Europe are similar to those over the Iberian Peninsula. The spread between models are smaller in winter than in summer, and the differences between GCMs and RCMs are smaller in winter than in summer. In summer the model spread is large, and in some cases, the differences between GCMs and RCMs are even larger. Almost all RCM give smaller changes in temperature and precipitation than the corresponding GCMs. In some cases the differences between GCMs and RCMs are large. One RCM changes the precipitation difference from c. -50% in the GCM to c. 30% in the RCM, and the temperature difference from a little more than 8°C to c. 5°C. For summer in both the Iberian Peninsula and South East Europe RCA4 tends to draw GCMs with large climatic response towards the rest of the ensemble, giving a reduction in spread between the GCM ensemble and the RCA4 ensemble (cf. Figure 23).

To conclude, it is clear that downscaling with a RCM changes the climate change signal and that different RCMs change it differently depending on model, region, season and parameter. All ensembles are unique and the choice of models to be included will affect the result. If the number of members in the ensemble is large, and outliers are not specifically chosen, the ensemble has a better chance of being representative of the whole set of models.

4.4   Choice of emissions scenario

How much do results based on different RCP scenarios differ from each other and how much do results based on RCP scenarios differ from SRES scenarios? This is illustrated by looking at two regions with different climate change signals. Figure 31 shows temperature and precipitation changes in different times according to different scenarios in Sweden and over the Iberian Peninsula. For wintertime conditions in Sweden there is a clear relationship between temperature and precipitation: when temperature increases so does precipitation. The situation is similar in summer, but with a larger spread in precipitation changes.

Over the Iberian Peninsula there is a large spread in precipitation differences in winter, differences range from -20% to 20%, even though precipitation decrease dominate towards the end of the century and in scenarios with high greenhouse gas emissions. In summer all scenarios and models agree on temperature increase and precipitation decrease. There are large variations in the simulations, however. For the time period 2071-2100 temperature change ranges between 1-7°C and precipitation change between -60-0%.

Generally, all models and scenarios agree on a relationship between temperature change and precipitation change. In some regions or seasons the spread is smaller (e.g. Sweden in winter) and in some larger (e.g. Iberian Peninsula in summer). In winter the Iberian Peninsula lies on the border between increasing and decreasing precipitation. Hence, some models give increasing precipitation and some decreasing, and the direction of change is uncertain. The uncertainty in the sign of change is larger when the climate signal is weak, i.e. in the close future and in scenarios with small green-house gas emissions while uncertainty in amplitude is as high or higher at the end of the century. As expected, the choice of scenario is of importance; especially in the last time period (cf. Figure 23). The choice of models is also of importance, all lines of the same colours in Figure 31 do not take the same path. Some models have a higher TCR and are thus more sensitive to changes in greenhouse gas concentrations than others, which results in that in some cases the high-end RCP 8.5 scenario shows weaker warming than the more moderate RCP 4.5 scenario even at the end of the century. Despite this, there is a robust agreement on in what way climate will change as an effect of greenhouse gas emissions. The question is how much it will change and how rapid the change will be; that depends

on the actual future greenhouse gas emissions and the regional response in the GCMs, including natural internal variability. This is evident when comparing the time evolution in scenario RCP 8.5 with the projections for the end of the 21st century in scenarios RCP 2.6 and RCP 4.5 (Figure 32). The temperature change according to RCP 8.5 at different times (top row in Figure 32) is very similar to the temperature change in the end of the century in other scenarios (bottom row in Figure 32). This figure has a very strong message as it shows the benefit of greenhouse gas mitigation in a clear way.
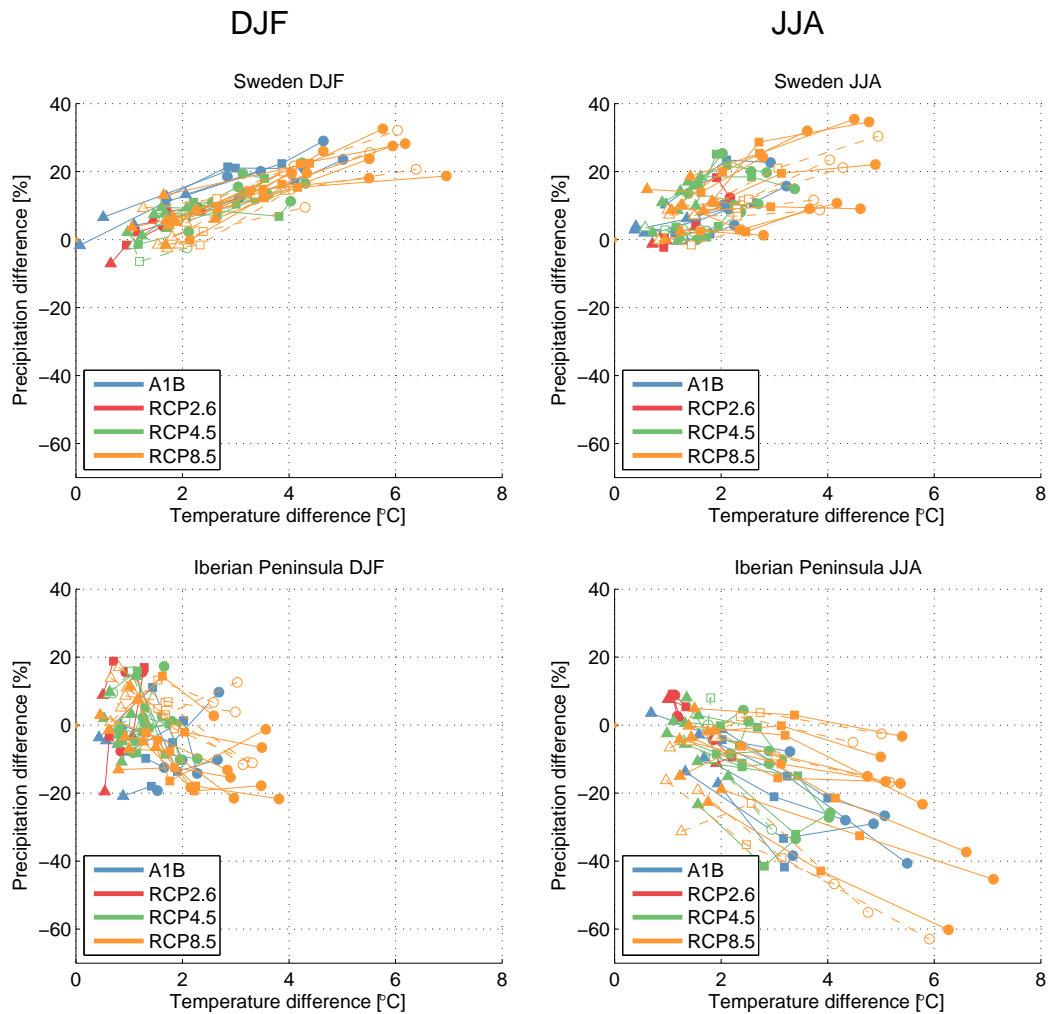

Figure 31. Temperature and precipitation change in RCP scenarios simulated with RCA4 compared to SRES scenarios simulated with RCA3. Every simulation is represented by a line showing climate change compared to 1971-2000 for three time periods: 2011-2040 (triangle), 2041-2070 (square) and 2071-2100 (circle). Filled symbols indicate RCA4 runs, open symbols indicate other RCM simulations. Colours represent different scenarios. Sweden (top row), Iberian Peninsula (bottom row). Winter (DJF, left column), summer (JJA, right column).
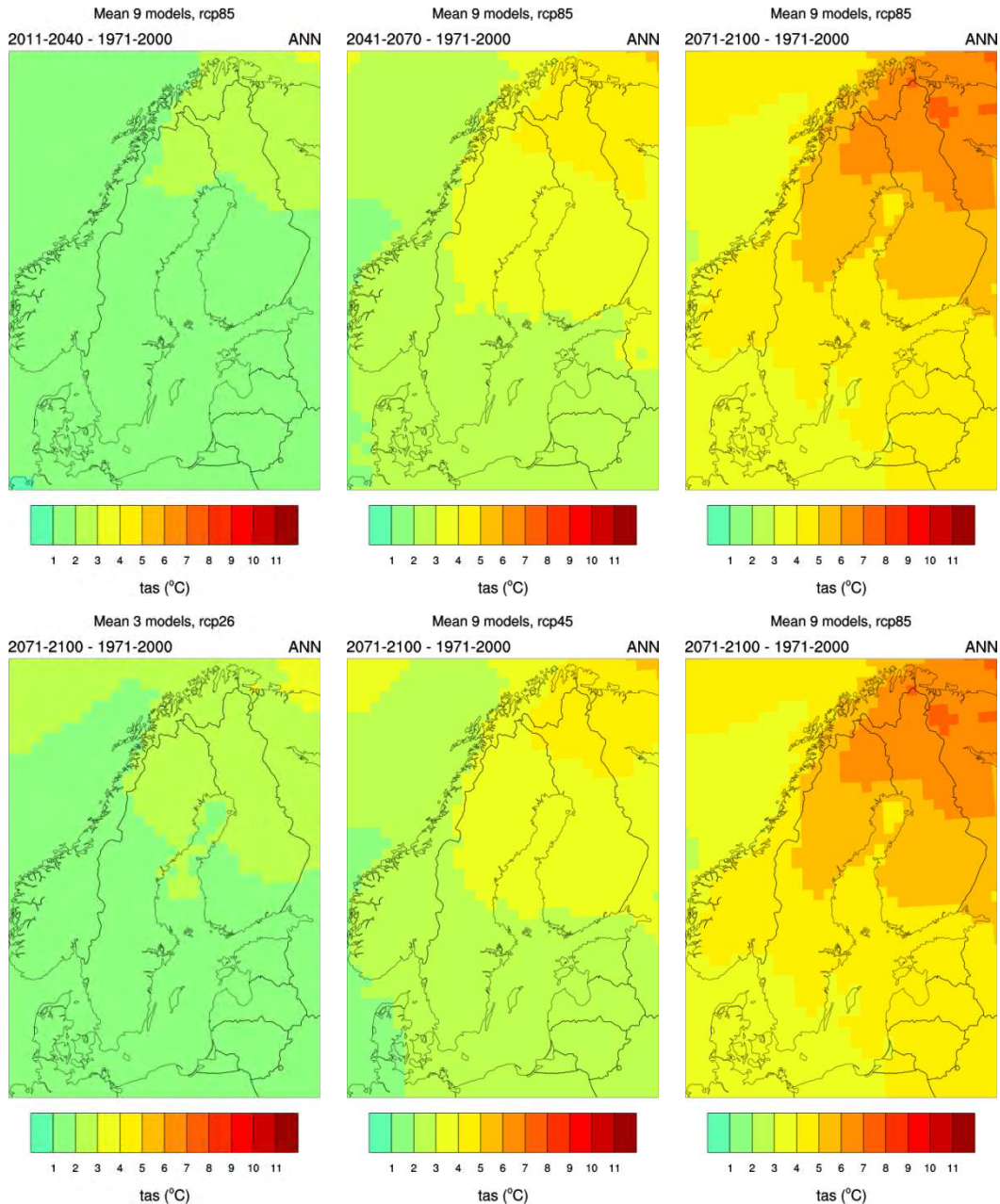
Figure 32. Top row: Simulated temperature change in three time periods (2011-2040 (left), 2041-2070 (middle), 2071-2100 (right)) compared to the period 1971-2000 according to scenario RCP 8.5. Bottom row: Simulated temperature change in 2071-2100 compared to 1971-2000 according to scenarios RCP 2.6 (left), RCP 4.5 (middle) and RCP 8.5 (right).

5   Summary and conclusions

This report focus on documenting Coordinated Regional Downscaling Experiment (CORDEX) simulations at 50 km horizontal resolution over Europe with the Rossby Centre regional atmospheric model (RCA4) for i) a ERA-Interim-driven (ERAINT) simulation used to evaluate model performance in the recent past climate, ii) historical simulations of the recent decades with forcing from nine different global climate models (GCMs) and iii) future scenarios RCP 4.5 and RCP 8.5 forced by the same nine different GCMs. Those simulations represent a subset of all CORDEX simulations produced at the

34

Rossby Centre and a general conclusion drawn at the Rossby Centre is that such large ensembles could not have been produced without the establishment of an efficient production chain as outlined here.

The first part of this report documents RCA4 and its performance in a perfect boundary simulation where ERAINT was downscaled. From this part of the work we conclude that:

- The large-scale circulation in the model domain is to a large extent replicating that in the forcing ERAINT boundaries. Some local biases in mean sea level pressure appear over the Mediterranean and over the eastern part of the domain, but the conditions over the North Atlantic are simulated in a good way indicating that the transport of mild and moist air from the west is captured in a good way.

- In general the seasonal cycles of temperature and precipitation are simulated in relatively close agreement to observations. Some biases occur, such as too much precipitation in northern Europe and too little in the south. In winter, there is also too much precipitation in eastern Europe, possibly related to the too low mean sea level pressure in that area which may reflect a too cyclonic activity in the area. Temperatures are generally biased low in northern Europe and in the Mediterranean region in winter while overestimated temperatures are seen in southeastern Europe in winter and in the Mediterranean area in summer. Seasonal mean biases are 1-3°C in these areas.

Next we examine the recent past climate when RCA4 takes boundary conditions from the GCMs. A large part of the RCA4 simulated climate is attributed to the driving GCMs; RCA4 creates its own climate inside the model domain and adds details due to higher resolution, however. In particular we note that:

- All nine downscaled GCMs share problems in their representation of the large-scale circulation in winter. In general there is a too strong north-south pressure gradient over the North Atlantic south of the British Isles and a too weak gradient north thereof. This feature is inherited in RCA4.

- The biases in large-scale circulation induce some biases in temperature and precipitation in RCA4. Alternatively, biases already existing in RCA4 driven by ERAINT are amplified or weakened. Examples include: a stronger warm bias in southeastern Europe in winter and a stronger cold bias in the north. Further, the wet biases in winter are amplified in many areas while there is a stronger dry bias along the Norwegian west coast.

- The spread in the results from the nine-member RCA4 ensemble are sometimes considerably reduced compared to that in the ensemble of the underlying GCMs. In particular we note this for precipitation in Eastern Europe in winter and parts of Scandinavia in summer and for temperature in Southeastern Europe in winter and for most of Europe in summer. This is likely a result of the fact that RCA4 only holds one description of the climate system while the GCMs have in total nine different ones. There are also areas where the spread is larger in the RCA4 ensemble. This is mostly in mountainous areas where the higher altitude in RCA4 can amplify differences in precipitation.

Next we analyse the climate change signal in the RCP 4.5 and RCP 8.5 ensembles. The patterns of change that show up are very similar to what has been presented previously and to a large extent the scenarios reflect that in the underlying GCMs. From this part of the work we note that:

- Both scenarios RCP 4.5 and RCP 8.5 project Europe to be warmer in the future. In winter the warming is largest in northern Europe (c. 4-8 °C in RCP 8.5) and in summer in southern Europe (c. 4-8 °C in RCP 8.5). The summer maximum daily temperature increases in a way similar to summer temperature, but somewhat

more in southern Europe (5-8 °C in RCP 8.5). The winter minimum daily temperature is the temperature that changes the most; more than 8 °C in large parts of northern Europe. In southern Europe this temperature is relatively unchanged.

- Precipitation is projected to increase in all seasons in northern Europe (c. 20-40 % in RCP 8.5) and decrease in southern Europe (10-40 % in RCP 8.5). The shift between increasing and decreasing precipitation is moving over the year. In winter the area of decreasing precipitation is confined to the Mediterranean region. In summer it stretches up to the North Sea and central Europe. Naturally, there are differences between individual ensemble members; some place the shift in precipitation farther north some farther south.

- The largest amount of rainfall per day (and per seven day period) is projected to increase in almost all of Europe and in all seasons. At the same time the longest period without precipitation is projected to be longer in southern Europe.

- Small changes in wind speed are generally projected. There are, however, regions (Baltic Sea, Aegean Sea) with significant changes in wind. Here we see an increase in mean wind of 10-15 %.

This report builds on a RCA4 ensemble driven by nine different GCMs. The ensemble approach is a way to describe the uncertainties in the scenarios, but there are other possible ensembles using other models which would give other results. Still, the ensemble used here is considered to be similar enough to these other possible ensembles to be representative of the whole set of GCMs. This is based on:

- The transient climate response of the GCMs used in this study (1.3-2.5 °C) almost captures the range estimated by IPCC (1.0-2.5 °C).

- The ensemble of nine GCMs used here captures the statistical properties of temperature and precipitation change in a way similar to an ensemble of 34 coupled model intercomparison project (CMIP5) GCMs.

- Dynamical downscaling using RCA4 changes the climate change signal, but the ensemble of nine RCA4 simulations, using different GCMs, is considered to be representative of the full ensemble. In some way the GCM RCA4 difference reflects the GCM spread and also the uncertainty in the climate change signal of that region/season/parameter.

- All scenarios agree on a climate change pattern; the amplitude of the change is determined by the choice of scenario. The relative importance of the chosen scenario increases with time.

Acknowledgements

References

Adler, R. F., Adler, Huffman, G. J., Chang, A., Ferraro, R., Xie, P., Janowiak, J., Rudolf, B., Schneider, U., Curtis, S., Bolvin, D., Gruber, A., Susskind, J., Arkin, P. and Nelkin, E.: The Version-2 Global Precipitation Climatology Project (GPCP) Monthly Precipitation Analysis (1979–Present). J. Hydrometeor, 4, 1147–1167, 2003.

Ban, N., Schmidli, J. and Schär, C.: Evaluation of the convection-resolving regional climate modeling approach in decade-long simulations, J. Geophys. Res. Atmos., 9, 7889–7907, doi:10.1002/2014JD021478, 2014.

Bechtold, P., Bazile, E., Guichard, F., Mascart, P. and Richard, E.: A mass-flux convection scheme for regional and global models, Q.J.R. Meteorol. Soc., 127: 869–886, 2001.

Bentsen, M., Bethke, I., Debernard, J.B., Iversen, T., Kirkevåg, A., Seland, Ø., Drange, H., Roelandt, C., Seierstad, I.A., Hoose, C. and Kristjánsson, J.E..: The Norwegian earth system model, NorESM1-M. Part 1: Description and basic evaluation, Geosci. Mod. Dev., 6, 687-720, doi:10.5194/gmd-6-687-2013, 2013.

Berg, P., Döscher, R., and Koenigk, T.: Impacts of using spectral nudging on regional climate model RCA4 simulations of the Arctic, Geosci. Model Dev., 6, 849-859, doi:10.5194/gmd-6-849-2013, 2013.

Boberg, F. and Christensen, J.H.: Overestimation of Mediterranean summer temperature projections due to model deficiencies, Nature Clim. Change, 2, 433–436, 2012.

Brands, S., Herrera, S., Fernández, J. and Gutiérrez, J.M.: How well do CMIP5 Earth System Models simulate present climate conditions in Europe and Africa? Clim. Dyn., 41, 803–817, DOI 10.1007/s00382-013-1742-8, 2013.

Cai, W., Borlace, S., Lengagne, M., van Rensch, P., Collins, M., Vecchi, G., Timmermann, A., Santoso, A., McPhaden M.J., Wu, L., England, M.H., Wang, G., Guilyardi, E. and Jin, F.-F.: Increasing frequency of extreme El Niño events due to greenhouse warming. Nature Climate Change, 4, 111–116 doi:10.1038/nclimate2100, 2014

Cattiaux, J., Douville, H. and Peings, Y.: European temperatures in CMIP5: origins of present-day biases and future uncertainties, Clim. Dyn., 41, 2889–2907, DOI 10.1007/s00382-013-1731-y, 2013.

Christensen, J.H. and Christensen, O.B.: Severe summertime flooding in Europe, Nature 421, 805–806, 2003.

Christensen, J.H. and Christensen, O.B.: A summary of the PRUDENCE model projections of changes in European climate by the end of the century, Clim. Change, 81, 7–30, 2007.

Christensen, J.H., Kjellström, E., Giorgi, F., Lenderink, G., Rummukainen, M.: Weight assignment in Regional Climate Models, Clim. Res., 44, 179–194, 2010.

Chylek, P., Li, J., Dubey, M. K., Wang, M. and Lesins. G.: Observed and model simulated 20th century Arctic temperature variability: Canadian Earth System Model CanESM2, Atmos. Chem. Phys. Discuss., 11, 22893-22907, 2011.

Collins, W.J., Bellouin, N., Doutriaux-Boucher, M., Gedney, N., Halloran, P., Hinton, T., Hughes, J., Jones, C.D., Joshi, M., Liddicoat, S., Martin, G., O'Connor, F., Rae J., Senior, C., Sitch, S., Totterdell, I., Wiltshire, A. and Woodward, S.: Development and evaluation of an Earth-System model-HadGEM2. Geosci. Model Dev., 4, 1051-1075, 2011.

Collins, M., Knutti, R., Arblaster, J., Dufresne, J.-L., Fichefet, T., Friedlingstein, P., Gao, X., Gutowski, W.J., Johns, T., Krinner, G., Shongwe, M., Tebaldi, C., Weaver, A.J. and Wehner, M.: Long-term Climate Change: Projections, Commitments and Irreversibility. In: Climate Change 2013: The Physical Science Basis. Contribution of Working Group I to the Fifth Assessment Report of the Intergovernmental Panel on Climate Change [Stocker, T.F., D. Qin, G.-K. Plattner, M. Tignor, S.K. Allen, J. Boschung, A. Nauels, Y. Xia, V. Bex and P.M. Midgley (eds.)]. Cambridge University Press, Cambridge, United Kingdom and New York, NY, USA, 2013.

Cubash, U., Meehl, G.A., Boer, G.J., Stouffer, R.J., Dix, M., Noda, A., Senior, C.A., Raper, S. and Yap, K.S.: Projections of Future Climate Change. In: Climate Change 2001: The Scientific Basis. Contribution of Working Group I to the Third Assessment Report of the Intergovernmental Panel on Climate Change [Houghton, J.T., Y. Ding, D.J. Griggs, M. Noguer, P.J. van der Linden, X. Dai, K. Maskell, and C.A. Johnson (eds.)]. Cambridge University Press, Cambridge, United Kingdom and New York, NY, USA, 881pp, 2001.

Cuxart, J., Bougeault, P. and Redelsperger, J.-L.: A turbulence scheme allowing for mesoscale and large-eddy simulations, Q.J.R. Meteorol. Soc., 126, 1–30, 2000.

Dee, D.P., Uppala, S.M., Simmons, A.J., Berrisford, P. Poli, P., Kobayashi, S., Andrae, U., Balmaseda, M. A., Balsamo, G., Bauer, P., Bechtold, P., Beljaars, A.C.M., van de Berg, L., Bidlot, J., Bormann, N., Delsol, C., Dragani, R., Fuentes, M., Geer, A. J., Haimberger, L., Healy, S. B., Hersbach, H., Hólm, E.V., Isaksen, L., Kållberg, P., Köhler, M., Matricardi, M., McNally, A.P., Monge-Sanz, B.M., Morcrette, J.-J., Park, B.-K. Peubey, C., de Rosnay, P., Tavolato, C., Thépaut, J.-N., and Vitart, F.: The ERA-Interim reanalysis: configuration and performance of the data assimilation system, Quart. J. Roy. Met. Soc., 137, 656, 553–597, 2011.

Dufresne, J.-L., Foujols, M.-A., Denvil, S., Caubel, A., Marti, O., Aumont, O., Balkanski, Y., Bekki, S., Bellenger, H., Benshila, R., Bony, S., Bopp, L., Braconnot, P., Brockmann, P., Cadule, P., Cheruy, F., Codron, F., Cozic, A., Cugnet, D., de Noblet, N., Duvel, J.-P., Ethé, C., Fairhead, L., Fichefet, T., Flavoni, S., Friedlingstein, P., Grandpeix, J.-Y., Guez, L., Guilyardi, E., Hauglustaine, D., Hourdin, F., Idelkadi, A., Ghattas, J., Joussaume, S., Kageyama, M., Krinner, G., Labetoulle, S., Lahellec, A., Lefebvre, M.-P., Lefevre, F., Levy, C., Li, Z.X., Lloyd, J., Lott, F., Madec, G., Mancip, M., Marchand, M., Masson, S., Meurdesoif, Y., Mignot, J., Musat, I., Parouty, S., Polcher, J., Rio, C., Schulz, M., Swingedouw, D., Szopa, S., Talandier, C., Terray, P., Viovy, N. and Vuichard, N.: Climate change projections using the IPSL-CM5 Earth system model: From CMIP3 to CMIP5. Clim. Dyn., 40, 2123-2165, 2013.

Dunne, J.P., John, J.G., Adcroft, A.J., Griffies, S.M., Hallberg, R.W., Shevliakova, E., Stouffer, R.J., Cooke, W., Dunne, K.A., Harrison, M.J., Krasting, J.P., Malyshev, S.L., Milly, P.C.D., Phillips, P.J., Sentman, L.T., Samuels, B.L., Spelman, M.J., Winton, M., Wittenberg, A.T., and Zadeh, N.: GFDL's ESM2 Global Coupled Climate-Carbon Earth System Models. Part I: Physical Formulation and Baseline Simulation Characteristics, Journal of Climate, 25, DOI: 10.1175/JCLI-D-11-00560.1, 2012.

Fischer, E. M. and Schär, C.: Future changes in daily summer temperature variability: driving processes and role for temperature extremes. Clim. Dyn. 33, 917–935 DOI 10.1007/s00382-008-0473-8, 2009.

Fischer, E.M., Beyerle, U. and Knutti, R.: Robust spatially aggregated projections of climate extremes. Nature Clim. C., 3, 1033-1038, 2013.

Giorgi, F., Jones, C. and Asrar, G.R.: Addressing climate information needs at the regional level: the CORDEX framework, WMO Bulletin, 58, 3, 2009.

Global Soil Data Task: Global gridded surfaces of selected soil characteristics (IGBPDIS). International Geosphere-Biosphere Programme. Data and Information Services. Available online [http://www.daac.ornl.gov/] from the ORNL Distributed Active Archive Center, Oak , 2000.

Grenier, H. and Bretherton, C.S.: A Moist PBL Parameterization for Large-Scale Models and Its Application to Subtropical Cloud-Topped Marine Boundary Layers, Mon. Wea. Rev., 129, 357–377, 2001.

van Haren, R. van Oldenborgh, G.J., Lenderink, G., Collins, M. and Hazeleger, W.: SST and circulation trend biases cause an underestimation of European precipitation trends. Clim. Dyn., 40, 1-2, 2013.

Harris, I., Jones, P.D., Osborn, T.J. and Lister, D.H.: Updated high-resolution grids of monthly climatic observations – the CRU TS3.10 Dataset, Int. J. Climatol., 34, 623–642, 2014.

Haugen, J. E. and Iversen, T.: Response in extremes of daily precipitation and wind from a downscaled multimodel ensemble of anthropogenic global climate change scenarios. Tellus 60A, 411–426, 2008.

Hawkins, E., Sutton, R.T.: Decadal predictability of the Atlantic Ocean in a coupled GCM: forecast skill and optimal perturbations using Linear Inverse Modelling, J. Clim., 22, 14, 3960-3978, doi:10.1175/2009JCLI2720.1, 2009.

Haylock, M.R., Hofstra, N., Klein Tank, A.M.G., Klok, E.J., Jones, P.D. and New, M.: A European daily high-resolution gridded data set of surface temperature and precipitation for 1950–2006. J. Geophys. Res., 113, 0119, doi:10.1029/2008JD010201, 2008.

Hazeleger, W., Severijns, C., Semmler, T., Ştefănescu, S., Yang, S., Wang, X., Wyser, K., Dutra, E., Baldasano, J.M., Bintanja, R., Bougeault, P., Caballero, R., Ekman, A.M.L., Christensen, J.H., van den Hurk, B., Jimenez, P., Jones, C., Kållberg, P., Koenigk, T., McGrath, R., Miranda, P., Van Noije, T., Palmer, T., Parodi, J.A., Schmith, T., Selten, F., Storelvmo, T., Sterl, A., Tapamo, H., Vancoppenolle, M., Viterbo, P. Willén, U.: EC-Earth: A seamless Earth-system prediction approach in action, Bull. Amer. Meteor. Soc., 91, 1357-1363, 2010.

IPCC: Climate Change 2013: The Physical Science Basis. Contribution of Working Group I to the Fifth Assessment Report of the Intergovernmental Panel on Climate Change [Stocker, T.F., D. Qin, G.-K. Plattner, M. Tignor, S.K. Allen, J. Boschung, A. Nauels, Y. Xia, V. Bex and P.M. Midgley (eds.)]. Cambridge University Press, Cambridge, United Kingdom and New York, NY, USA, 1535 pp, 2013.

Jacob, D., Barring, L., Christensen, O.B., Christensen, J.H., de Castro, M., Deque, M., Giorgi, F., Hagemann, S., Hirschi, M., Jones, R., Kjellstrom, E., Lenderink, G., Rockel, B., van Ulden, A.P. and van den Hurk, B.J.J.M.: An inter-comparison of regional climate models for Europe: model performance in present-day climate. Climatic Change, doi:10.1007/s10584-006-9213-4, 2007.

Jacob, D., Petersen, J., Eggert, B., Alias, A., Christensen, O.B., Bouwer, L.M., Braun, A., Colette, A., Déqué, M., Georgievski, G., Georgopoulou, E., Gobiet, A., Menut, L., Nikulin, G., Haensler, A., Hempelmann, N., Jones, C., Keuler, K., Kovats, S., Kröner, N., Kotlarski, S., Kriegsmann, A., Martin, E., van Meijgaard, E., Moseley, C., Pfeifer, S., Preuschmann, S., Radermacher, C., Radtke, K., Rechid, D., Rounsevell, M., Samuelsson, P., Somot, S., Soussana, J.-F., Teichmann, C., Valentini, R., Vautard, R., Weber, B., Yiou, P.: EURO-CORDEX: new high-resolution climate change projections for European impact research, Regional Environmental Change, 14, 2, 563-578, doi: 10.1007/s10113-013-0499-2, 2013.

Jiao, Y. and Jones, C.: Comparison Studies of Cloud- and Convection-Related Processes Simulated by the Canadian Regional Climate Model over the Pacific Ocean, Mon. Wea. Rev., 136, 4168–4187, 2008.

Jones, C. G., Ullerstig, A., Willén, U. and Hansson, U.: The Rossby Centre regional atmospheric climate model (RCA). Part I: model climatology and performance characteristics for present climate over Europe, AMBIO, 33, 199–210, 2004.

Kain, J.S. and Fritsch, J.M.: A One-Dimensional Entraining/Detraining Plume Model and Its Application in Convective Parameterization, J. Atmos. Sci., 47, 2784–2802, 1990.

Kendon, E.J., Roberts, N.M., Senior, C.A., and Roberts, M.J.: Realism of Rainfall in a Very High-Resolution Regional Climate Model. J. Climate, 25, 5791–5806. doi: http://dx.doi.org/10.1175/JCLI-D-11-00562.1, 2012.

Kjelllström, E. and Giorgi, F.: Introduction. Clim. Res., 44, 117-119, 2010.

Kjellström, E. and Ruosteenoja, K.: Present-day and future precipitation in the Baltic Sea region as simulated in a suite of regional climate models. Climatic Change. 81 (Suppl. 1), 281-291. doi:10007/s10584-006-9219-y, 2007.

Kjellström, E., Bärring, L., Gollvik, S., Hansson, U., Jones, C., Samuelsson, P., Rummukainen, M., Ullerstig, A., Willén, U and Wyser, K.: A 140-year simulation of European climate with the new version of the Rossby Centre regional atmospheric climate model (RCA3). In: Reports Meteorology and Climatology. Volume 108, SMHI, SE-60176 Norrköping, Sweden, 54, 2005.

Kjellström, E., Nikulin, G., Hansson, U., Strandberg, G. and Ullerstig, A.: 21st century changes in the European climate: uncertainties derived from an ensemble of regional climate model simulations. Tellus, 63A, 1, 24-40, 2011.

Kjellström, E., Thejll, P., Rummukainen, M., Christensen, J.H., Boberg, F., Christensen, O.B., Fox Maule, C.: Emerging regional climate change signals for Europe under varying large-scale circulation conditions, Clim. Res. 56, 103–119, doi: 10.3354/cr01146, 2013.

Knutti, R. and Sedláček, J.: Robustness and uncertainties in the new CMIP5 climate model projections, Nature Clim. Change, 3, 369–373, doi:10.1038/nclimate1716, 2013.

Kourzeneva, E.V.: External data for lake parameterization in numerical weather prediction and climate modelling, Boreal Env. Res. 15, 165–177, 2010.

Lenderink, G. and Holtslag, A.A.M.: An updated length-scale formulation for turbulent mixing in clear and cloudy boundary layers, Q.J.R. Meteorol. Soc., 130, 3405–3427, 2004.

Madec, G.: NEMO ocean engine, User Manual 3.3 , IPSL, Paris, France, 2011.

Masson, V., Champeaux, J.-L., Chauvin, F., Meriguet, C. and Lacaze, R.: A global database of Land Surface Parameters at 1-km Resolution in Meteorological and Climate Models, Journal of Climate, 16, 9, 1261- 1282, 2003.

Maraun, D., Wetterhall, F., Ireson, A.M., Chandler, R.E., Kendon, E.J., Widmann, M., Brienen, S., Rust, H.W., Sauter, T., Themeßl, M., Venema, V.K.C., Chun, K.P., Goodess, C.M., Jones, R.G., Onof, C., Vrac, M., and I. Thiele-Eich, I.: Precipitation downscaling under climate change: Recent developments to bridge the gap between dynamical models and the end user, Rev. Geophys, 48, RG3003, doi:10.1029/2009RG000314, 2010.

Moss., R.H., Edmonds, J.A., Hibbard, K.A., Manning, M.R., Rose, S.K., van Vuuren, D.P., Carter, T.R., Emori, S., Kainuma, M., Kram, T., Meehl, G.A., Mitchell,

J.F.B., Nakicenovic, N., Riahi, K., Smith, S.J., Stouffer, R.J., Thomson, A.M., Weyant, J.P. and Wilbanks, T.J.: The next generation of scenarios for climate change research and assessment, Nature, Vol 463, 11 February 2010, doi:10.1038/nature08823, 2010.

Nikulin, G., Kjellström, E., Hansson, U., Jones, C., Strandberg, G. and Ullerstig, A.: Evaluation and Future Projections of Temperature, Precipitation and Wind Extremes over Europe in an Ensemble of Regional Climate Simulations, Tellus, 63A, 1, 41-55. DOI: 10.1111/j.1600-0870.2010.00466.x, 2011.

Popke, D., Stevens, B. and Voigt, A.: Climate and climate change in a radiative-convective equilibrium version of ECHAM6, Journal of Advances in Modeling Earth Systems, Vol.. 5, 1-14, doi:10.1029/2012MS000191, 2013.

Prein, A. F., Gobiet, A., Truehetz, H., Keuler, K., Goergen, K., Teichmann, C., Fox Maule, C., van Meijgaard, E., Déqué, M., Nikulin, G., Vautard, R., Colette, A., Kjellström, E. and Jacob, D.: Precipitation in the EURO-CORDEX 0.11˚ and 0.44˚ simulations: high resolution, high benefits? Accepted for publication in Climate Dynamics, 2015.

Rauscher, S.A., Coppola, E., Piani, C., Giorgi, F.: Resolution effects on regional climate model simulations of seasonal precipitation over Europe. Clim. Dyn., 35:685–711, DOI 10.1007/s00382-009-0607-7, 2010.

Rossow, W. B. and Schiffer, R. A.: Advances in understanding clouds from ISCCP, Bull. Am. Meteorol. Soc., 80, 2261–2287, 1999.

Rowell, D. P. and Jones, R. G.: Causes and uncertainty of future summer drying over Europe. Clim. Dyn. 27, 281-299, DOI 10.1007/s00382-006-0125-9, 2006.

Rubel, F., and Hantel, M.: BALTEX 1/6-degree daily precipitation climatology 1996-1998, Meteorol. Atmos. Phys., 77, 155-166, 2001.

Rummukainen, M.: State-of-the-art with regional climate models. WIREs Clim. Change 1, 82–96, 2010.

Rummukainen, M., Räisänen, J., Ullerstig, A., Bringfelt, B., Hansson, U., Graham, P. and Willén, U.: RCA – Rossby Centre regional Atmospheric climate model: model description and results from the first multi-year simulation, Reports Meteorology and Climatology 83,SMHI, SE-601 76 Norrköping, Sweden, 76 pp, 1998.

Rummukainen, M., Räisänen, J., Bringfelt, B., Ullerstig, A., Omstedt, A., Willén, U., Hansson, U. and Jones, C.: A regional climate model for northern Europe: model description and results from the downscaling of two GCM control simulations. Clim. Dyn., 17, 339-359, 2001.

Räisänen, J., Hansson, U., Ullerstig, A., Döscher, R., Graham, L.P., Jones, C., Meier, M., Samuelsson, P. and Willén, U.: GCM driven simulations of recent and future climate with the Rossby Centre coupled atmosphere – Baltic Sea regional climate model RCAO. Reports Meteorology and Climatology 101, SMHI, SE 60176 Norrköping, Sweden, 61 pp, 2003.

Räisänen, J., Hansson, U., Ullerstig, A., Döscher, R., Graham, L.P., Jones, C., Meier, H.E.M., Samuelsson, P. and Willén, U.: European climate in the late 21st century: regional simulations with two driving global models and two forcing scenarios. Clim. Dyn., 22, 13-31, 2004.

Samuelsson, P., Kourzeneva, E., and Mironov, D.: The impact of lakes on the European climate as simulated by a regional climate model, Boreal Env. Res., 15, 113-129, 2010.

Samuelsson, P., Jones, C. G., Willen, U., Ullerstig, A., Gollvik, S., Hansson, U., Jansson, C., Kjellström, E., Nikulin, G., and Wyser, K.: The Rossby Centre regional climate model RCA3: model description and performance, Tellus A, 63, 4–23, doi:10.1111/j.1600-0870.2010.00478.x, 2011.

Samuelsson, P., Gollvik, S., Jansson, C., Kupiainen, M., Kourzeneva, E., van de Berg, W. J.: The surface processes of the Rossby Centre regional atmospheric climate model (RCA4). Report in Meteorology 157, SMHI, SE-601 76 Norrköping, Sweden, 2014.

Sillmann, J., Kharin, V.V., Zwiers, F.W., Zhang, X. and Bronaugh, D.: Climate extremes indices in the CMIP5 multimodel ensemble: Part 2. Future climate projections, J. Geophys. Res. Atmos., 118, 2473–2493, doi:10.1002/jgrd.50188, 2013.

Smith, B., Prentice, I. C., and Sykes, M. T.: Representation of vegetation dynamics in the modelling of terrestrial ecosystems: comparing two contrasting approaches within European climate space, Global Ecol. Biogeogr., 10, 621–637, doi:10.1046/j.1466-822X.2001.t01-1-00256.x, 2001.

Takala, M., Luojus, K., Pulliainen, J., Derksen, C., Lemmetyinen, J., Kärnä, J.-P., Koskinen, J. and Bojkov, B.: Estimating Northern Hemisphere snow water equivalent for climate research through assimilation of space-borne radiometer and ground-based measurements. Remote Sens. Environ., 115, 3517–3529, 2011.

Taylor, K.E., Stouffer, R.J. and Meehl, G.A.: An Overview of CMIP5 and the Experiment Design, Bull. Met. Am. Soc., 93, 485–498, doi: http://dx.doi.org/10.1175/BAMS-D-11-00094.1, 2012.

Tiedtke, M., An extension of cloud-radiation parameterization in the ECMWF model: The representation of subgrid-scale variations of optical depth. Mon. Weather Rev., 12, 745-750, 1996.

Undén, P., Rontu, L., Järvinen, H., Lynch, P., Calvo, J., Cats, G., Cuxart, J., Eerola, K., Fortelius, K., Garcia-Moya, J. A., Jones, C., Lenderlink, G., McDonald, A., McGrath, R., Navascues, B., Nielsen, N. W., Ødegaard, V., Rodrigues, E., Rummukainen, M., Rõõm, R., Sattler, K., Sass, B. H., Savijärvi, H., Schreuer, B. W., Sigg, R., The, H., Tijm, A.: HIRLAM-5 Scientific Documentation. HIRLAM Report, SMHI, SE-601 76 Norrköping, Sweden, 144 pp, 2002.

USGS: Global 30 Arc-Second Elevation (GTOPO30) . https://lta.cr.usgs.gov/GTOPO30, 1996.

Valcke, S.: The OASIS3 coupler: a European climate modelling community software, Geosci. Model Dev., 6, 373388, doi:10.5194/gmd63732013, 2013.

Vancoppenolle, M., Fichefet, T.,Goosse, H., Bouillon, S., Madec,G. and Maqueda, M.A.M.: Simulating the mass balance and salinity of arctic and antarctic sea ice, Ocean Modelling, 27, 33–53, 2009.

Vautard, R., Gobiet, A., Jacob, D., Belda, M., Colette, A., Déqué, M., Fernández, J., García-Díez, M., Goergen, K., Güttler, I., Halenka, T., Karacostas, T., Katragkou, E., Keuler, K., Kotlarski, S., Mayer, S., van Meijgaard, E., Nikulin, G., Patarčić, M., Scinocca, J., Sobolowski, S., Suklitsch, M., Teichmann, C., Warrach-Sagi, K., Wulfmeyer, V. and Yiou, P.: The simulation of European heat waves from an ensemble of regional climate models within the EURO-CORDEX project, Clim Dyn, 41, 2555–2575, DOI 10.1007/s00382-013-1714-z. 2013.

Voldoire, A., Sánchez-Gómez, E., Salas y Mélia, D., Decharme, B., Cassou, C., Sénési, S., Valcke, S., Beau, I., Alias, A., Chevallier, M., Déqué, M., Deshayes, J., Douville, H., Fernandez, E., Madec, G., Maisonnave, E., Moine, M-P., Planton, S., Saint-Martin, D., Szopa, S., Tyteca, S., Alkama, R., Belamari, S., Braun, A.,

Coquart, L., Chauvin, F.: The CNRM-CM5.1 global climate model: description and basic evaluation, Clim Dyn. doi:10.1007/s00382-011-1259-y, 2012.

Wang, S., Dieterich, C., Döscher, R., Höglund, A., Hordoir, R., Meier, H.E.M., Samuelsson, P. and Schimanke, S.: Development and evaluation of a new regional coupled atmosphere-ocean model in the North Sea and the Baltic Sea, Submitted to Tellus, 2015.

Watanabe, S., Hajima, T., Sudo, K., Nagashima, T., Takemura, T., Okajima, H., Nozawa, T., Kawase, H., Abe, M., Yokohata, T., Ise, T., Sato, H., Kato, E., Takata, K., Emori, S. and Kawamiya, M.: MIROC-ESM 2010: Model description and basic results of CMIP5-20c3m experiments, Geosci. Model Dev., 4, 845-872, 2011.

Wern, L.: Snödjup i Sverige 1904/05–2013/14. Report in Meteorology 158, SMHI, SE-601 76 Norrköping, Sweden, 2014.

Wibig, J., Mauran, D., Benestad, R., Kjellström, E., Lorenz, P, and Christensen, O.B.: Projected Change—Models and Methodology. In Second Assessment of Climate Change for the Baltic Sea Basin. The BACC II Author Team. Regional Climate Studies, 189-216. DOI 10.1007/978-3-319-16006-1_102015, 2015.

Willmott, C. J. and Matsuura, K.: Smart interpolation of annually averaged air temperature in the United States. J. Appl. Met. 34, 2577–2586, 1995.

Wu, M., Smith, B., Schurgers, G., Siltberg, J., Rummukainen, M., Samuelsson, P. and Jansson, C.: Potential mechanism of vegetation-induced reduction in tropical rainfall in Africa: Analysis based on regional Earth system model simulations, 3rd International Lund Regional-scale climate modelling workshop, International Baltic Earth Secretariat Publication No. 3, June 2014, 78. ISSN 2198-4247, 2014.

Yamazaki, D., Kanae,S., Kim, H. and Oki, T.: A physically based description of flood plain inundation dynamics in a global river routing model, Water Resour. Res. 47,W04501, doi:10.1029/2010WR009726, 2011.

Zhang, W., Jansson, C., Miller, P.A., Smith, B. and Samuelsson, P.: Biogeophysical feedbacks enhance Arctic terrestrial carbon sink in regional Earth system dynamics, Biogeosciences, 11, 5503–5519, doi:10.5194/bg-11-5503-2014, 2014.

44

Appendix

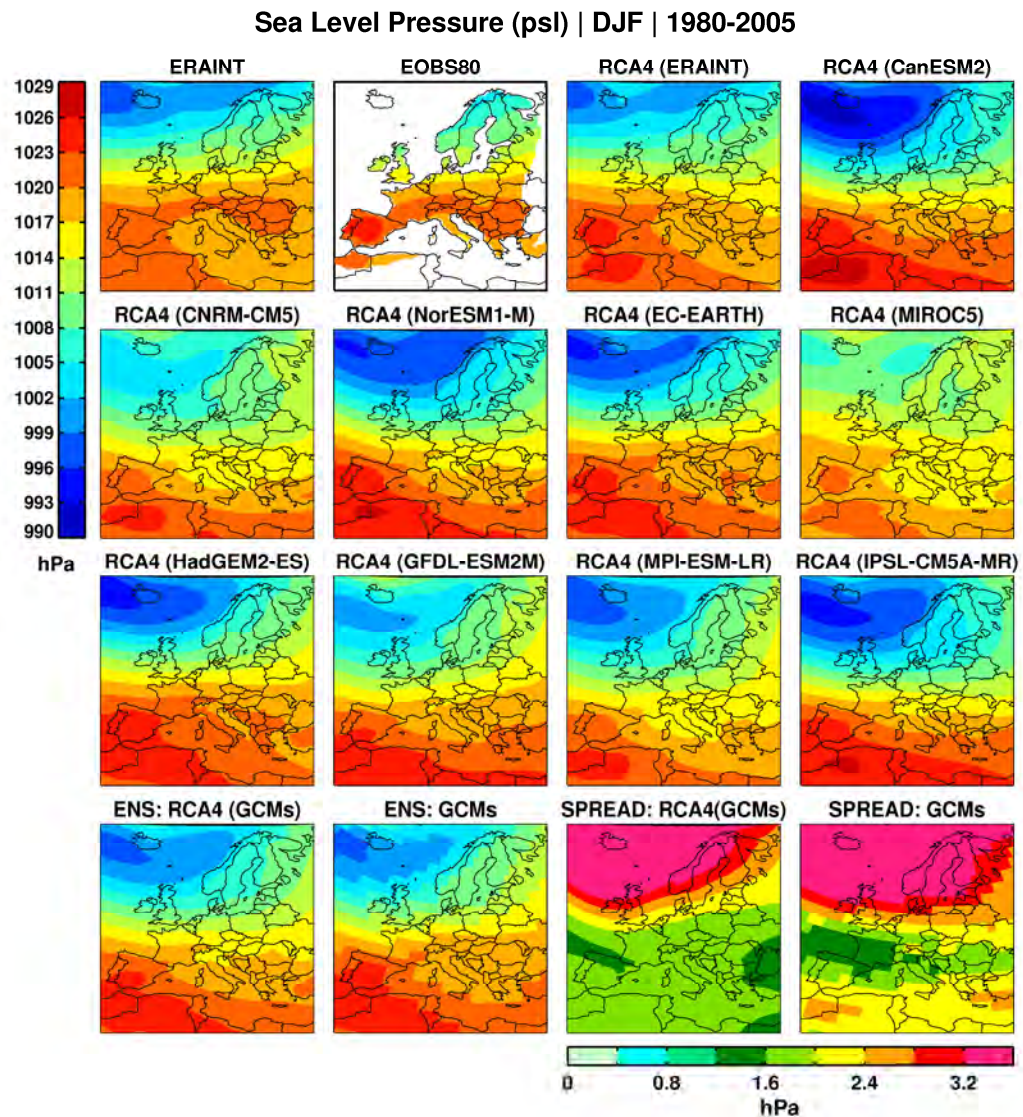The following pages present further information on RCA4 evaluation and scenarios.

Figure A1. Winter (December – February) sea level pressure (hPa) in the recent past climate, 1980-2005, according to ERAINT, E-OBS, RCA4 forced with ERAINT and RCA4 forced with 9 different GCMs (rows 1-3). Bottom row: ensemble mean in RCA4 forced by GCMs, ensemble mean in GCMs, spread between the members in the RCA4 GCM ensemble and spread in the GCM ensemble given as the standard deviation.
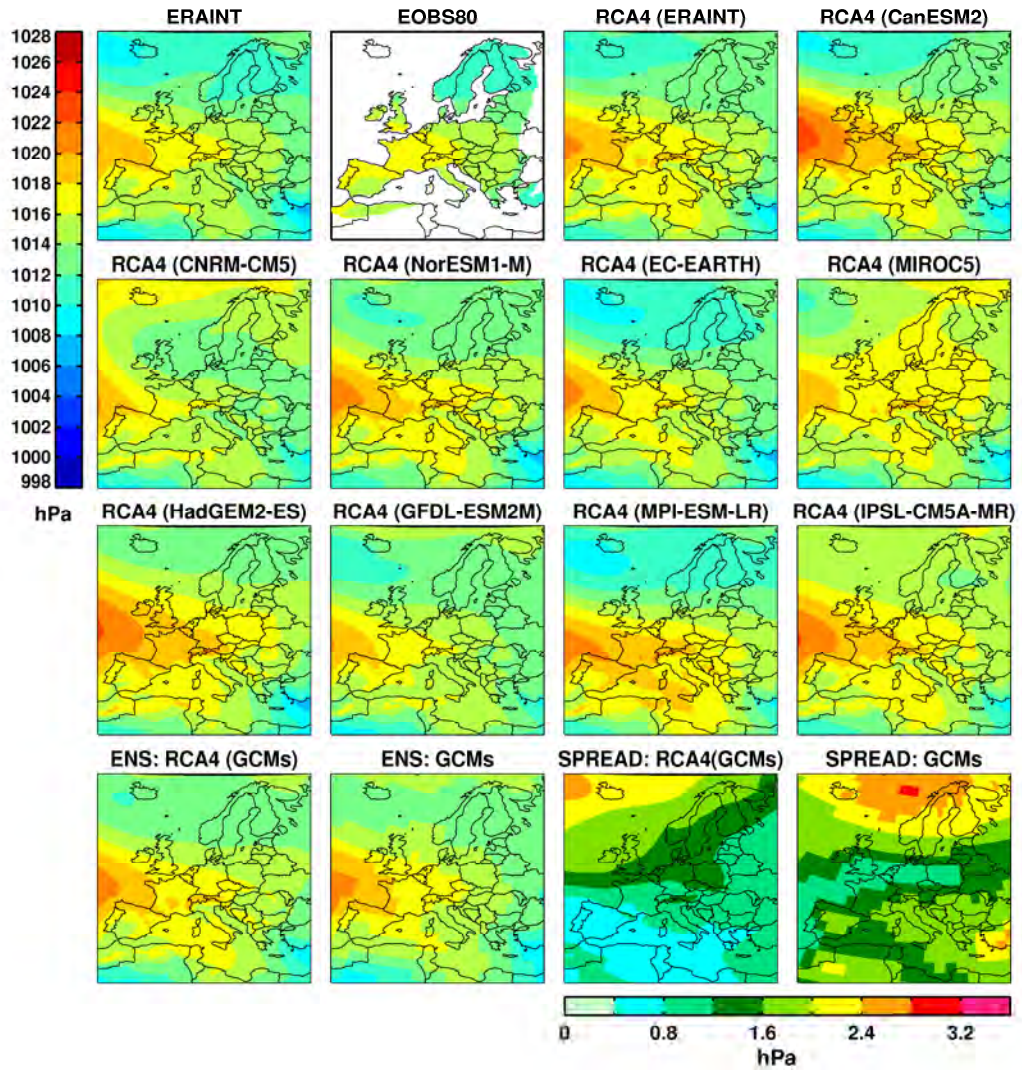
Figure A2. Summer (June – August) sea level pressure (hPa) in the recent past climate, 1980-2005, according to ERAINT, E-OBS, RCA4 forced with ERAINT and RCA4 forced with 9 different GCMs (rows 1-3). Bottom row: ensemble mean in RCA4 forced by GCMs, ensemble mean in GCMs, spread between members in the RCA4 GCM ensemble and spread in the GCM ensemble given as standard deviation.
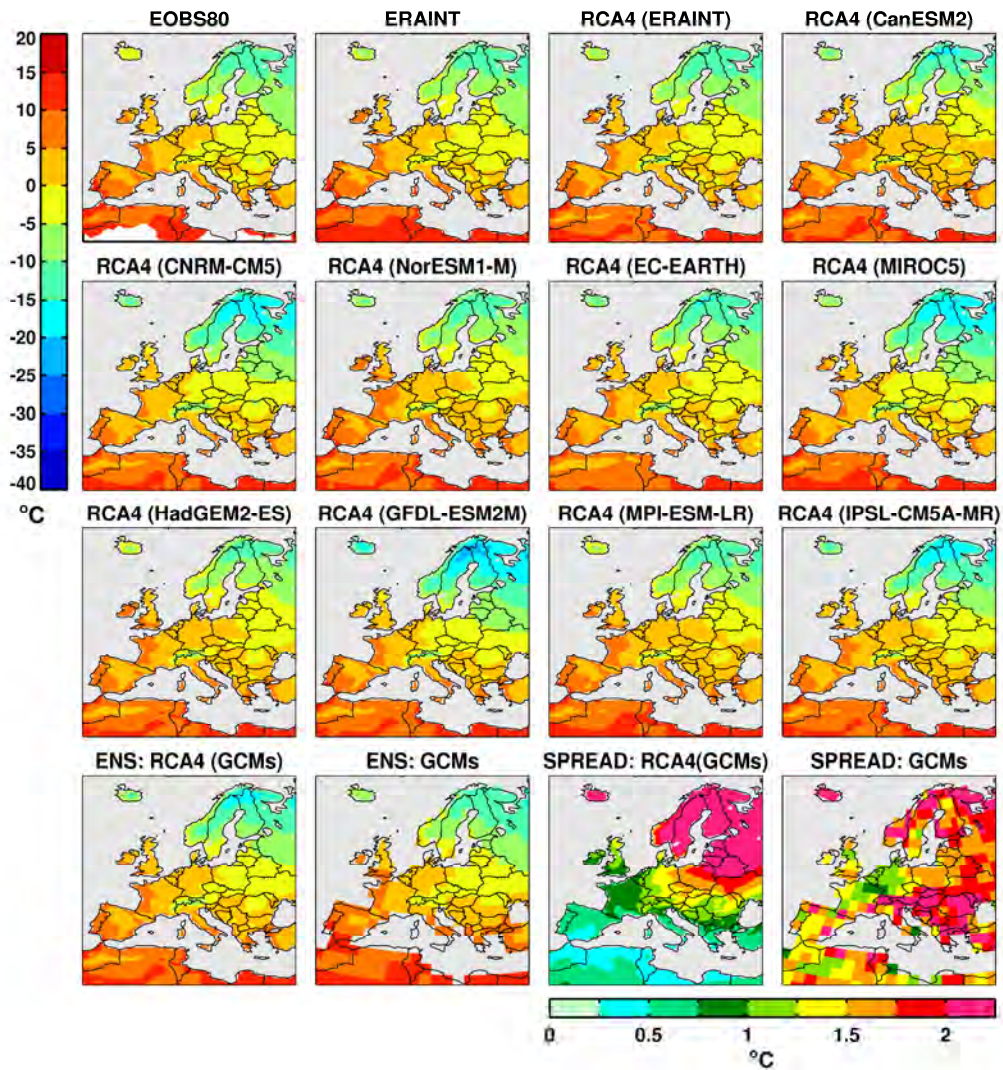
Figure A3. Winter (December – February) temperature (°C) in the recent past climate, 1980-2005, according to E-OBS, ERAINT, RCA4 forced with ERAINT and RCA4 forced with 9 different GCMs (rows 1-3). Bottom row: ensemble mean in RCA4 forced by GCMs, ensemble mean in GCMs, spread between members in the RCA4 GCM ensemble and spread in the GCM ensemble given as standard deviation.

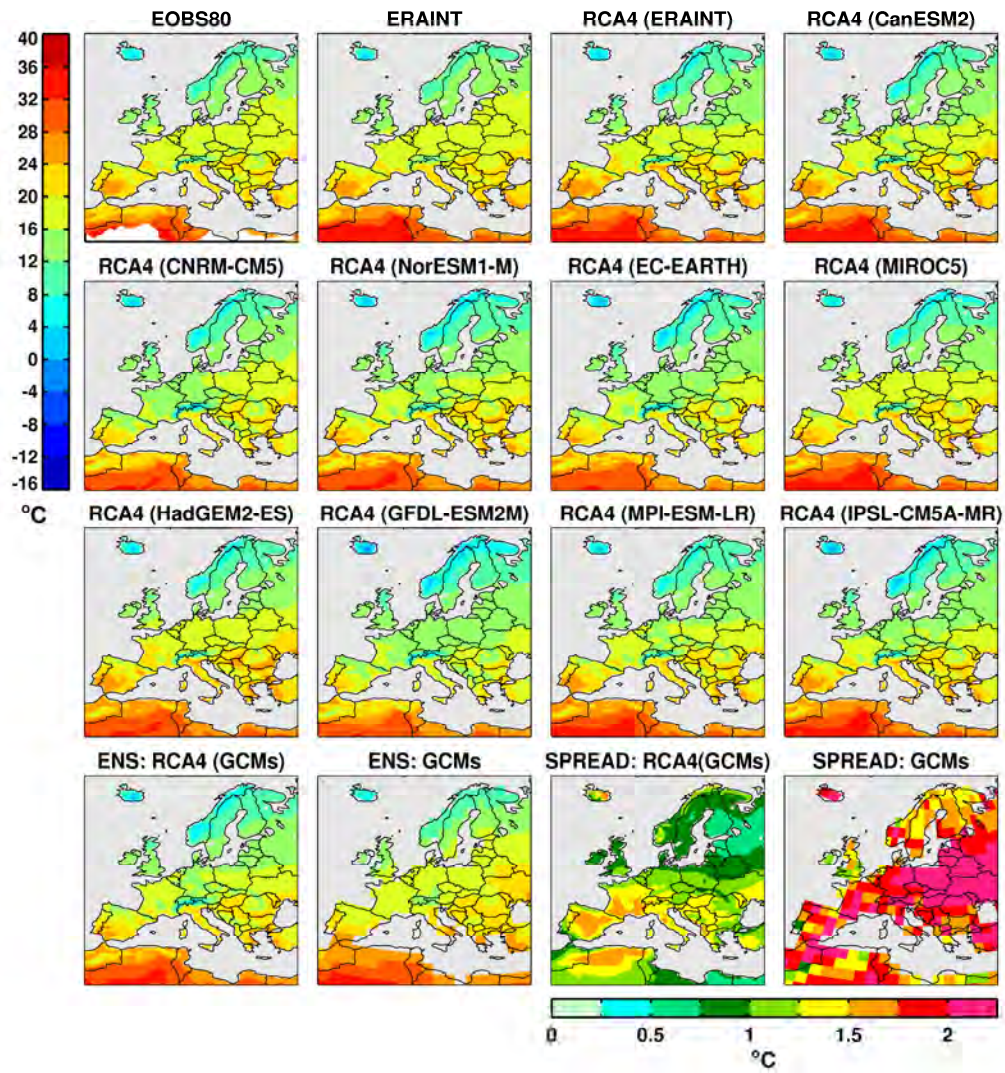**2m Temperature (tas) | JJA | 1980-2005**

Figure A4. Summer (June – August) temperature (°C) in the recent past climate, 1980-2005, according to E-OBS, ERAINT, RCA4 forced with ERAINT and RCA4 forced with 9 different GCMs (rows 1-3). Bottom row: ensemble mean in RCA4 forced by GCMs, ensemble mean in GCMs, spread between members in the RCA4 GCM ensemble and spread in the GCM ensemble given as standard deviation.

Precipitation (pr) | DJF | 1980-2005
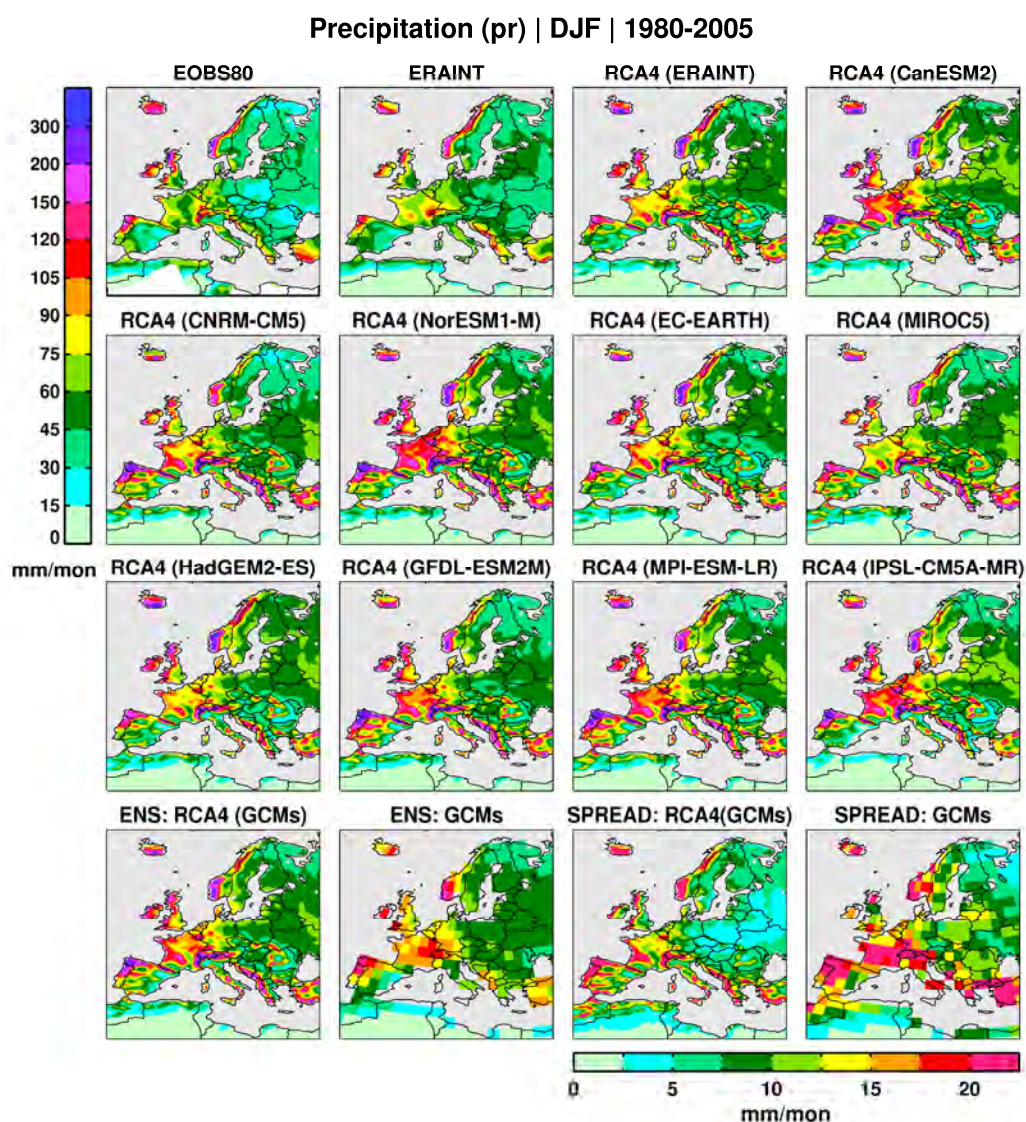

Figure A5. Winter (December – February) precipitation (mm/mon) in the recent past climate, 1980-2005, according to E-OBS, ERAINT, RCA4 forced with ERAINT and RCA4 forced with 9 different GCMs (rows 1-3). Bottom row: ensemble mean in RCA4 forced by GCMs, ensemble mean in GCMs, spread between members in the RCA4 GCM ensemble and spread in the GCM ensemble given as standard deviation.

Precipitation (pr) | JJA | 1980-2005
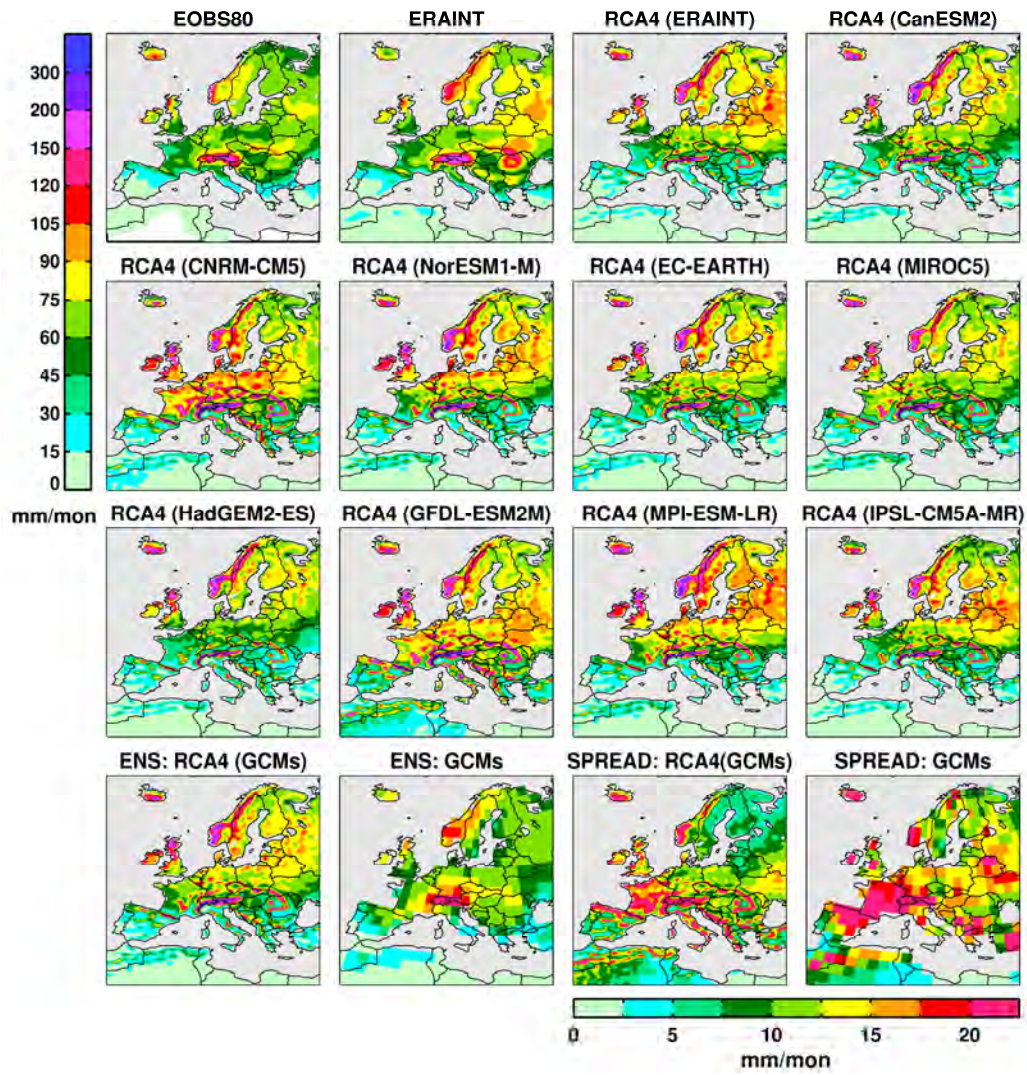
Figure A6. Summer (June – August) precipitation (mm/mon) in the recent past climate, 1980-2005, according to E-OBS, ERAINT, RCA4 forced with ERAINT and RCA4 forced with 9 different GCMs (rows 1-3). Bottom row: ensemble mean in RCA4 forced by GCMs, ensemble mean in GCMs, spread between members in the RCA4 GCM ensemble and spread in the GCM ensemble given as standard deviation.
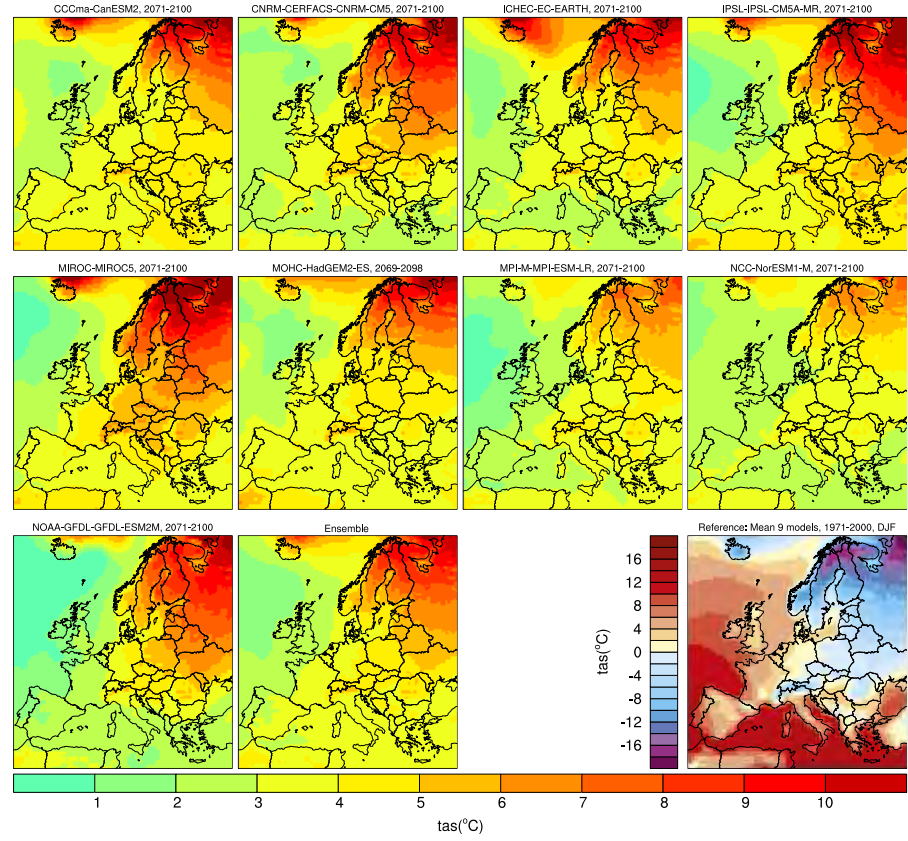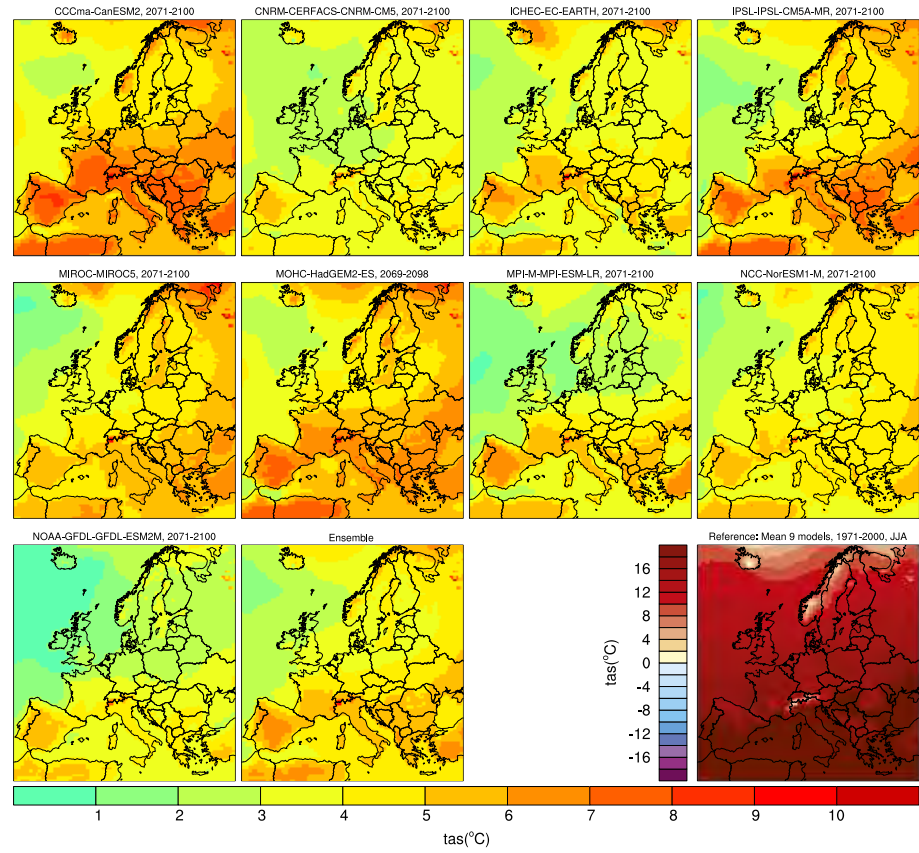
Figure A7. Difference in temperature (°C) 2071-2100 compared to 1971-2000 in RCA4 forced with 9 different GCMs and the RCA4 ensemble mean according to RCP 8.5. The ensemble mean of the absolute temperature (°C), 1971-2000, is shown in the bottom right corner. A: winter (December – February), B: summer (June – August).
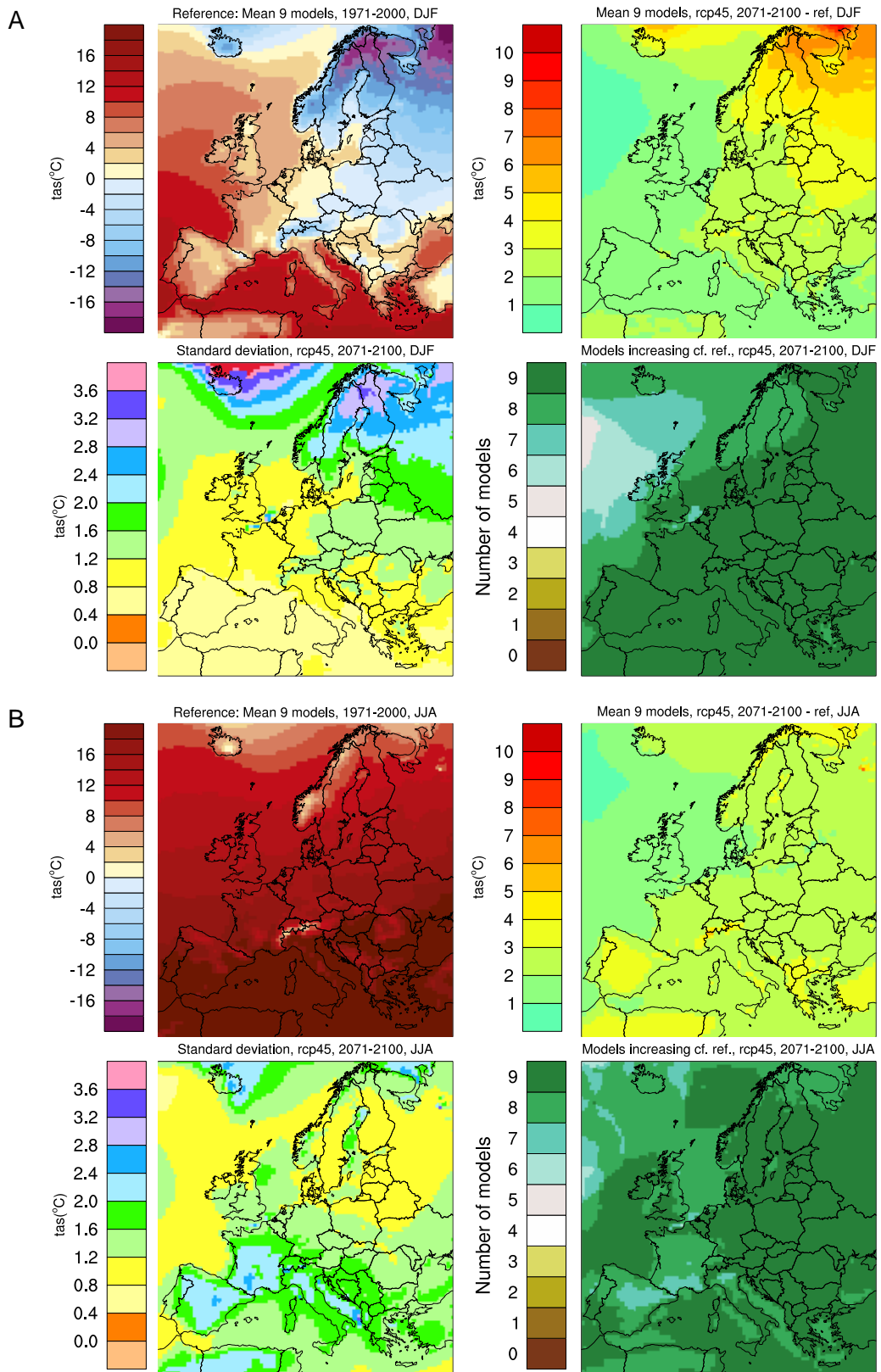
Figure A8. Ensemble mean temperature (°C) in the control period 1971-2000 (upper left). Change in ensemble mean (°C) for 2071-2100 compared with 1971-2000 (upper right). Standard deviation (°C) for members of the ensemble for the period 2071-2100 (lower left). Number of climate scenarios in the ensemble that show an increase for the period 2071-2100 compared to the control period 1971-2000 (lower right). All according to the RCP 4.5 scenario. A: winter (December – February), B: summer (June – August).
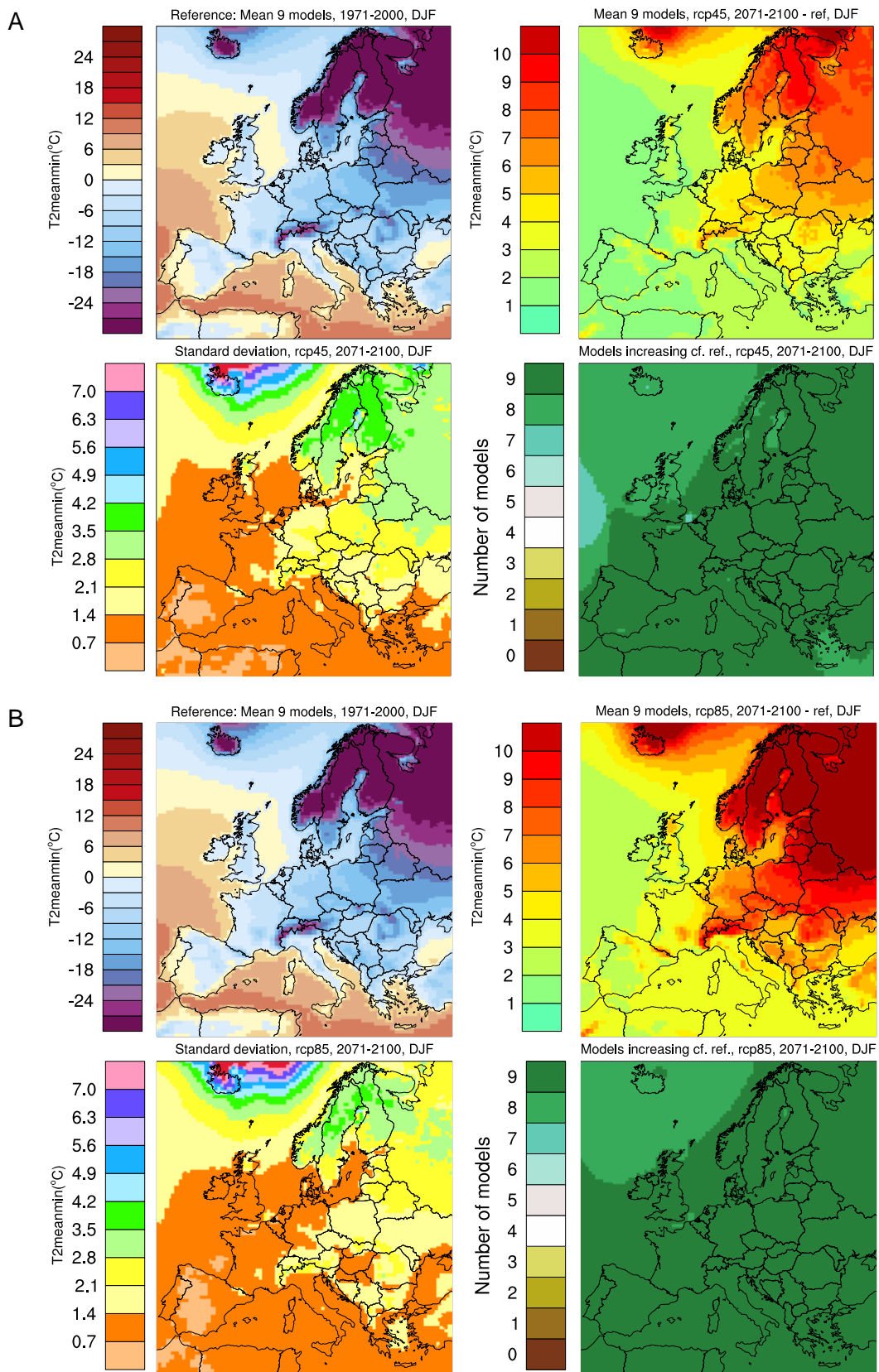
Figure A9. Ensemble mean minimum winter (December - February) temperature (˚C) in the control period 1971-2000 (upper left). Change in ensemble mean (°C) for 2071-2100 compared with 1971-2000 (upper right). Standard deviation (°C) for members of the ensemble for the period 2071-2100 (lower left). Number of climate scenarios in the ensemble that show an increase for the period 2071-2100 compared to the control period 1971-2000 (lower right). According to the scenarios RCP 4.5 (A) and RCP 8.5 (B).

Figure A10. Ensemble mean maximum summer (June – August) temperature (°C) in the control period 1971-2000 (upper left). Change in ensemble mean (°C) for 2071-2100 compared with 1971-2000 (upper right). Standard deviation (°C) for members of the ensemble for the period 2071-2100 (lower left). Number of climate scenarios in the ensemble that show an increase for the period 2071-2100 compared to the control period 1971-2000 (lower right). According to the scenarios RCP 4.5 (A) and RCP 8.5 (B).

Figure A11. A: Ensemble mean start of the vegetation period (day number) in
the control period 1971-2000 (upper left). Change in ensemble mean (day no.)
for 2071-2100 compared with 1971-2000 (upper right). Standard deviation (day
no.) for members of the ensemble for the period 2071-2100 (lower left).
Number of climate scenarios in the ensemble that show an increase for the
period 2071-2100 compared to the control period 1971-2000 (lower right),
according to scenario RCP 8.5. B: same as A, but for the end of the vegetation
period.
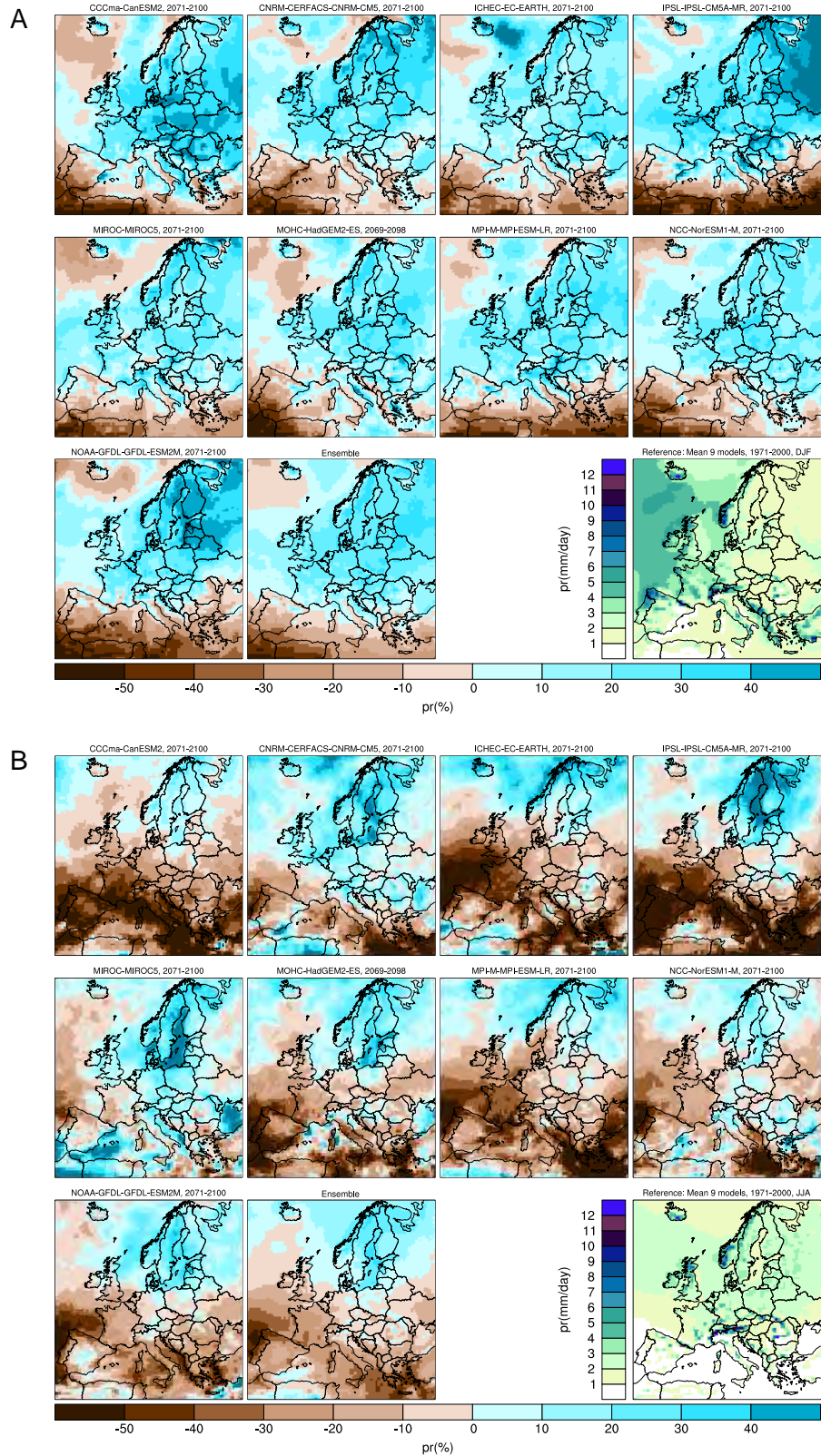
Figure A12. Difference in precipitation (%) 2071-2100 compared to 1971-2000 in RCA4 forced with 9 different GCMs and the RCA4 ensemble mean according to RCP 8.5. The ensemble mean of the absolute precipitation (mm/day), 1971-2000, is shown in the bottom right corner. A) winter (December – February), B) summer (June – August).
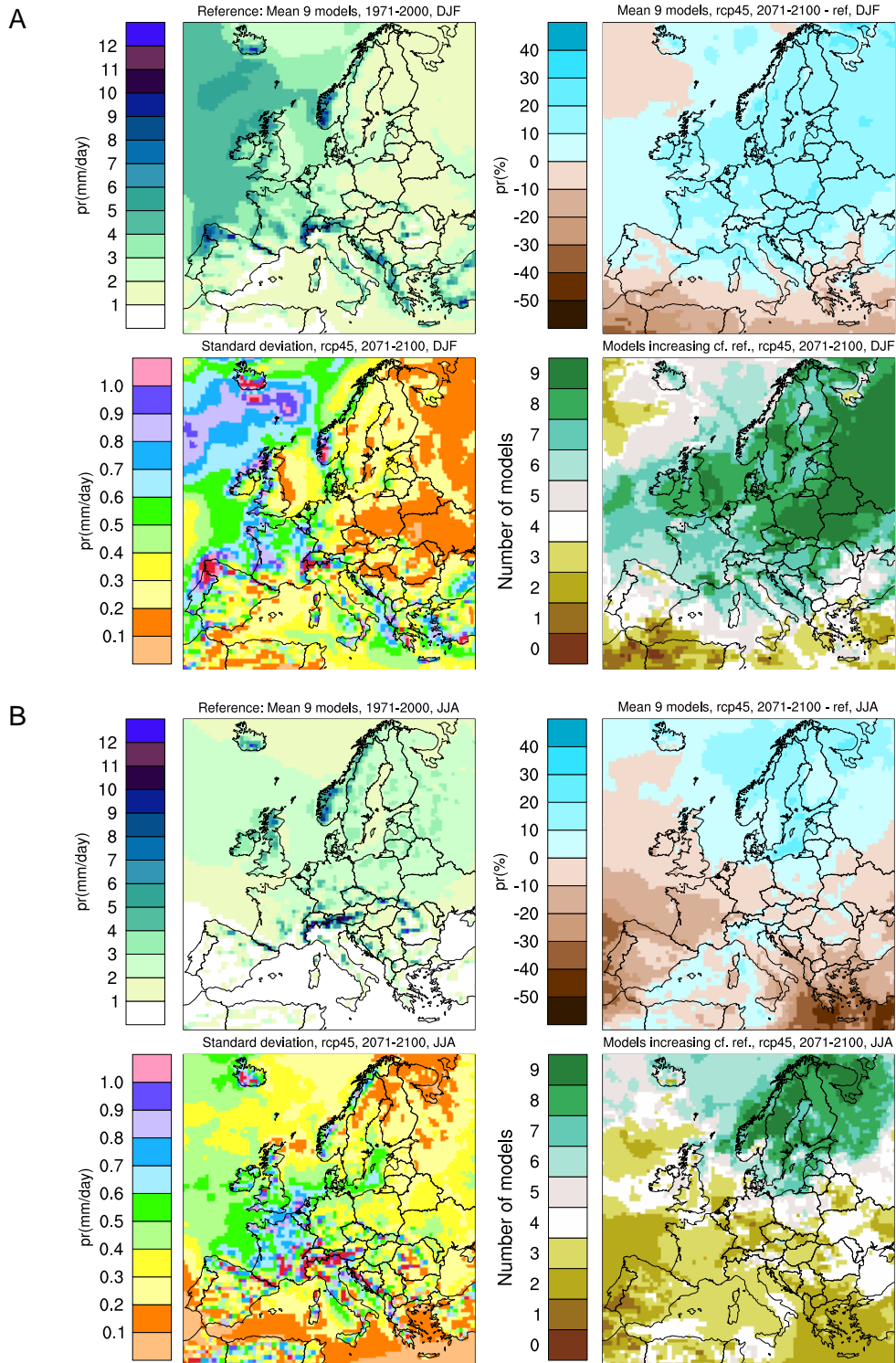
Figure A13. Ensemble mean precipitation (mm/day) in the control period 1971-2000 (upper left). Change in ensemble mean (%) for 2071-2100 compared with 1971-2000 (upper right). Standard deviation (mm/day) for members of the ensemble for the period 2071-2100 (lower left). Number of climate scenarios in the ensemble that show an increase for the period 2071-2100 compared to the control period 1971-2000 (lower right). All according to the RCP 4.5 scenario. A: winter (December – February), B: summer (June – August).
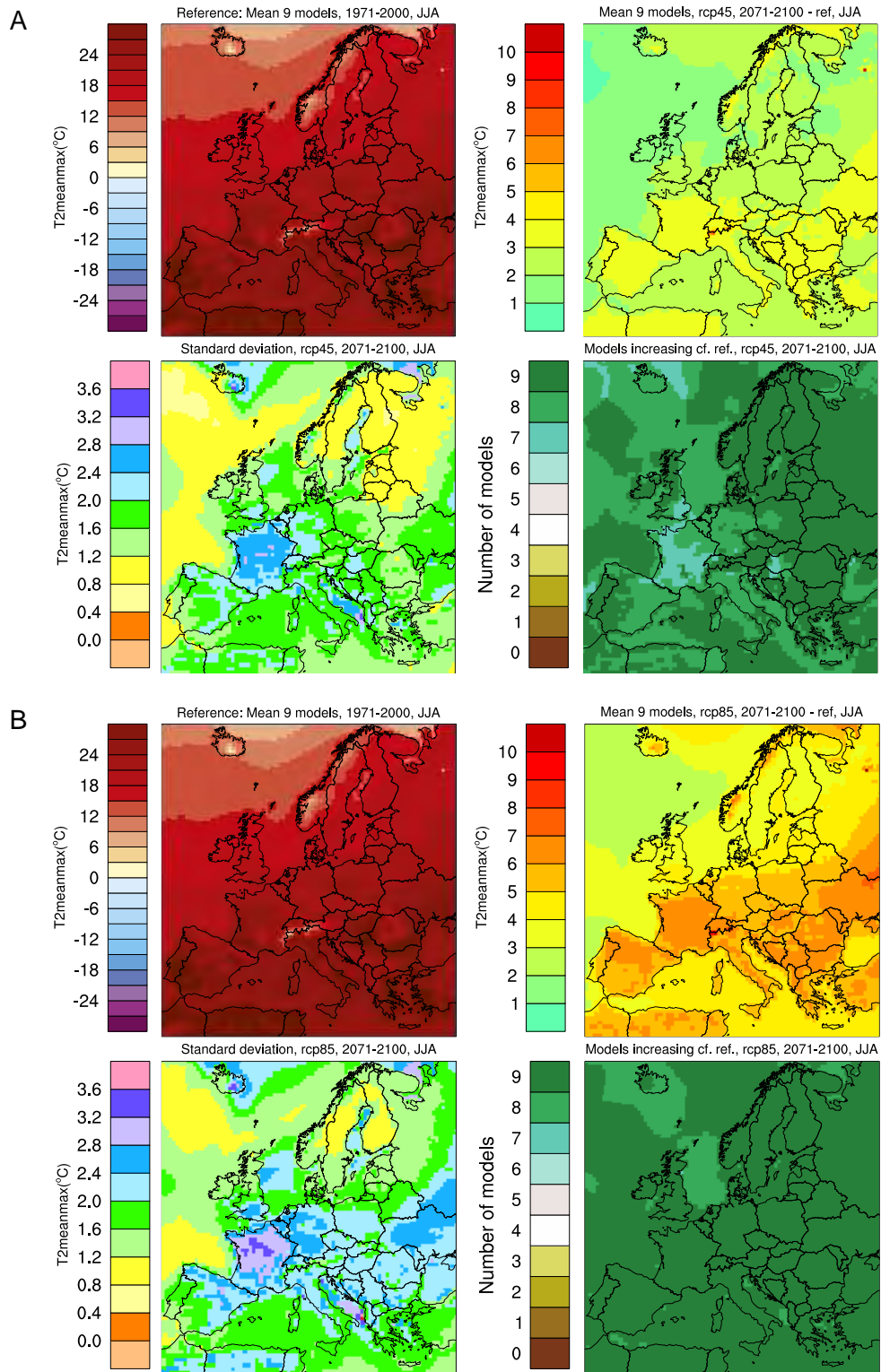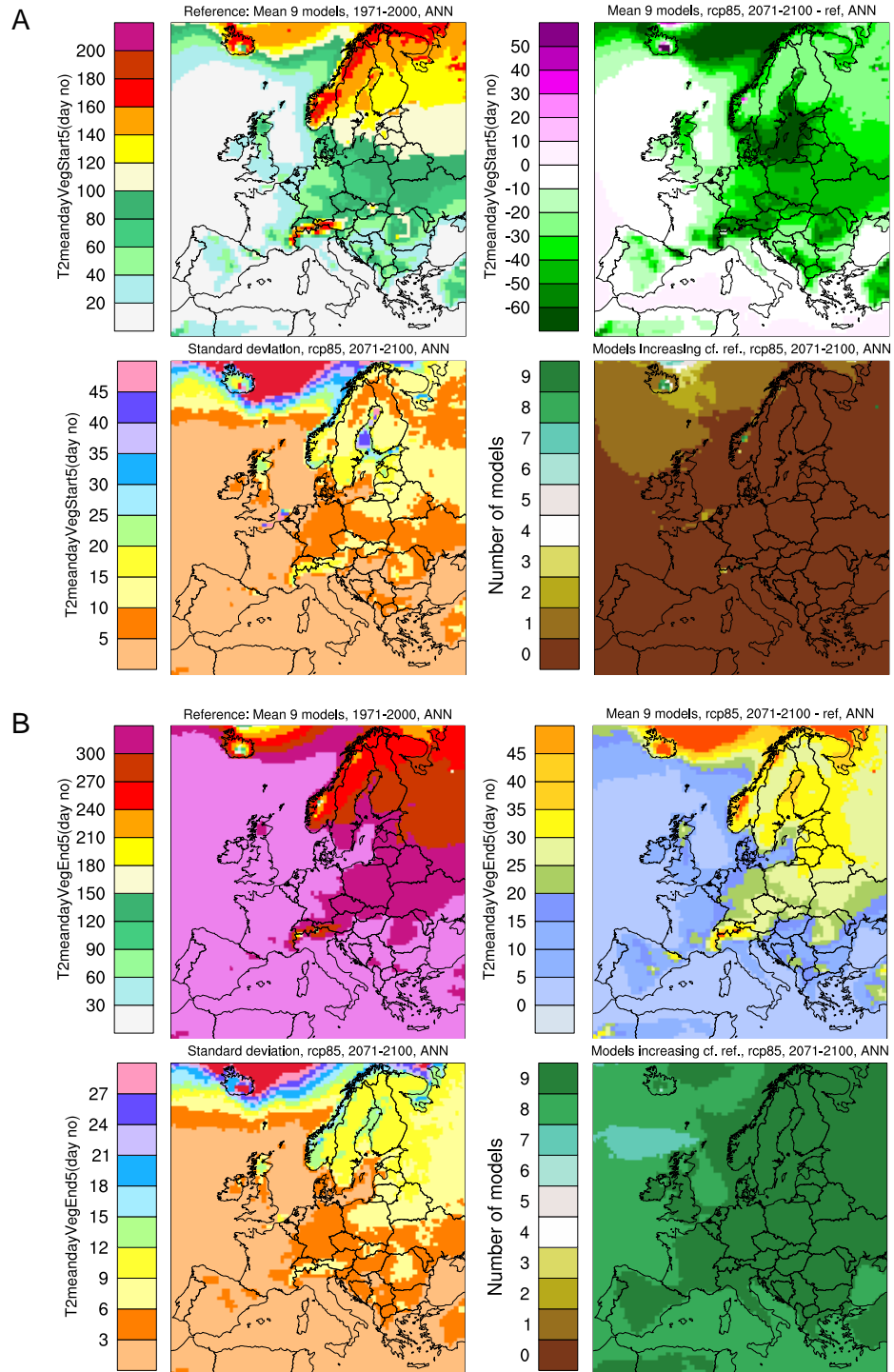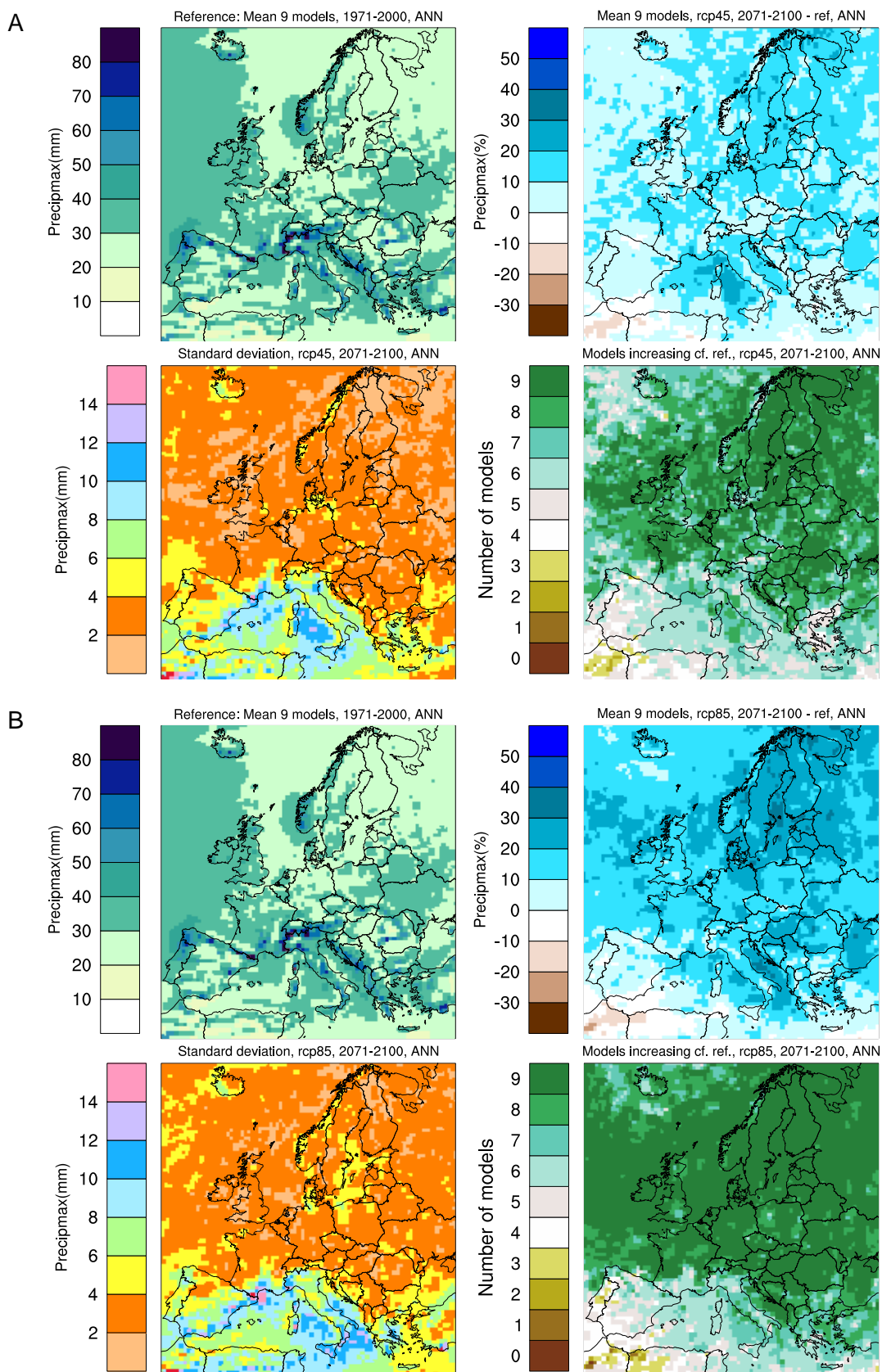
Figure A14. Ensemble annual mean maximum daily precipitation (mm) in the control period 1971-2000 (upper left). Change in ensemble mean (%) for 2071-2100 compared with 1971-2000 (upper right). Standard deviation (mm) for members of the ensemble for the period 2071-2100 (lower left). Number of climate scenarios in the ensemble that show an increase for the period 2071-2100 compared to the control period 1971-2000 (lower right). A: RCP 4.5, B: RCP 8.5.
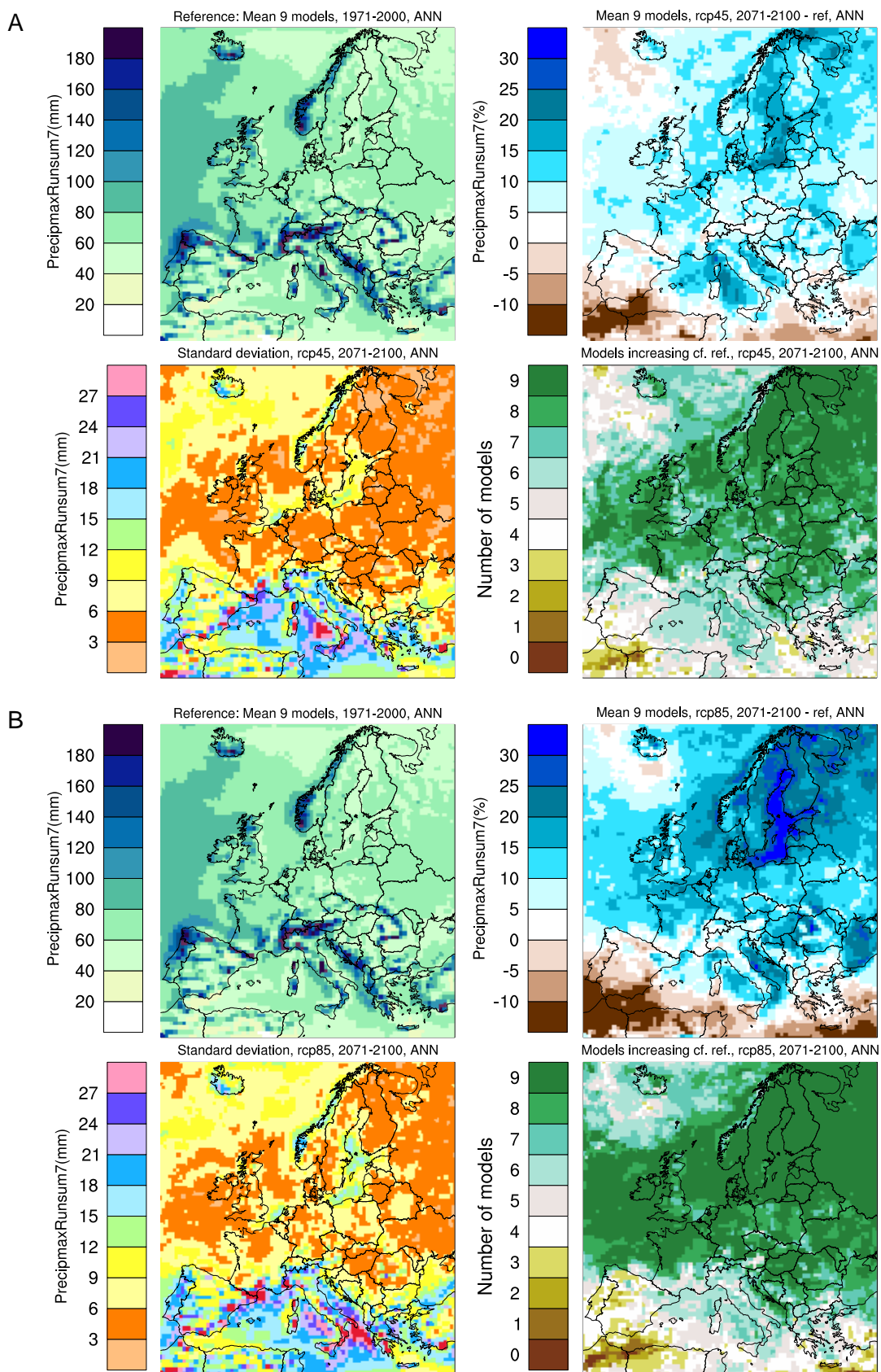
Figure A15. Ensemble annual mean of maximum precipitation amount during seven consecutive days (mm) in the control period 1971-2000 (upper left). Change in ensemble mean (%) for 2071-2100 compared with 1971-2000 (upper right). Standard deviation (mm) for members of the ensemble for the period 2071-2100 (lower left). Number of climate scenarios in the ensemble that show an increase for the period 2071-2100 compared to the control period 1971-2000 (lower right). A: RCP 4.5, B: RCP 8.5.
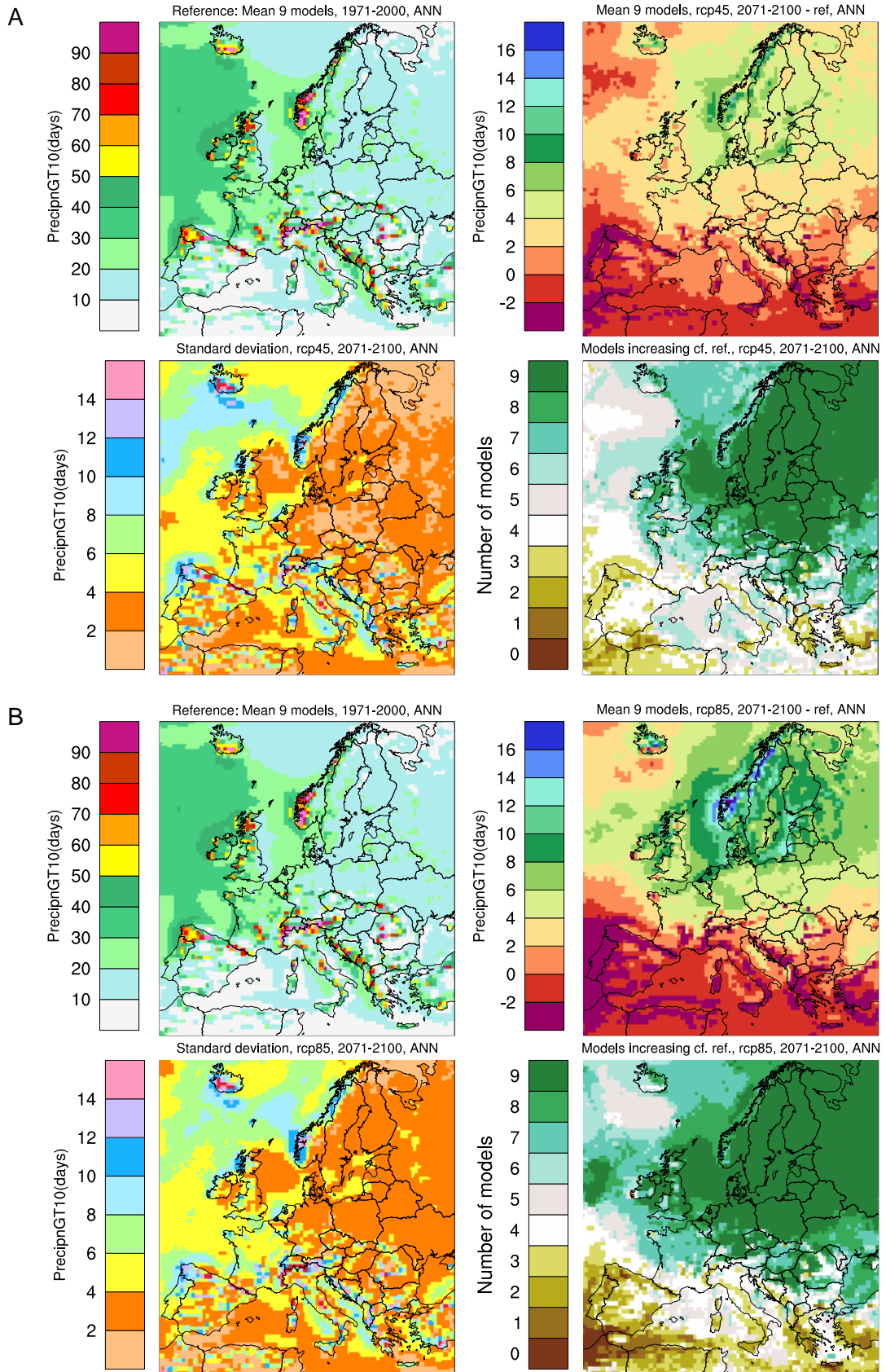
Figure A16. Ensemble annual mean of number of days with heavy precipitation (no. of days with precipitation over 10 mm) in the control period 1971-2000 (upper left). Change in ensemble mean (days) for 2071-2100 compared with 1971-2000 (upper right). Standard deviation (days) for members of the ensemble for the period 2071-2100 (lower left). Number of climate scenarios in the ensemble that show an increase for the period 2071-2100 compared to the control period 1971-2000 (lower right). A: RCP 4.5, B: RCP 8.5.

Figure A17. Ensemble annual mean of number of dry days (no. days with precipitation less than 1 mm) in the control period 1971-2000 (upper left). Change in ensemble mean (days) for 2071-2100 compared with 1971-2000 (upper right). Standard deviation (days) for members of the ensemble for the period 2071-2100 (lower left). Number of climate scenarios in the ensemble that show an increase for the period 2071-2100 compared to the control period 1971-2000 (lower right). A: RCP 4.5, B: RCP 8.5.
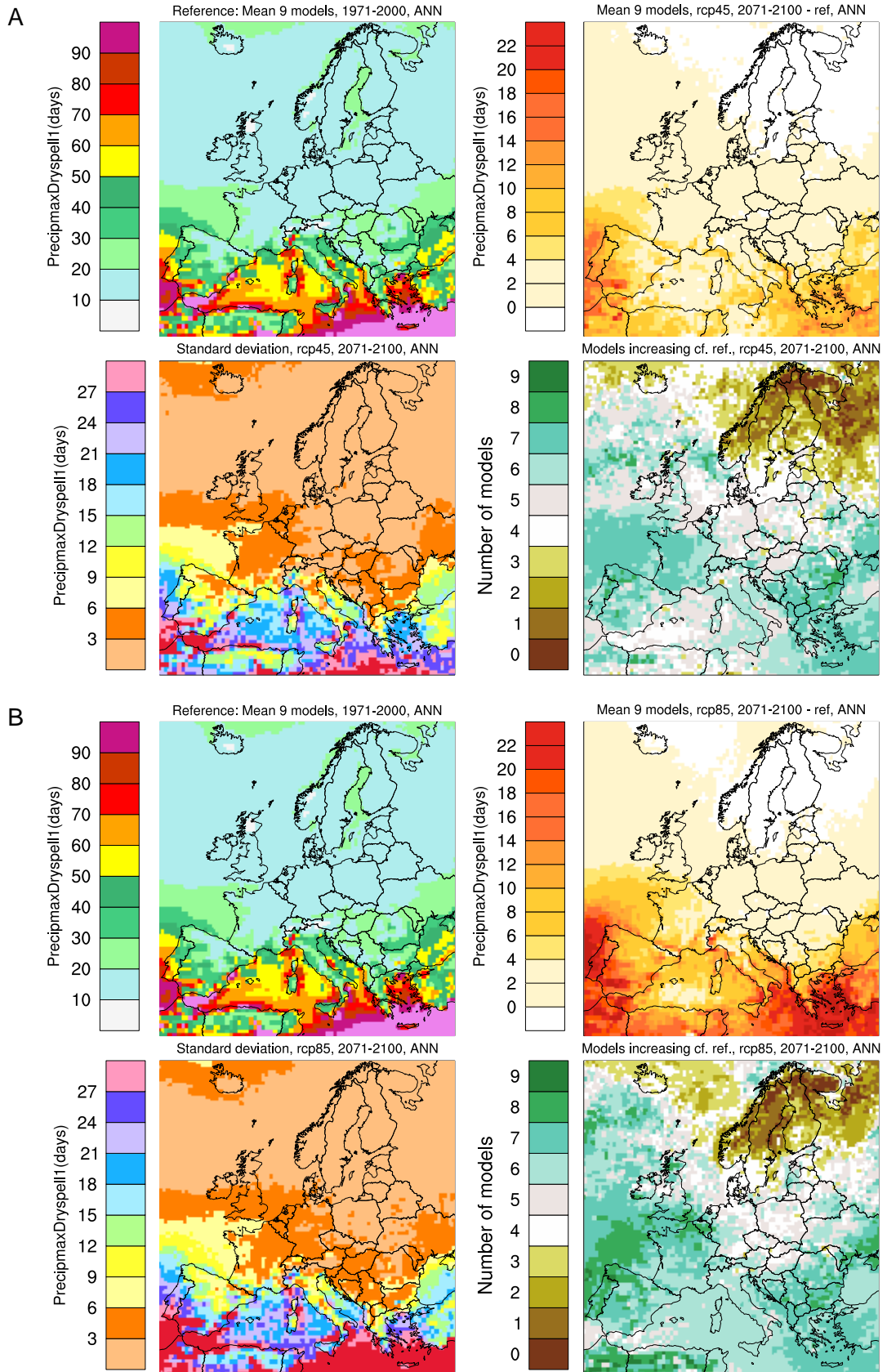
Table A1. Statistical properties in an ensemble using all GCMs (All), the nine GCMs used by
RCA4 (Ens), four randomly selected ensembles of nine GCMs (Rnd1-4) and the down-scaled
RCA4 ensemble (RCA); for mean temperature and precipitation (T mean(°C), P mean(%)),
standard deviation of temperature and precipitation (T std(°C), P std(%)) and the correlation
between temperature and precipitation (Corr); for Sweden (SWE), West Continental Europe
(WCE), Iberian Peninsula (IBP) and South East Europe (SEE).

```
--- SWE ANN RCP85 ---
          All    Ens    Rnd1   Rnd2   Rnd3   Rnd4    RCA
T mean:   4.86   4.81   4.44   4.95   5.38   4.17   4.58
T std :   1.25   0.86   1.63   1.14   1.05   0.47   0.66
P mean:  15.85  17.15  18.82  12.22  17.89  14.91  22.19
P std :   7.86   5.22   8.91   4.47   9.00   4.64   5.08
Corr. :   0.38  -0.16   0.73   0.19   0.28   0.03   0.55


--- SWE DJF RCP85 ---
          All    Ens    Rnd1   Rnd2   Rnd3   Rnd4    RCA
T mean:   5.48   5.14   5.15   5.92   6.16   4.67   5.43
T std :   1.55   0.61   1.82   1.76   1.06   0.54   0.94
P mean:  23.91  22.95  25.35  18.98  28.42  20.67  23.75
P std :  10.86   6.49  12.96   6.95  13.76   9.03   5.14
Corr. :   0.37  -0.22   0.46   0.51   0.02  -0.28   0.23


--- SWE JJA RCP85 ---
          All    Ens    Rnd1   Rnd2   Rnd3   Rnd4    RCA
T mean:   4.72   4.69   4.12   4.65   5.22   4.02   3.98
T std :   1.45   1.36   1.49   1.19   1.55   1.10   0.81
P mean:   5.54   7.98   9.39   5.69   4.11  10.21  19.82
P std :  16.95  19.59  18.08  12.71  15.57  17.76  12.72
Corr. :  -0.00  -0.25   0.58  -0.49  -0.11  -0.36   0.35


--- WCE ANN RCP85 ---
          All    Ens    Rnd1   Rnd2   Rnd3   Rnd4    RCA
T mean:   4.30   4.29   3.87   3.97   4.71   3.58   3.73
T std :   1.14   1.02   1.25   1.05   1.33   1.03   0.68
P mean:   1.42   4.00   4.99   1.41  -0.06   1.00   5.41
P std :   7.25   6.82   7.24   8.16   4.95   4.80   4.39
Corr. :  -0.10   0.10   0.19   0.14  -0.08  -0.16  -0.28


--- WCE DJF RCP85 ---
          All    Ens    Rnd1   Rnd2   Rnd3   Rnd4    RCA
T mean:   3.87   3.73   3.70   3.65   4.07   3.13   3.58
T std :   1.04   0.65   1.19   1.20   1.05   0.72   0.57
P mean:  14.02  21.57  15.92  11.36  13.31  17.03  19.89
P std :  10.73  10.22   9.44  10.20  14.04   7.07   7.41
Corr. :   0.07  -0.02   0.33   0.38   0.12   0.57  -0.45


--- WCE JJA RCP85 ---
          All    Ens    Rnd1   Rnd2   Rnd3   Rnd4    RCA
T mean:   5.45   5.51   4.56   4.87   6.25   4.52   4.47
T std :   1.93   1.85   1.96   1.65   2.42   1.71   1.15
```

```
P mean: -14.96 -18.77  -3.24  -9.12 -16.42 -17.20 -16.51
P std :  21.02  22.38  19.05  18.86  22.69  15.72  14.04
Corr. :  -0.56  -0.60  -0.41  -0.45  -0.48  -0.79  -0.63


--- IBP ANN RCP85 ---
          All    Ens   Rnd1   Rnd2   Rnd3   Rnd4    RCA
T mean:  4.68   4.69   4.39   4.27   5.06   4.12   4.37
T std :  1.03   0.82   1.18   0.84   1.33   0.95   0.75
P mean: -22.75 -22.16 -21.27 -20.81 -25.00 -23.04 -20.29
P std :  8.45   8.85  10.75   7.65   8.23   8.53   7.43
Corr. : -0.52  -0.48  -0.27  -0.43  -0.61  -0.48  -0.60


--- IBP DJF RCP85 ---
          All    Ens   Rnd1   Rnd2   Rnd3   Rnd4    RCA
T mean:  3.36   3.39   3.07   3.07   3.43   2.90   3.09
T std :  0.79   0.53   0.84   0.77   0.91   0.81   0.54
P mean: -13.86 -14.14 -11.52 -13.09 -15.93 -14.89 -12.56
P std :  15.44  13.87  19.99  10.12  19.13  13.41   8.88
Corr. : -0.24   0.03  -0.29   0.13  -0.55  -0.20  -0.03


--- IBP JJA RCP85 ---
          All    Ens   Rnd1   Rnd2   Rnd3   Rnd4    RCA
T mean:  6.27   6.34   5.91   5.73   7.05   5.61   5.71
T std :  1.52   1.10   1.71   1.19   2.10   1.09   0.80
P mean: -33.53 -35.38 -30.80 -26.23 -34.84 -33.02 -25.29
P std :  15.78  21.64  10.74  13.59  13.58  18.51  18.55
Corr. : -0.29  -0.60  -0.25  -0.55  -0.17  -0.30  -0.80


--- SEE ANN RCP85 ---
          All    Ens   Rnd1   Rnd2   Rnd3   Rnd4    RCA
T mean:  4.99   5.12   4.63   4.58   5.19   4.46   4.31
T std :  1.23   1.06   1.27   1.05   1.45   1.30   0.74
P mean: -8.08  -7.19  -6.09  -6.36 -10.60  -9.11  -0.80
P std :  8.63  11.00   7.15   7.12   9.46   9.29   5.38
Corr. : -0.21  -0.15   0.07   0.19  -0.08  -0.31  -0.32


--- SEE DJF RCP85 ---
          All    Ens   Rnd1   Rnd2   Rnd3   Rnd4    RCA
T mean:  4.39   4.48   4.24   4.15   4.44   3.99   4.11
T std :  1.13   0.82   1.05   1.34   1.25   0.91   0.50
P mean:  0.74   6.25   0.23   2.66  -1.84   2.95   9.17
P std :  13.13  13.11  12.66  11.10  18.26  11.13   8.02
Corr. :  0.06   0.38   0.39   0.15   0.18   0.21   0.14


--- SEE JJA RCP85 ---
          All    Ens   Rnd1   Rnd2   Rnd3   Rnd4    RCA
T mean:  6.55   6.72   5.86   5.85   7.06   5.77   5.37
T std :  1.95   1.79   1.90   1.68   2.48   2.03   1.17
P mean: -21.39 -22.88 -15.45 -19.06 -23.97 -23.78 -10.28
P std :  15.35  18.62  12.43  12.82  11.63  17.41   9.39
Corr. : -0.45  -0.46  -0.29  -0.51  -0.35  -0.54  -0.46
```

```
--- GBR ANN RCP85 ---
          All    Ens   Rnd1   Rnd2   Rnd3   Rnd4    RCA
T mean:   3.52   3.67   3.30   3.25   3.68   3.19   3.80
T std :   0.66   0.65   0.63   0.53   0.80   0.74   0.64
P mean:  -0.62  -1.85   0.45  -0.77  -1.16  -2.64  -8.44
P std :   4.91   4.98   5.80   3.90   6.56   2.84   4.91
Corr. :   0.25  -0.09   0.44   0.41  -0.03   0.76  -0.12


--- GBR DJF RCP85 ---
          All    Ens   Rnd1   Rnd2   Rnd3   Rnd4    RCA
T mean:   3.33   3.45   3.16   3.13   3.45   3.03   3.24
T std :   0.57   0.58   0.55   0.50   0.66   0.68   0.49
P mean:   0.84  -0.58   0.80   0.37   2.72  -2.36  -0.21
P std :   5.69   4.53   7.90   3.85   5.44   4.05   5.83
Corr. :   0.56   0.74   0.62   0.54   0.55   0.74   0.09


--- GBR JJA RCP85 ---
          All    Ens   Rnd1   Rnd2   Rnd3   Rnd4    RCA
T mean:   3.72   3.88   3.46   3.40   3.95   3.38   4.35
T std :   0.74   0.69   0.70   0.60   0.95   0.78   0.71
P mean:  -3.48  -5.92  -1.42  -3.24  -5.47  -5.47 -19.34
P std :   6.46   7.20   6.49   4.46   9.75   3.20  13.21
Corr. :  -0.09  -0.49   0.27   0.18  -0.28   0.09  -0.28


--- EUR ANN RCP85 ---
          All    Ens   Rnd1   Rnd2   Rnd3   Rnd4    RCA
T mean:   4.82   4.92   4.48   4.58   5.12   4.32   4.08
T std :   0.98   0.80   1.07   0.87   1.22   0.85   0.65
P mean:   1.38   1.83   1.68   0.95   2.25   0.55   4.17
P std :   4.32   4.79   5.63   3.28   4.50   4.03   2.64
Corr. :   0.38   0.29   0.69   0.30   0.57  -0.07   0.57


--- EUR DJF RCP85 ---
          All    Ens   Rnd1   Rnd2   Rnd3   Rnd4    RCA
T mean:   4.65   4.67   4.32   4.63   4.90   4.31   4.16
T std :   0.82   0.64   0.79   0.86   0.93   0.71   0.55
P mean:   7.07   7.54   5.08   6.08   8.08   6.52   6.21
P std :   5.27   6.01   5.96   5.32   7.24   4.70   3.57
Corr. :   0.51   0.65   0.47   0.45   0.42   0.72   0.59


--- EUR JJA RCP85 ---
          All    Ens   Rnd1   Rnd2   Rnd3   Rnd4    RCA
T mean:   5.31   5.45   4.91   4.90   5.73   4.68   4.25
T std :   1.27   1.16   1.27   1.08   1.66   1.15   0.85
P mean:  -8.69  -9.00  -5.90  -6.52  -7.99  -8.73  -0.00
P std :  10.97  10.28  11.91  10.25  11.69   8.89   5.22
Corr. :  -0.14  -0.46   0.31  -0.25   0.00  -0.76   0.04
```

SMHI Publications

SMHI publish seven report series. Three of these, the R-series, are intended for international readers and are in most cases written in English. For the others the Swedish language is used.

Name of the series	Published since
RMK (Report Meteorology and Climatology)	1974
RH (Report Hydrology)	1990
RO (Report Oceanography)	1986
METEOROLOGI	1985
HYDROLOGI	1985
OCEANOGRAFI	1985
KLIMATOLOGI	2009

Earlier issues published in serie RMK

1   Thompson, T., Udin, I. and Omstedt, A. (1974)
Sea surface temperatures in waters surrounding Sweden.

2   Bodin, S. (1974)
Development on an unsteady atmospheric boundary layer model.

3   Moen, L. (1975)
A multi-level quasi-geostrophic model for short range weather predictions.

4   Holmström, I. (1976)
Optimization of atmospheric models.

5   Collins, W.G. (1976)
A parameterization model for calculation of vertical fluxes of momentum due to terrain induced gravity waves.

6   Nyberg, A. (1976)
On transport of sulphur over the North Atlantic.

7   Lundqvist, J.-E. and Udin, I. (1977)
Ice accretion on ships with special emphasis on Baltic conditions.

8   Eriksson, B. (1977)
Den dagliga och årliga variationen av temperatur, fuktighet och vindhastighet vid några orter i Sverige.

9   Holmström, I., and Stokes, J. (1978)
Statistical forecasting of sea level changes in the Baltic.

10   Omstedt, A. and Sahlberg, J. (1978)
Some results from a joint Swedish-Finnish sea ice experiment, March, 1977.

11   Haag, T. (1978)
Byggnadsindustrins väderberoende, seminarieuppsats i företagsekonomi, B-nivå.

12   Eriksson, B. (1978)
Vegetationsperioden i Sverige beräknad från temperaturobservationer.

13   Bodin, S. (1979)
En numerisk prognosmodell för det atmosfäriska gränsskiktet, grundad på den turbulenta energiekvationen.

14   Eriksson, B. (1979)
Temperaturfluktuationer under senaste 100 åren.

15   Udin, I. och Mattisson, I. (1979)
Havsis- och snöinformation ur datorbearbetade satellitdata - en modellstudie.

16   Eriksson, B. (1979)
Statistisk analys av nederbördsdata. Del I. Arealnederbörd.

17   Eriksson, B. (1980)
Statistisk analys av nederbördsdata. Del II. Frekvensanalys av månadsnederbörd.

18   Eriksson, B. (1980)
Årsmedelvärden (1931-60) av nederbörd, avdunstning och avrinning.

19   Omstedt, A. (1980)
A sensitivity analysis of steady, free floating ice.

20 Persson, C. och Omstedt, G. (1980)
En modell för beräkning av
luftföroreningars spridning och
deposition på mesoskala.

21 Jansson, D. (1980)
Studier av temperaturinversioner och
vertikal vindskjuvning vid Sundsvall-
Härnösands flygplats.

22 Sahlberg, J. and Törnevik, H. (1980)
A study of large scale cooling in the
Bay of Bothnia.

23 Ericson, K. and Hårsmar, P.-O. (1980)
Boundary layer measurements at
Klock-rike. Oct. 1977.

24 Bringfelt, B. (1980)
A comparison of forest
evapotranspiration determined by some
independent methods.

25 Bodin, S. and Fredriksson, U. (1980)
Uncertainty in wind forecasting for
wind power networks.

26 Eriksson, B. (1980)
Graddagsstatistik för Sverige.

27 Eriksson, B.(1981)
Statistisk analys av nederbördsdata.
Del III. 200-åriga nederbördsserier.

28 Eriksson, B. (1981)
Den "potentiella" evapotranspirationen
i Sverige.

29 Pershagen, H. (1981)
Maximisnödjup i Sverige (perioden
1905-70).

30 Lönnqvist, O. (1981)
Nederbördsstatistik med praktiska
tillämpningar.
(Precipitation statistics with practical
applications.)

31 Melgarejo, J.W. (1981)
Similarity theory and resistance laws
for the atmospheric boundary layer.

32 Liljas, E. (1981)
Analys av moln och nederbörd genom
automatisk klassning av AVHRR-data.

33 Ericson, K. (1982)
Atmospheric boundary layer field
experiment in Sweden 1980, GOTEX
II, part I.

34 Schoeffler, P. (1982)
Dissipation, dispersion and stability of
numerical schemes for advection and
diffusion.

35 Undén, P. (1982)
The Swedish Limited Area Model. Part
A. Formulation.

36 Bringfelt, B. (1982)
A forest evapotranspiration model
using synoptic data.

37 Omstedt, G. (1982)
Spridning av luftförorening från
skorsten i konvektiva gränsskikt.

38 Törnevik, H. (1982)
An aerobiological model for
operational forecasts of pollen
concentration in the air.

39 Eriksson, B. (1982)
Data rörande Sveriges
temperaturklimat.

40 Omstedt, G. (1984)
An operational air pollution model
using routine meteorological data.

41 Persson, C. and Funkquist, L. (1984)
Local scale plume model for nitrogen
oxides. Model description.

42 Gollvik, S. (1984)
Estimation of orographic precipitation
by dynamical interpretation of synoptic
model data.

43 Lönnqvist, O. (1984)
Congression - A fast regression
technique with a great number of
functions of all predictors.

44 Laurin, S. (1984)
Population exposure to SO and NO_x
from different sources in Stockholm.

45 Svensson, J. (1985)
Remote sensing of atmospheric
tempera-ture profiles by TIROS
Operational Vertical Sounder.

46 Eriksson, B. (1986)
Nederbörds- och humiditetsklimat i
Sverige under vegetationsperioden.

47 Taesler, R. (1986)
Köldperioden av olika längd och
förekomst.

48   Wu Zengmao (1986)
Numerical study of lake-land breeze over Lake Vättern, Sweden.

49   Wu Zengmao (1986)
Numerical analysis of initialization procedure in a two-dimensional lake breeze model.

50   Persson, C. (1986)
Local scale plume model for nitrogen oxides. Verification.

51   Melgarejo, J.W. (1986)
An analytical model of the boundary layer above sloping terrain with an application to observations in Antarctica.

52   Bringfelt, B. (1986)
Test of a forest evapotranspiration model.

53   Josefsson, W. (1986)
Solar ultraviolet radiation in Sweden.

54   Dahlström, B. (1986)
Determination of areal precipitation for the Baltic Sea.

55   Persson, C., Rodhe, H. and De Geer, L.-E. (1986)
The Chernobyl accident - A meteorological analysis of how radionucleides reached Sweden.

56   Persson, C., Robertson, L., Grennfelt, P., Kindbom, K., Lövblad, G. och Svanberg, P.-A. (1987)
Luftföroreningsepisoden över södra Sverige 2 - 4 februari 1987.

57   Omstedt, G. (1988)
An operational air pollution model.

58   Alexandersson, H. and Eriksson, B. (1989)
Climate fluctuations in Sweden 1860 - 1987.

59   Eriksson, B. (1989)
Snödjupsförhållanden i Sverige - Säsongerna 1950/51 - 1979/80.

60   Omstedt, G. and Szegö, J. (1990)
Människors exponering för luftföroreningar.

61   Mueller, L., Robertson, L., Andersson, E. and Gustafsson, N. (1990)
Meso-□ scale objective analysis of near surface temperature, humidity and wind, and its application in air pollution modelling.

62   Andersson, T. and Mattisson, I. (1991)
A field test of thermometer screens.

63   Alexandersson, H., Gollvik, S. and Meuller, L. (1991)
An energy balance model for prediction of surface temperatures.

64   Alexandersson, H. and Dahlström, B. (1992)
Future climate in the Nordic region - survey and synthesis for the next century.

65   Persson, C., Langner, J. and Robertson, L. (1994)
Regional spridningsmodell för Göteborgs och Bohus, Hallands och Älvsborgs län. (A mesoscale air pollution dispersion model for the Swedish west-coast region. In Swedish with captions also in English.)

66   Karlsson, K.-G. (1994)
Satellite-estimated cloudiness from NOAA AVHRR data in the Nordic area during 1993.

67   Karlsson, K-G. (1996)
Cloud classifications with the SCANDIA model.

68   Persson, C. and Ullerstig, A. (1996)
Model calculations of dispersion of lindane over Europe. Pilot study with comparisons to easurements around the Baltic Sea and the Kattegat.

69   Langner, J., Persson, C., Robertson, L. and Ullerstig, A. (1996)
Air pollution Assessment Study Using the MATCH Modelling System. Application to sulfur and nitrogen compounds over Sweden 1994.

70   Robertson, L., Langner, J. and Engardt, M. (1996)
MATCH - Meso-scale Atmosperic Transport and Chemistry modelling system.

71   Josefsson, W. (1996)
Five years of solar UV-radiation monitoring in Sweden.

72 Persson, C., Ullerstig, A., Robertson, L., Kindbom, K. and Sjöberg, K. (1996)
The Swedish Precipitation Chemistry Network. Studies in network design using the MATCH modelling system and statistical methods.

73 Robertson, L. (1996)
Modelling of anthropogenic sulfur deposition to the African and South American continents.

74 Josefsson, W. (1996)
Solar UV-radiation monitoring 1996.

75 Häggmark, L. Ivarsson, K.-I. and Olofsson, P.-O. (1997)
MESAN - Mesoskalig analys.

76 Bringfelt, B., Backström, H., Kindell, S., Omstedt, G., Persson, C. and Ullerstig, A. (1997)
Calculations of PM-10 concentrations in Swedish cities- Modelling of inhalable particles

77 Gollvik, S. (1997)
The Teleflood project, estimation of precipitation over drainage basins.

78 Persson, C. and Ullerstig, A. (1997)
Regional luftmiljöanalys för Västmanlands län baserad på MATCH modell-beräkningar och mätdata - Analys av 1994 års data

79 Josefsson, W. and Karlsson, J.-E. (1997)
Measurements of total ozone 1994-1996.

80 Rummukainen, M. (1997)
Methods for statistical downscaling of GCM simulations.

81 Persson, T. (1997)
Solar irradiance modelling using satellite retrieved cloudiness - A pilot study

82 Langner, J., Bergström, R. and Pleijel, K. (1998)
European scale modelling of sulfur, oxidized nitrogen and photochemical oxidants. Model development and evaluation for the 1994 growing season.

83 Rummukainen, M., Räisänen, J., Ullerstig, A., Bringfelt, B., Hansson, U., Graham, P. and Willén, U. (1998)
RCA - Rossby Centre regional Atmospheric climate model: model description and results from the first multi-year simulation.

84 Räisänen, J. and Döscher, R. (1998)
Simulation of present-day climate in Northen Europé in the HadCM2 OAGCM.

85 Räisänen, J., Rummukainen, M., Ullerstig, A., Bringfelt, B., Hansson, U. and Willén, U. (1999)
The First Rossby Centre Regional Climate Scenario - Dynamical Downscaling of CO_2-induced Climate Change in the HadCM2 GCM.

86 Rummukainen, M. (1999)
On the Climate Change debate

87 Räisänen, J. (2000)
CO_2-induced climate change in northern Europé: comparison of 12 CMIP2 experiments.

88 Engardt, M. (2000)
Sulphur simulations for East Asia using the MATCH model with meteorological data from ECMWF.

89 Persson, T. (2000)
Measurements of Solar Radiation in Sweden 1983-1998

90 Michelson, D. B., Andersson, T., Koistinen, J., Collier, C. G., Riedl, J., Szturc, J., Gjertsen, U., Nielsen, A. and Overgaard, S., (2000)
BALTEX Radar Data Centre Products and their Methodologies

91 Josefsson, W. (2000)
Measurements of total ozone 1997 – 1999

92 Andersson, T. (2000)
Boundary clear air echos in southern Sweden

93 Andersson, T. (2000)
Using the Sun to check some weather radar parameters

94 Rummukainen, M., Bergström, S., Källén, E., Moen, L., Rodhe, J. and

Tjernström, M. (2000)
SWECLIM – The First Three Years

95 Meier, H. E. M. (2001)
The first Rossby Centre regional
climate scenario for the Baltic Sea
using a 3D coupled ice-ocean model

96 Landelius, T., Josefsson, W. and
Persson, T. (2001)
A system for modelling solar radiation
parameters with mesoscale spatial
resolution

97 Karlsson, K.-G. (2001)
A NOAA AVHRR cloud climatology
over Scandinavia covering the period
1991-2000

98 Bringfelt, B., Räisänen, J., Gollvik, S.,
Lindström, G., Graham, P. and
Ullerstig, A., (2001)
The land surface treatment for the
Rossby Centre Regional Atmospheric
Climate Model - version 2 (RCA2)

99 Kauker, F. and Meier, H. E. M., (2002)
Reconstructing atmospheric surface
data for the period 1902-1998 to force
a coupled
ocean-sea ice model of the Baltic Sea.

100 Klein, T., Bergström, R. and Persson,
C. (2002)
Parameterization of dry deposition in
MATCH

101 Räisänen, J., Hansson, U., Ullerstig A.,
Döscher, R., Graham, L. P., Jones, C.,
Meier, M., Samuelsson, P.and Willén,
U. (2003)
GCM driven simulations of recent and
future climate with the Rossby Centre
coupled atmosphere - Baltic Sea
regional climate model RCAO

102 Tjernström, M., Rummukainen, M.,
Bergström, S., Rodhe, J. och Persson,
G., (2003)
Klimatmodellering och klimatscenarier
ur SWECLIMs perspektiv.

103 Segersson, D. (2003)
Numerical Quantification of Driving
Rain on Buildings

104 Rummukainen, M. and the SWECLIM
participants (2003)
The Swedish regional climate

modeling program 1996-2003. Final
report.

105 Robertson, L. (2004)
Extended back-trajectories by means of
adjoint equations

106 Rummukainen, M., Bergström S.,
Persson G., Ressner, E (2005)
Anpassningar till klimatförändringar

107 Will not be published

108 Kjellström, E., Bärring, L., Gollvik, S.,
Hansson, U., Jones, C., Samuelsson, P.,
Rummukainen, M., Ullerstig, A.,
Willén, U., Wyser, K., (2005)
A 140-year simulation of European
climate with the new version of the
Rossby Centre regional atmospheric
climate model (RCA3).

109 Meier, H.E.M., Andréasson, J.,
Broman, B., Graham, L. P.,
Kjellström, E., Persson, G., and
Viehhauser, M., (2006)
Climate change scenario simulations of
wind, sea level, and river discharge in
the Baltic Sea and Lake Mälaren region
– a dynamical downscaling approach
from global to local scales.

110 Wyser, K., Rummukainen, M.,
Strandberg, G., (2006)
Nordic regionalisation of a greenhouse-
gas stabilisation scenario

111 Persson, G., Bärring, L., Kjellström, E.,
Strandberg G., Rummukainen, M.,
(2007).
Climate indices for vulnerability
assessments

112 Jansson, A., Persson, Ch., Strandberg,
G., (2007)
2D meso-scale re-analysis of
precipitation, temperature and wind
over Europe -ERAMESAN

113 Lind, P., Kjellström, E., (2008)
Temperature and Precipitation changes
in Sweden; a wide range of model-
based projections for the 21st century

114 Klein, T., Karlsson, P-E., Andersson,
S., Engardt, M., Sjöberg, K (2011)
Assessing and improving the Swedish
forecast and information capabilities
for ground-level ozone

115. Camilla Andersson, Robert Bergström,
Cecilia Bennet, Manu Thomas, Lennart
Robertson SMHI. Harri Kokkola,
Hannele Korhonen, Kari Lehtinen
FMI (2013)
MATCH-SALSA Multi-scale
Atmospheric Transport and Chemistry
model coupled to the SALSA aerosol
microphysics model.

SMHI